Astronomy & Astrophysics manuscript no. aa7838
August 28, 2021

The VLT-FLAMES survey of massive stars: Evolution of surface N abundances and effective temperature scales in the Galaxy and Magellanic Clouds. ⋆,⋆⋆

C.Trundle[1], P.L. Dufton[1], I. Hunter[1,2], C.J. Evans[3], D.J. Lennon[2], S.J Smartt[1], R.S.I. Ryans[1]

[1] Astronomy Research Centre, Department of Physics & Astronomy, School of Mathematics & Physics, The Queen's University of Belfast, Belfast, Northern Ireland, UK
[2] The Isaac Newton Group of Telescopes, Apartado de Correos 321, E-38700, Santa Cruz de La Palma, Canary Islands, Spain
[3] UK Astronomy Technology Centre, Royal Observatory, Blackford Hill, Edinburgh, EH9 3HJ, UK

ABSTRACT

We present an analysis of high resolution VLT-FLAMES spectra of 61 B-type stars with relatively narrow-lined spectra located in 4 fields centered on the Milky Way clusters; NGC3293 & NGC4755 and the Large and Small Magellanic cloud clusters; NGC2004 and NGC330. For each object a quantitative analysis was carried out using the non-LTE model atmosphere code TLUSTY; resulting in the determination of their atmospheric parameters and photospheric abundances of the dominant metal species (C, N, O, Mg, Si, Fe). The results are discussed in relation to our earlier work on 3 younger clusters in these galaxies; NGC6611, N11 and NGC346 paying particular attention to the nitrogen abundances which are an important probe of the role of rotation in the evolution of stars. This work along with that of the younger clusters provides a consistent dataset of abundances and atmospheric parameters for over 100 B-type stars in the three galaxies. We provide effective temperature scales for B-type dwarfs in all three galaxies and for giants and supergiants in the SMC and LMC. In each galaxy a dependence on luminosity is found between the three classes with the unevolved dwarf objects having significantly higher effective temperatures. A metallicity dependence is present between the SMC and Galactic dwarf objects, and whilst the LMC stars are only slightly cooler than the SMC stars, they are significantly hotter than their Galactic counterparts.

Key words. stars: atmospheres – stars: early-type – stars: B-type – stars: abundances - Magellanic Clouds - Galaxies: abundances - open clusters and associations: individual: NGC3293, NGC4755, NGC2004, NGC330 – stars: evolution

1. Introduction.

Rotation was introduced as a crucial dynamical process in understanding the evolution of massive stars due to a number of discrepancies found between stellar evolution models and observations (Meynet & Maeder 1997). Amongst these were the discovery of surface enrichments of helium and nitrogen in OBA-type supergiants (Jaschek & Jaschek 1967; Dufton 1972; Walborn 1972; Venn 1999) and helium excesses in fast rotating O-type stars (Herrero et al. 1992), which provided observational evidence that additional mixing mechanisms were required in the models. Important breakthroughs by Zahn (1992) on the theory of the transport mechanisms caused by rotation, and subsequent work in that area has allowed for the introduction of rotation in the stellar evolution models (Meynet & Maeder 2000; Heger & Langer 2000). Additionally metallicity may play an important role in the evolution of rotational velocities in massive stars through the more compact structures and lower mass-loss rates predicted at low metallicities (Maeder & Meynet 2001). Yet discrepancies still remain as previous studies show significant surface enrichments which require more efficient rotational mixing at earlier stages of evolution than the models predict (Lennon et al. 2006).

In recent years there has been a strong motivation in observational astronomy to study the correlation of rotational velocities of OB-type stars and their surface composition together with understanding the roles of metallicity and the density of the stellar environment. Keller (2004) presented the first extragalactic study of the distribution of rotational velocities of B-type main-sequence stars. They showed that young cluster objects rotate more rapidly than field objects, whilst LMC objects rotate faster than their Galactic counterparts, highlighting the existence of a metallicity dependence. Confirming the report by Keller, Strom et al. (2005) found that BA-type stars close to the ZAMS in the h and χ Persei clusters had projected rotational velocities twice that of a similar aged field population. Martayan et al. (2006) investigated the projected rotational velocity distribution of both B-type and Be stars in the Large Magellanic Cloud cluster, NGC2004, with the result that the latter population are rotating faster in their initial ascent along the main-sequence. Subsequently Wolff et al. (2007) have studied the role of the initial density conditions of the star-forming regions on the rotational velocity distributions in seven galactic clusters. They found that stars formed in low density regions have a higher number of slow rotators in comparison to those formed in high density clusters.

To study the roles of rotation, mass-loss and metallicity on the evolution of massive stars, we have undertaken a high res-

Send offprint requests to: C.Trundle, e-mail: c.trundle@qub.ac.uk.

⋆ Based on observations at the European Southern Observatory Very Large Telescope in programmes 68.D-0369 and 171.D-0237.

⋆⋆ Tables A.1-C.4 are only available in electronic form at http://www.edpsciences.org

Table 1. Observational details of the telescope/instrument combinations used for this paper. The second column presents the complete wavelength coverage of the data, whilst the numbers in parentheses are the number of wavelength settings required to obtain this coverage. The third and fourth columns display the mean signal-to-noise (S/N) ratio and resolution of the data.

Telescope/Instrument	λ-range (Å)	S/N	R
VLT/FLAMES	3850-4755, 6380-6620 (6)	100-150	20000-30000
VLT/UVES[1]	3750-5000, 5900-7700, 7750-9600 (3)	40	20000
ESO2.2m/FEROS	3600-9300 (1)	>100	48000

[1]UVES data only used for one object NGC330-124

olution spectroscopic survey of approximately 750 OB stars towards seven young clusters in the Galaxy, LMC and SMC (the VLT-FLAMES Survey of Massive Stars). The Galactic and Magellanic Cloud samples have been discussed in Evans et al. (2005, 2006) respectively. The O stars in the sample were analysed by Mokiem et al. (2006, 2007), who derive their atmospheric & wind parameters, helium abundances and rotational velocities. Helium enrichments were found to be present at the surface of many of these stars, implying significant rotational mixing. However the models considered by Mokiem et al. still underpredicted the degree of helium enrichment observed. They also found that the more evolved objects rotated slower than the unevolved stars and that within the population of unevolved stars there was an excess of fast rotators in the SMC compared to Galactic objects.

Analysis of the much larger sample of B-type stars is currently underway; Dufton et al. (2006) have derived the rotational velocities of all the Galactic stars. They confirmed the result of Strom et al. that the cluster objects rotate faster than their field counterparts and confirm predictions that the higher-mass stars with strong stellar winds have lower rotational velocities due to the loss of surface angular momentum. To understand the efficiency of rotation in mixing chemically processed material from the interior of a star to the photospheric layers, it is important to study the surface chemical composition of these objects in conjunction with their rotational velocity distribution. Hunter et al. (2007, hereafter Paper IV) have derived the atmospheric parameters and surface composition of 50 narrow lined B-type stars in the youngest of our target clusters (NGC6611, N11, NGC346). In this paper we extend that analysis to the older clusters in the survey studying 61 narrow lined stars in NGC3293, NGC4755, NGC2004 & NGC330. As these stars have low projected rotational velocities, a detailed atmospheric analysis can provide highly accurate atmospheric parameters and surface composition, thus providing the baseline metallicities of these seven regions and an insight into the evolution of nitrogen as a function of environment. Additionally we will provide effective temperature scales as a function of spectral type, luminosity and metallicity for these narrow lined objects which can be applied to the fast rotators, in which the blending of the lines makes it impossible to determine effective temperatures directly from the spectra. These effective temperature scales will have important applications in many areas of astrophysics such as for comparison with stellar evolution models, determining cluster properties and understanding the properties of ionising stars.

2. Observations.

The spectroscopic data analysed in this paper are from an ESO large programme using the Fibre Large Array Multi-Element Spectrograph (FLAMES) on the VLT, primarily with the Giraffe spectrograph, but also using the fibre-feed to UVES (Ultraviolet and Visual Echelle Spectrograph). In addition spectra from the Fibre-Fed Extended Range Optical Spectrograph (FEROS) and UVES (without FLAMES feed) were obtained for a number of targets in the Galactic clusters. The former had been omitted from the FLAMES setups as they were too bright, whilst the UVES data had been obtained prior to the large survey. As explained in Sect. 2.1, we have enforced certain criteria to select the dataset for this analysis which left only one suitable UVES target. The properties of the datasets are summarised in Table 1, while the target selection, data reduction and observational details of all the observations have been discussed in Evans et al. (2005, hereafter Paper I) and Evans et al. (2006, hereafter Paper II). Their target identifications will be used throughout this paper. Whilst the survey covers seven clusters in three distinct metallicity regimes; Galactic (NGC6611, NGC4755, NGC3293), LMC (N11, NGC2004) and SMC (NGC346, NGC330), this paper will concentrate on the narrow lined stars (*i.e.* those with small projected rotational velocities) in the older clusters NGC4755, NGC3293, NGC2004, and NGC330.

2.1. Selection of narrow lined stars.

Our selection of objects follows closely the criteria set out in Paper IV. The main objective was to select the highest quality spectra suitable for a reliable model atmosphere analysis. Fast rotators were excluded because rotational-broadening blends the absorption lines, thereby decreasing the accuracy with which equivalent widths can be measured. The criteria applied were as follows:

- Spectral types earlier than O9 were excluded as they are more suited to analyses which utilise unified model atmosphere codes, and can model the stronger stellar winds of these stars (Mokiem et al. 2006, 2007).

- Any object whose spectrum was deemed to be contaminated by a secondary object and for which the lines were not clearly separated from those of the secondary, was omitted from the analysis.

- Only objects for which the effective temperature could be accurately measured using the silicon ionisation equilibrium (viz. Si III/Si IV or Si III/Si II) were considered.

In the case of the NGC2004 targets, the Si III lines at 4560 Å, used for the temperature determination, were observed in two wavelength settings. Therefore in addition to the criteria listed above, if the measurement of the equivalent widths from the two spectra did not agree to within 10% the object was omitted from this analysis.

After applying the above criteria, we were left with 61 objects in total; 8 stars in NGC3293, 10 in NGC4755, 23

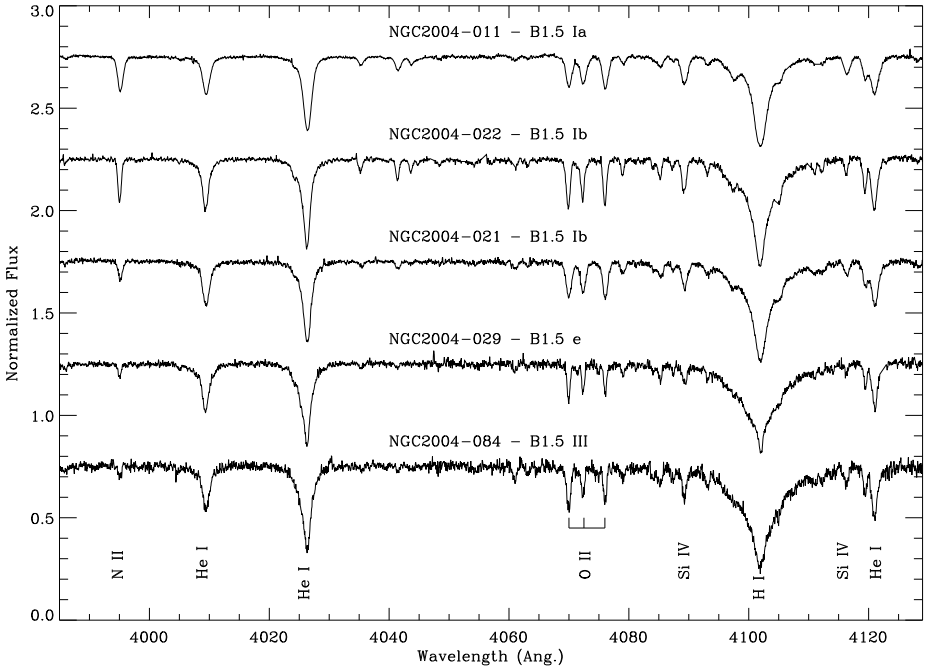

Fig. 1. Examples of the FLAMES-Giraffe Spectra for B1.5 stars in NGC2004, additional examples can be seen in Papers 1 & 2. The spectra are shifted to rest wavelengths. The identified lines are: N II λ3995, He I $\lambda\lambda$4009, 4026, 4120, O II $\lambda\lambda$4069, 4072,4076, Si IV$\lambda\lambda$4089, 4116 and H I δ. Note the range in line intensity of the N II line at 3995 Å.

in NGC2004 and 20 in NGC330. These objects are listed in Tables 3 & 4, whilst comments on two objects which were considered during object selection, but that did not fulfill all our criteria, are included in Appendix A.

2.2. Data Reduction.

The FLAMES-Giraffe spectra were reduced using the Giraffe Base-Line Reduction Software (Blecha et al. 2003, girBLDRS) as discussed in Paper I & II. An inherent drawback in multi-fibre spectroscopy is the difficulty in sky subtraction particularly when treating nebular emission. To deal with this, typically 15 sky fibres were allocated in each FLAMES plate, those with significant nebular emission were omitted prior to making a master sky spectrum. The maximum variations in counts from the sky fibres across the FLAMES plate were on the order of 10%, which is comparable to the fibre throughputs and would be difficult to disentangle from this effect. We carried out significant testing of the sky subtraction. Initially the sky spectra were smoothed but this did not remove very narrow absorption lines in the fainter targets. Finally we used a master sky, which was scaled to the appropriate fibre throughput and subtracted from all objects. Further to these steps and those outlined in Papers I & II additional steps were required before the spectra were suitable for analysis with the model atmosphere codes and these are outlined here.

FLAMES observations were taken in six separate wavelength settings, and in the case of the Magellanic Cloud fields, multiple exposures were taken for each setting. These are summarized in Table 2 together with the maximum time separation of the individual exposures for a given wavelength region; further information can be found in Paper I. As some of the wavelength settings were observed over an extended period, (34 days for NGC2004 and 4 days for NGC330) careful corrections for velocity shifts were required. For each wavelength setting, each exposure was cross-correlated with the others, identifying any radial velocity shifts. Stars were classified as *possible* single-lined spectroscopic binaries if the mean radial velocity of any two sets of exposures differed at the 3σ level, and are noted as such in Table 4. This method of cross-correlation to determine if there were any radial velocity shifts was dependent on sampling the binaries over a significant part of their orbit. Hence it was of limited utility for some of the clusters analysed here, and in particular for the NGC330 cluster where it was unlikely to identify long period binaries. For the Galactic cluster objects and the one UVES object, NGC330-124, no cross correlation was possible as only one exposure was taken for each of these objects.

Table 2. Details of the Magellanic Cloud observations for FLAMES. Columns denoted by (a) give the number of exposures, where as columns denoted by (b) give the maximum separation in days between exposures. Only single exposures were obtained for the galactic objects and hence they are not included in this table.

λ Setting	λ_c (Å)	NGC2004		NGC330	
		(a)	(b)	(a)	(b)
HR02	3958	6	6	9	3
HR03	4124	4	0	6	4
HR04	4297	6	2	6	4
HR05	4471	6	1	3	3
HR06	4656	6	0	6	3
HR14	6515	6	34	6	1

A few objects were identified with significant radial velocity shifts and are likely to be in binary systems, but a number of objects have also been identified with very small shifts of < 5 kms^{-1}. Objects with similarly low velocity shifts were highlighted in Paper IV. These shifts may be significant but require further sampling in time for corroboration and we simply label these objects as radial velocity variables (see Table 4).

Once the spectra had been cross-correlated, the individual exposures were combined and any cosmic rays were removed using the SCOMBINE procedure in IRAF[1]. The combined spectra, and in the case of the Galactic stars the single exposures, were then normalised and individual wavelength settings merged using the spectral analysis package DIPSO (Howarth et al. 1994). The spectra from the four clusters were then inspected for 53 prominent metal lines, the equivalent widths of these lines were measured if they were clearly visible and unblended with neighbouring lines. The low order Balmer lines plus the neutral helium lines in each star were then normalised for comparison with the theoretical models. Additionally when observed, the singly ionised helium lines at 4199, 4541 and 4686 Å were also normalised as they provide useful supplementary checks on the effective temperature estimates. Figure 1 displays some examples of the FLAMES-Giraffe spectra of B1.5 type stars in NGC2004, additional examples can be seen in Papers 1 & 2.

3. Spectral Analysis: tools and techniques.

Our analysis follows the methodology presented in Paper IV, as we have strived to provide a consistent analysis of the entire FLAMES dataset. This is important as later in this paper the implications from the results of both the young and old clusters will be discussed together. Due to the similarities with Paper IV the details of the spectral analysis will not be reiterated here but we will simply provide a summary.

The spectra were analysed with the Queen's University Belfast (QUB) B-type star grid (Ryans et al. 2003; Dufton et al. 2005), which was generated using the non-LTE model atmosphere code TLUSTY and line formation code SYNSPEC. For Hydrogen Lyman and Balmer lines the broadening tables of Vidal et al. (1973) were used, whilst for the higher members of the spectral series the approach described by Hubeny et al. (1994) was applied. Further details can be found in the SYNSPEC user manual. The QUB grid has been created specifically for B-type stars of all luminosity classes, covering the effective temperatures ($T_{\rm eff}$), surface gravities ($\log g$) and microturbulent velocities (ξ) appropriate for late O to late B-type stars ($T_{\rm eff}$: 35-12 kK, steps of 2.5 kK; $\log g$: 4.5 down to the Eddington limit, steps of 0.25; ξ: 0, 5, 10, 15, 20 and 30 kms^{-1}). The grid covers a range of metallicities appropriate to the Milky Way, LMC and SMC. In addition, for each of these metallicity grids the light elements are varied around their normal abundances by +0.8, +0.4, -0.4 and -0.8. The atmospheric parameters along with the photospheric abundances were determined for each star by interpolation within this grid via QUB IDL routines (Ryans et al. 2003). The energy levels and oscillator strengths relating to the transitions for the metal lines considered in this work are available online at http://star.pst.qub.ac.uk/~pld/line_identifications.html.

[1] IRAF is distributed by the National Optical Astronomy Observatories, which are operated by the Association of Universities for Research in Astronomy, Inc., under agreement with the National Science Foundation.

4. Stellar parameters

A static stellar atmosphere is characterised by four parameters: $T_{\rm eff}$, $\log g$, ξ and metallicity (Z). These parameters are interdependent and hence are determined through an iterative procedure, that assumes an appropriate metallicity (which depends on the cluster/galaxy) and estimates of the atmospheric parameters based on the spectral type of the star. By choosing suitable initial estimates of the stars properties, one can significantly reduce the number of iterations required. The stellar parameters of our targets, are presented in Tables 3 & 4.

Effective temperatures were determined using the silicon ionisation balance *i.e.* that the abundance estimates derived from the Si III lines (4552, 4567 & 4574 Å) agree with that from the Si IV line (4116 Å) for hot objects, or those from the Si II lines (4128 & 4131 Å) for cooler objects. Several of the B1 & B2 objects in the galactic cluster, NGC3293, had all three ionisation stages present in their spectra. However the temperatures determined from the Si III/IV and Si III/II ionisation stages differed, with the latter generally requiring higher temperatures. For NGC3293-007 where the Si IV line is relatively strong and well observed this difference is only 200 K, but for NGC3293-010,-018, & -026 the differences are $\sim$ 2000 to 2500 K. As the Si II spectrum is the weakest of the three ionisation stages the $T_{\rm eff}$ estimated from the Si III/IV lines have been adopted for these stars. NGC4755-004 also has the three silicon ionisation stages present in its spectra and for this object the estimates were in excellent agreement.

For the hotter objects (with spectral types earlier than B1), the He II 4541 and 4199 Å lines were used as an additional check on the temperature. The estimates from the two elements normally agreed to within 500K with the He lines implying slightly higher temperature. For one star, NGC2004-090, a significant discrepancy was found with the estimate from the Si lines being 31750 K, whilst the He II lines implied a temperature of 33000 K. However the Si III lines are relatively weak in this spectrum increasing the uncertainty in this effective temperature estimate.

We believe that our effective temperature estimates should have an uncertainty of typically $\pm$1000 K. However there are a number of other objects for which larger error estimates are appropriate, due to either the Si lines from one of the ionisation stages being very weak or the difficulty in constraining the microturbulence. In these cases, errors of up to 2000 K have been adopted when estimating uncertainties in the derived abundances.

Surface gravities were determined by comparing theoretical spectra with the observed profiles of the hydrogen Balmer lines, H_γ and H_δ. This was achieved using automated procedures developed in IDL, to fit models within the TLUSTY grids using χ^2 techniques. To increase the accuracy of our estimates, a higher resolution TLUSTY grid has been generated in gravity space, with steps of 0.1 dex in $\log g$ from 4.5 dex down to the Eddington limit. The estimates derived from the two hydrogen lines normally agree to within 0.1 dex, with any differences mainly arising from errors in the normalisation of the observed spectra.

Microturbulences have been derived from the Si III lines 4552, 4567 & 4574 Å, by ensuring that the abundance estimates were consistent (*i.e.* a slope of zero is obtained in a plot of equivalent widths against abundance estimates). For a number of objects in our sample, and those presented in Paper IV, a microturbulence of 0 kms^{-1} has been adopted. Unfortunately this did not produce a slope of zero in the equivalent-width versus

Table 3. Atmospheric parameters for B-type stars in NGC3293 & NGC4755 as derived from non-LTE TLUSTY model atmospheres. The majority of the data comes from FEROS however those taken with FLAMES are marked with [1]. Identifications and spectral classifications are taken from Paper I. Both the initial and corrected atmospheric parameters are shown following the discussion in Sect. 4. The uncertainties in these parameters are typically 1000K for $T_{\rm eff}$, 0.20 dex for $\log g$, 3-5 kms^{-1} for ξ and 5 kms^{-1} for $v \sin i$.

		Initial Parameters			Corrected Parameters					
Star	Sp.Typ	$T_{\rm eff}$ (K)	$\log g$ (cm^{-2})	$\xi_{\rm Si}$ (kms^{-1})	$T_{\rm eff}$ (K)	$\log g$ (cm^{-2})	$\xi_{\rm Si}$ (kms^{-1})	$v \sin i$ (kms^{-1})	$M_\star$ ($M_\odot$)	$\log(L_\star)$ ($L_\odot$)
NGC3293-003	B1 III	20700	2.75	15	20500	2.75	13	80	18± 2	4.92
NGC3293-004	B1 III	22700	3.13	13	22700	3.13	13	105	17± 1	4.76
NGC3293-007	B1 III	22700	3.10	12	22600	3.10	11	65	15^{+2}_{-1}	4.86
NGC3293-010	B1 III	21325	3.20	10	21450	3.20	11	70	12± 1	4.37
NGC3293-012	B1 III	21150	3.30	10	21500	3.30	11	100	12± 1	4.37
NGC3293-018	B1 V	23250	3.75	3	23450	3.75	5	26	12± 1	4.23
NGC3293-026[1]	B2 III	21700	3.65	<0	22100	3.65	2	30	9± 1	3.83
NGC3293-043[1]	B3 V	19500	4.05	<0	19500	4.05	<0	14	7± 1	3.32
NGC4755-002	B3 Ia	15950	2.20	19	15950	2.20	18	70	22± 1	5.15
NGC4755-003	B2 III	17600	2.50	17	17700	2.50	15	38	19^{+1}_{-2}	4.97
NGC4755-004	B1.5 Ib	19400	2.60	18	19550	2.60	17	75	19^{+1}_{-2}	5.00
NGC4755-006	B1 III	19000	2.85	14	19900	2.95	17	100	11± 1	4.36
NGC4755-015	B1 V	21800	3.65	2	22400	3.70	5	48	10± 1	3.98
NGC4755-017	B1.5 V	20500	3.90	6	20400	3.90	3	75	9± 1	3.83
NGC4755-020[1]	B2 V	21800	3.95	3	21700	3.95	1	120	9± 1	3.78
NGC4755-033[1]	B3 V	18000	3.90	10	17300	3.85	6	75	6± 1	3.11
NGC4755-040[1]	B2.5 V	18250	4.00	<0	18900	4.10	2	65	6± 1	3.25
NGC4755-048[1]	B3 V	18200	3.95	6	17800	3.95	4	55	6± 1	2.98

[1]Spectra from FLAMES with Giraffe spectrograph.

abundance-estimate diagram but was the value of microturbulence which brought the slope the closest to zero (these values are denoted in Tables 3 & 4 with < 0 kms^{-1}). The cause for this discrepancy is unclear and has been discussed in detail in Paper IV. The uncertainties in the adopted microturbulence depend on the accuracy of the measured equivalent widths with typical errors of 3-5 kms^{-1}. Uncertainties of 5 kms^{-1} are only required for those objects with large microturbulences (*i.e.* $\xi >$ 10 kms^{-1}), whose derived silicon (and indeed other) abundances are less sensitive to the value adopted. The microturbulence can also be estimated from other species and this can lead to values that are generally consistent with our adopted uncertainties. Again a detailed discussion of this can be found in Paper IV and will not be repeated here.

In Paper IV, a microturbulence for each object which provides a silicon abundance equal to the median of that from all targets in the cluster was also considered. This significantly reduces the scatter in the abundances derived for elements (excluding nitrogen) within a cluster. The changes in the microturbulence are normally consistent with the errors discussed above and in most cases the effect of these changes on the other atmospheric parameters are minor, typically less than 200 K for $T_{\rm eff}$ and negligible for $\log g$. However for a small number of objects the changes in microturbulence had a significant effect on the other atmospheric parameters due to their interdependence. Hence, we decided to carry out our abundance analysis in three steps:

1. Using the microturbulence determined from the Si III lines we derived the stellar parameters and surface abundances as described above (see Table A.1).
2. For each star in a cluster, the microturbulence was varied until the abundance estimate from the Si III lines was that of the median silicon abundance of the cluster. The abundances of other elements were then recalculated with this new value of microturbulence (see Table A.2).
3. Finally, since the ionisation balance and microturbulence are reliant on the silicon lines, the $T_{\rm eff}$ and $\log g$ were reiterated, where necessary, for the new value of microturbulence, whilst maintaining the median silicon abundance of the cluster. This required, on occasions, an additional reiteration of the microturbulence due to the interdependency of the parameters. The other abundances were then recalculated with these parameters resulting in the abundances presented in Table 6.

The estimates of the atmospheric parameters from step one and three are listed in Tables 3 & 4 as initial and corrected parameters, respectively. Nine out of the sixty-one targets analysed in this work have microturbulent velocities in the range of 15-18 kms^{-1}. These velocities are typical of the sound speeds in NLTE model atmospheres at the line formation depths of the metal lines considered in the abundance analysis of these stars. (The sound speeds of such models have been discussed by McErlean et al. (1998) and the reader is referred there for further details.) Assuming that microturbulence represents a true microscopic velocity field in the atmospheres and as this turbulent velocity is a significant fraction of the sound speed in these nine stars, one would expect this to result in the formation of shocks. This casts some doubt on the validity of applying static atmospheres rather than hydrodynamical atmospheres in the interpretation of these stars. However this should not affect the main results of this paper, in particular the large range in nitrogen

Table 4. Atmospheric parameters for B-type stars in NGC2004 & NGC330 as derived from non-LTE TLUSTY models. Identifications and spectral classifications are taken from Paper II. The uncertainties are as described in Table 3.

Star	Sp.Typ	Initial Parameters			Corrected Parameters					
		$T_{\rm eff}$ (K)	log g ($\rm cm^{-2}$)	$\xi_{\rm Si}$ ($\rm kms^{-1}$)	$T_{\rm eff}$ (K)	log g ($\rm cm^{-2}$)	$\xi_{\rm Si}$ ($\rm kms^{-1}$)	$v \sin i$ ($\rm kms^{-1}$)	$M_\star/M_\odot$ ($M_\odot$)	$\log(L_\star/L_\odot)$ ($L_\odot$)
NGC2004-003^{R5}	B5 Ia	14450	2.10	14	14450	2.10	15	42	20^{+2}_{-1}	5.10
NGC2004-005^{R5}	B8 Ia	12600	1.90	24:	12390	1.90	12	31	18 ± 2	4.93
NGC2004-007	B8 Ia	12560	2.00	29:	12250	2.00	10	25	17 ± 2	4.88
NGC2004-010	B2.5 Iab	17050	2.40	16	17160	2.40	14	45	19 ± 2	5.02
NGC2004-011	B1.5 Ia	21300	2.75	14	21250	2.75	13	62	24 ± 2	5.22
NGC2004-012	B1.5 Iab	21270	2.87	12	21270	2.87	12	47	18 ± 2	4.92
NGC2004-014	B3 Ib	17660	2.85	14	17800	2.85	10	20	15^{+2}_{-1}	4.72
NGC2004-021	B1.5 Ib	21400	3.00	12	21450	3.00	14	59	16^{+2}_{-1}	4.82
NGC2004-022	B1.5 Ib	21700	3.15	10	21780	3.15	11	42	16^{+2}_{-1}	4.79
NGC2004-026^{R}	B2 II	22700	3.65	1	22900	3.65	0	19	14 ± 1	4.68
NGC2004-029^{R}	B1.5 e	23100	3.50	1	23100	3.50	1	30	14 ± 1	4.65
NGC2004-036	B1.5 III	22200	3.35	5	22870	3.35	7	42	13 ± 1	4.58
NGC2004-042	B2.5 III	20930	3.45	3	20980	3.45	2	42	12 ± 1	4.45
NGC2004-046	B1.5 III	25770	3.80	<0	26090	3.85	2	32	15 ± 1	4.62
NGC2004-053	B0.2Ve	32000	4.15	3	31500	4.15	6	7	18 ± 1	4.77
NGC2004-061	B2 III	21090	3.35	<0	20990	3.35	1	40	11 ± 1	4.31
NGC2004-064	B0.7-B1 III	25700	3.70	3	25900	3.70	6	28	13 ± 1	4.48
NGC2004-070	B0.7-B1 III	27200	3.90	<0	27400	3.90	4	46	14 ± 1	4.51
NGC2004-084	B1.5 III	27170	4.00	<0	27395	4.00	3	36	14 ± 1	4.46
NGC2004-090	O9.5 III	31750	4.05	3	32500	4.10	<0	16	17 ± 1	4.64
NGC2004-091^{R5}	B1.5 III	26600	4.05	1	26520	4.05	0	40	13 ± 1	4.42
NGC2004-108^{R}	B2.5 III	22600	4.00	<0	22600	4.00	<0	13	10 ± 1	4.21
NGC2004-119	B2 III	23210	3.75	<0	23210	3.75	<0	15	10 ± 1	4.15
NGC330-002	B3 Ib	14500	2.15	20	14590	2.15	16	14	15 ± 2	4.73
NGC330-003	B2 Ib	17250	2.25	15	17210	2.25	20	49	16^{+2}_{-1}	4.84
NGC330-004	B2.5 Ib	17000	2.30	16	17000	2.30	16	36	15 ± 1	4.77
NGC330-005	B5 Ib	13700	2.25	8	13700	2.25	8	16	13 ± 2	4.54
NGC330-009	B5 Ib	14000	2.45	10	13940	2.45	6	29	12 ± 2	4.41
NGC330-010	B5 Ib	14900	2.60	9	14820	2.60	4	0	12 ± 1	4.40
NGC330-014	B1.5 Ib	20000	2.75	15	20130	2.75	18	81	14 ± 1	4.64
NGC330-016	B5: II	14300	2.60	10	14220	2.60	5	40	10 ± 1	4.20
NGC330-017	B2 II	22000	3.35	<0	22000	3.35	<0	14	14 ± 1	4.62
NGC330-018	B3 II	18000	2.95	5	18000	2.95	5	46	12 ± 1	4.41
NGC330-020	B3 II	16400	2.85	2	16720	2.85	5	44	11 ± 1	4.31
NGC330-022	B3 II	18450	3.00	7	18860	3.00	1	23	12 ± 1	4.38
NGC330-026	B2.5 II	22500	3.40	<0	22500	3.40	<0	71	12 ± 1	4.46
NGC330-027	B1 V	22000	3.20	6	22040	3.20	7	80	12 ± 1	4.42
NGC330-032	B0.5 V	29700	4.15	<0	29700	4.15	<0	17	16 ± 1	4.63
NGC330-042	B2 II	25650	3.75	3	25450	3.75	1	26	12 ± 1	4.34
NGC330-047	B1 V	26700	4.05	0	26700	4.05	0	28	12 ± 1	4.30
NGC330-074	B0 V	32300	4.20	2	32020	4.20	4	29	15 ± 1	4.31
NGC330-114	B2 III	23800	3.90	3	23800	3.90	4	17	9 ± 1	3.79
NGC330-124	B0.2 V	31150	4.25	<0	30980	4.25	2	95	15 ± 1	4.38

^{R} Radial velocity variations detected at the 3σ level, these objects are candidates for binaries, see Sect. 2.2.
'R5' indicates that the radial velocity variation is less than $5\rm kms^{-1}$.

abundances observed in these stars. Whilst these nine objects are amongst those with the highest nitrogen abundances they are not the only objects with significant enrichments of nitrogen in their atmospheres.

In order to fit theoretical spectra to the observed data, any additional broadening of the spectral lines due to, for example, rotation or macroturbulence must be included. Here we have assumed that rotational broadening will be the dominant mechanism and have estimated its magnitude from the line profiles of the He I 4026 Å line for objects where the projected rotational velocity ($v \sin i$) was greater than 50 $\rm kms^{-1}$ and from the Si III lines where it was less than 50 $\rm kms^{-1}$. Details of the methodology have been presented in Paper IV & Hunter et al. (2007, hereafter Paper V) and the estimates are listed in Tables 3 & 4

In the case of dwarfs and giants these estimates can be safely considered to be a measurement of the projected rotational velocity as the instrumental broadening and microturbulence have been taken into account. However for most of the supergiants this excess broadening is likely to be a convolution of rotational broadening and other broadening mechanisms as

has been discussed by Ryans et al. (2002), Dufton et al. (2006), Simón-Díaz et al. (2006) & Simón-Díaz & Herrero (2007). In Paper V, a Fourier method (Simón-Díaz & Herrero 2007) has been applied to these supergiants to deconvolve the rotational broadening from other mechanisms and more realistic estimates of the projected rotational velocities were obtained. However we emphasize that the values quoted here have only been used to account for additional broadening in the line profile when comparing observation and theory, for which purpose we believe them to be adequate.

Luminosities and masses were estimated for each object and are presented in Tables 3 & 4. Luminosities for all the Milky Way cluster targets in our survey have been presented in Paper III, but here we have recalculated them following the same technique, based on the new, more accurate atmospheric parameters. For the Magellanic Cloud stars, the luminosities of each object were determined by assuming a constant reddening towards each cluster, Bolometric correction from the empirical solutions of Vacca et al. (1996) and Balona (1994), and the apparent magnitudes presented in Paper II. For the LMC a standard Galactic extinction law of $A_{\rm V}$ = 3.1E(B-V) was used whilst for NGC330 we took $A_{\rm V}$ = 2.72E(B-V) from Bouchet et al. (1985). We adopt an E(B-V) of 0.09 for NGC2004 (Sagar & Richtler 1991) and NGC330 (Lennon 1997). The distance moduli (DM) adopted were 18.91 and 18.56 for NGC330 and NGC2004, respectively (Hilditch et al. 2005; Gieren et al. 2005). The masses were then derived by plotting luminosity and temperature for each object on a Hertzsprung-Russell (HR) diagram and interpolating between stellar evolutionary tracks of varying masses. The evolutionary tracks adopted are from Meynet et al. (1994) together with those of Schaller et al. (1992) for the Milky Way clusters, and Schaerer et al. (1993) and Charbonnel et al. (1993) for NGC2004 and NGC330, respectively. Quoted uncertainties in the derived masses assumed an uncertainty of 0.1 dex in log $L_\star/L_\odot$ and a negligible error from the uncertainty in the effective temperature estimates.

5. Photospheric Abundances.

This Paper is concerned with analyzing the photospheric abundance patterns, specifically of C, N, and O, of the selected targets. Therefore we have used the atmospheric parameters, discussed in the previous sections, to derive absolute abundances of these stars by interpolating between models with the same atmospheric parameters but differing light element abundances. Using the equivalent widths measured for each line in the spectra arising from C, N, O, Mg, Si and Fe we have derived abundance estimates for each line of a given species (see Tables C.1 - C.4), and from these the mean abundances in a given star were determined and are presented in Tables A.1, A.2, & 6. Abundances of C, N, O, Mg & Si were determined using the non-LTE model atmospheres and line formation calculations. As will be discussed later in this section, the Fe abundances were also derived using non-LTE model atmosphere structures but with LTE line formation calculations. Table A.1 presents the abundances derived using the initial atmospheric parameters from Tables 3 & 4.

5.1. Errors in abundances.

There are several factors which contribute to the uncertainties in the mean abundances derived in the manner described above, including the atomic data adopted in the model atmosphere code, errors in EW measurements from normalisation problems or blending with other lines and errors in the stellar parameters. The former two will be decreased for species for which there are many lines, whereas the latter arises mainly from the interdependence of the parameters. The random uncertainty arising from the atomic data and observational data are accounted for in the standard error in the mean of the abundances. The systematic errors which arise from the uncertainties in the atmospheric parameters were then accounted for by changing these in turn by their relevant uncertainties and re-determining the abundance estimates. The random and systematic errors (from each parameter) were then summed in quadrature to give the uncertainties listed in Tables A.1, A.2, & 6. In the case of species for which only one or two lines (viz. Si IV and Mg II) were observed, we have adopted the random error of a better-sampled species (viz. oxygen). Since we have not explicitly accounted for the interdependence of the stellar parameters, specifically $T_{\rm eff}$ and log g, the uncertainties may be slightly overestimated.

5.2. Effect of Microturbulence on abundances.

As discussed in Section 4, for a number of objects it was difficult to obtain a microturbulence from the silicon lines and so the silicon abundance in each star was fixed to the mean cluster abundance (NGC3293: [Si/H]=7.45; NGC4755: [Si/H]=7.41; NGC2004: [Si/H]=7.21; NGC330: [Si/H]=6.81) by adjusting the microturbulence. The abundances derived using the initial $T_{\rm eff}$ and log g but with the microturbulence fixed to give the desired Si abundance ($\xi_{\rm ave}$) are presented in Table A.2. A comparison with Table A.1 shows that the Si III abundances are now more consistent within the clusters. Nevertheless, in comparing the Si III abundances with those from the other Si ionisation stages one can see that the ionisation balance is no longer maintained. Table 6 presents the abundances derived with the new microturbulence and appropriate $T_{\rm eff}$ and log g (*i.e.* using the corrected atmospheric parameters from Tables 3 & 4) to maintain the mean cluster Si abundance in each object, whilst also maintaining the ionisation balance. By fixing the microturbulence the scatter in Si abundances is greatly reduced as those objects with [Si/H] > [Si/H]$_{\rm cluster}$ can be easily brought into agreement with the [Si/H]$_{\rm cluster}$, by increasing ξ (see Tables A.2 & 6). This procedure only slightly reduces the scatter in abundances from the other elements (by less than 0.03 dex), except for the mean oxygen abundance. For those targets with [Si/H] significantly ($\sim$ 0.2 dex) above the mean cluster [Si/H], their oxygen abundances were also quite high (see Table A.1). By increasing the microturbulence in these objects, their silicon and oxygen abundances are reduced putting them into better agreement with the mean values of the cluster (see Table 6). For some objects, where the silicon abundance was significantly lower than the desired cluster abundance ([Si/H] $\leq$ [Si/H]$_{\rm cluster}$), it was not possible to increase the silicon abundance as the microturbulence was close to/or at zero and would need to be lowered further still (see for example NGC2004: #91, #108, #119).

5.3. Abundances of individual species.

Before discussing the final results it is worth mentioning a few general points on the mean abundances for the individual elements:

Carbon is a problematic species in B-type stars, a result of the C II lines being very sensitive to non-LTE effects. In the spectra of our targets the strongest carbon lines are at 3921, 4267, 6578 & 6582 Å. The carbon model atom in TLUSTY fails to reproduce consistent abundances from these 4 lines, with the car-

Table 5. Results of analysis of HR3468. The first column are the TLUSTY atmospheric parameters and abundances obtained following the procedures described in Sects. 2 & 4, the third column are the TLUSTY results using the parameters from Nieva & Przybilla (2007), and the fourth column are those from Nieva & Przybilla. Nieva & Przybilla estimate the $T_{\rm eff}$ from the C II/C III ionisation equilibrium and derive the microturbulence from the carbon lines not the silicon lines, as done in the TLUSTY analysis. Abundances are presented as [X]=12 + log([X/H]) in units of dex.

	HR 3468		
	Tlusty		Nieva & Przybilla
$T_{\rm eff}$(K)	22800	22900	22900
log g(cms^{-2})	3.55	3.60	3.60
ξ(kms^{-1})	10 (Si)	5	5 (C)
C II 3921	7.92	8.14	8.34
C II 4267	7.83	7.95	8.33
C II 6578	8.05	8.37	8.40
C II 6582	7.96	8.17	8.40

bon abundance estimated from the 4267 Å line normally found to be lower than for the other three lines.

Recently Nieva & Przybilla (2006, 2007) have constructed a new comprehensive non-LTE carbon model atom and have shown that for six slowly-rotating early B-type stars their model can produce consistent carbon abundances from 21 C II lines (including those mentioned above) in the visible spectrum. To investigate the offsets between the C abundances derived with TLUSTY in this work and those derived by Nieva & Przybilla using their C II model atom and a hybrid approach to the non-LTE line formation, we have analysed one of their stars in the same way as our targets. Using the same equivalent widths and spectra as Nieva & Przybilla, we analysed HR3468 a Galactic B1.5 III star. In Table 5 we present the results of this comparison, the $T_{\rm eff}$ and log g estimated in the two analyses are in good agreement. This is reassuring as there were a number of differences in the analyses viz. (1) Nieva & Przybilla estimated the $T_{\rm eff}$ from the C II/C III ionisation equilibrium and (2) they derived the microturbulence from the 17 carbon lines. This last point is the reason for the differences in the values of microturbulence in Table 5. The difference in abundances from the two analyses are quite significant, and vary from line to line. The C II 4267 Å line differs the most by 0.5 dex, this difference is reduced to a factor of 2.5 if the carbon abundances are derived using the lower microturbulence of 5 kms^{-1} in the TLUSTY analysis.

Two factors prevent us from adopting these offsets and applying them to the carbon abundances derived here using TLUSTY. Firstly, the carbon abundances derived by Nieva & Przybilla were estimated using a profile fitting technique and not the curve-of-growth technique applied here. Profile fitting is very reliant on the $v \sin i$ values adopted and results in uncertainties of up to 0.15 dex. More importantly, a comparison with only one object does not allow us to get a clear picture of the offsets in the carbon abundances derived throughout the entire parameter range covered by our targets. As each of the carbon lines behaves differently and since the C II 4267 Å line is the only line detectable throughout our spectral range, we have taken the absolute abundance of this line to represent the carbon abundance in these stars. In Tables A.1, A.2, & 6 the absolute carbon abundances are those derived from the C II 4267 Å line without any applied offsets but with the caveat that the absolute value is likely to be *significantly* lower than the true value and should only be used differentially. The abundances estimated from the other carbon lines are presented in Tables C.1 -C.4 for comparison.

Nitrogen abundances in B-type stars generally span a large range as a result of being processed in the CNO-cycle and this element being present in the photosphere through some, much debated, mechanism. The range of nitrogen abundances in our targets are again large: NGC3293: 7.45- 7.66 dex, NGC4755: 7.43 - 8.18 dex, NGC2004: 6.81 - 8.16 dex, NGC330: 6.76 - 7.83 dex. The spread in the nitrogen abundances of the stars in the Galactic cluster NGC3293, is smaller that of NGC4755 (also a Galactic cluster), but the former has no supergiants present in the analysed data. The three objects in NGC4755 with significant nitrogen enrichments are the three most massive and luminous Galactic objects in our sample. In each of the other clusters, it is the supergiants which have the highest nitrogen abundances, although there is a significant range in nitrogen abundances derived from the main sequence and dwarf objects. The nitrogen abundances will be discussed further in Sect. 6.

Oxygen has several strong features in the spectra of B-type stars and as such its mean abundance is very dependent on the microturbulence adopted for a given star. It has been previously noted that microturbulent velocities when derived from a range of oxygen lines are generally higher than that derived from the Si III 4560 Å multiplet (Vrancken et al. 2000; Trundle et al. 2002). However in Paper IV it was shown that by selecting the lines from a single oxygen multiplet, the microturbulence estimated from both oxygen and silicon were in better agreement (in some cases to within 1 kms^{-1}). The oxygen abundances are reasonably consistent within a cluster but a comparison of Tables A.1, A.2, & 6 reveals the strong dependence of oxygen on the microturbulence. For example, the oxygen abundances are lower than the mean cluster abundances for a number of objects where the microturbulence adopted was 0 but for which an even lower value, if realistic, could have been adopted (NGC3293-043, NGC2004-108, NGC330-017 & -026). The two B8Ia objects in NGC2004 (#005 & #007) have large oxygen abundances compared to the cluster mean, by almost a factor of 3. Although the $T_{\rm eff}$ and log g derived for these objects are reasonable, the oxygen abundances of these objects are highly dependent on the microturbulence, varying from 8.56 & 8.46 dex to 8.84 dex in both objects. These objects are also very luminous lying close to the edge of the grid and have a very weak oxygen spectrum so should be treated with caution.

Magnesium like silicon is an α-processed element and so should follow the same trend as silicon. There is only one strong line which can be seen over our wavelength range, that is the doublet at Mg II 4481 Å. The derived Mg abundances are normally in very good agreement throughout the clusters.

Silicon is one of the main diagnostic elements. As a result of its sensitivity to both temperature and microturbulence, we tend to see a large range in silicon abundances (Table A.1). However as discussed above we have fixed the Si abundance in each star to reflect the median abundance of the cluster, where possible. Those objects which have <0 in the microturbulence column for the corrected parameters in Tables 3 & 4 are those for which we could not obtain the desired Si abundance by changing the microturbulence. For these objects a zero microturbulence was adopted as this provided the closest possible Si abundance to that desired.

During our analysis we have encountered a problem with the Si II spectrum, where the Si abundances from the two Si II lines at 4128 & 4131 Å differ on average by 0.13 dex with the former resulting in a higher abundance. We expect that this is related to the oscillator strengths (log gf) included in TLUSTY calculations which have a ratio of 0.66. If the two lines were to follow LS coupling we would expect the ratio to be approximately 0.70.

Table 6. Absolute Abundances of NGC3293, NGC4755, NGC2004 & NGC330 stars. Presented are the mean of the absolute abundances for each species studied, obtained using the final corrected atmospheric parameters from Tables 3 & 4. Those objects with <0 in the microturbulence column are those for which the microturbulence could not be lowered any further to obtain a Si abundance close to or at the mean silicon abundance of the cluster. Carbon abundances presented here are based solely on the C II 4267 Å line and should only be used as a guide to the relative carbon abundance between the stars (see Sect. 5.3). Uncertainties on the abundances account for both random and systematic errors as discussed in Sect. 5.1. Abundances are presented as [X]=12 + log([X/H]) in units of dex, $T_{\rm eff}$ in K, log g in cms^{-2} and ξ in kms^{-1}.

Star	Sp.Typ	$T_{\rm eff}$	log g	ξ_{Ave}	C II	N II	O II	Mg II	Si II	Si III	Si IV	Fe III
NGC3293-003	B1 III	20500	2.75	13	7.84	7.52 ± 0.07	8.75 ± 0.28	7.29 ± 0.27		7.48 ± 0.33	7.49 ± 0.64	7.27 ± 0.31
NGC3293-004	B1 III	22700	3.13	13	7.89	7.55 ± 0.09	8.74 ± 0.23	7.44 ± 0.29		7.45 ± 0.22	7.45 ± 0.60	
NGC3293-007	B1 III	22600	3.10	11	7.86	7.50 ± 0.08	8.71 ± 0.22	7.26 ± 0.23	7.32 ± 0.39	7.44 ± 0.24	7.44 ± 0.59	7.24 ± 0.24
NGC3293-010	B1 III	21450	3.20	11	7.66	7.45 ± 0.11	8.82 ± 0.31	7.17 ± 0.24	6.89 ± 0.26	7.49 ± 0.33	7.53 ± 0.58	7.30 ± 0.24
NGC3293-012	B1 III	21500	3.30	11	7.67	7.45 ± 0.16	8.83 ± 0.33	7.29 ± 0.21		7.50 ± 0.33	7.51 ± 0.56	
NGC3293-018	B1 V	23450	3.75	5	7.66	7.56 ± 0.11	8.71 ± 0.28	7.15 ± 0.18	6.88 ± 0.23	7.49 ± 0.36	7.49 ± 0.57	7.70 ± 0.26
NGC3293-026	B2 III	22100	3.65	2	7.79	7.66 ± 0.17	8.75 ± 0.31	7.22 ± 0.29	6.95 ± 0.25	7.47 ± 0.35	7.46 ± 0.64	7.66 ± 0.18
NGC3293-043	B3 V	19500	4.05	< 0	7.91	7.55 ± 0.26	8.50 ± 0.34	7.14 ± 0.26	7.31 ± 0.37	7.31 ± 0.34		7.51 ± 0.25
NGC4755-002	B3 Ia	15950	2.20	18	7.87	8.18 ± 0.31	8.59 ± 0.43	7.30 ± 0.32	7.40 ± 0.30	7.40 ± 0.46		7.54 ± 0.22
NGC4755-003	B2 III	17700	2.50	15	7.78	8.12 ± 0.27	8.52 ± 0.36	7.33 ± 0.26	7.40 ± 0.26	7.40 ± 0.43		7.47 ± 0.18
NGC4755-004	B1.5 Ib	19550	2.60	17	7.76	8.07 ± 0.14	8.64 ± 0.28	7.29 ± 0.29	7.39 ± 0.35	7.38 ± 0.38	7.32 ± 0.67	7.38 ± 0.25
NGC4755-006	B1 III	19900	2.95	17	7.60	7.63 ± 0.19	8.90 ± 0.32	7.21 ± 0.21		7.43 ± 0.37	7.47 ± 0.52	
NGC4755-015	B1 V	22400	3.70	5	7.64	7.81 ± 0.21	8.80 ± 0.33	7.09 ± 0.23		7.47 ± 0.38	7.46 ± 0.64	7.73 ± 0.38
NGC4755-017	B1.5 V	20400	3.90	3	7.93	7.74 ± 0.37	8.71 ± 0.45	7.32 ± 0.34	7.44 ± 0.36	7.44 ± 0.44		
NGC4755-020	B2 V	21700	3.95	1	8.01	7.68 ± 0.22	8.51 ± 0.31	7.44 ± 0.29	7.38 ± 0.29	7.39 ± 0.34		7.84 ± 0.25
NGC4755-033	B3 V	17300	3.85	6	8.17	7.44 ± 0.36	8.72 ± 0.43	7.15 ± 0.35	7.38 ± 0.49	7.39 ± 0.39		
NGC4755-040	B2.5 V	18900	4.10	2	8.31	7.69 ± 0.39	8.98 ± 0.40	7.19 ± 0.40	7.43 ± 0.44	7.44 ± 0.34		
NGC4755-048	B3 V	17800	3.95	4	8.30	7.45 ± 0.34	9.00 ± 0.36	7.08 ± 0.30	7.36 ± 0.40	7.39 ± 0.34		
NGC2004-003	B5 Ia	14450	2.10	15	7.66	7.85 ± 0.40	8.45 ± 0.55	7.02 ± 0.26	7.22 ± 0.25	7.22 ± 0.50		7.29 ± 0.23
NGC2004-005	B8 Ia	12390	1.90	12	7.77	7.86 ± 0.37	8.84 ± 0.57	6.98 ± 0.46	7.22 ± 0.36	7.22 ± 0.44		7.20 ± 0.23
NGC2004-007	B8 Ia	12250	2.00	10	7.73	7.78 ± 0.28	8.84 ± 0.53	6.95 ± 0.43	7.21 ± 0.39	7.21 ± 0.44		7.11 ± 0.26
NGC2004-010	B2.5 Iab	17160	2.40	14	7.53	8.16 ± 0.29	8.29 ± 0.37	7.11 ± 0.26	7.21 ± 0.25	7.20 ± 0.43		7.26 ± 0.12
NGC2004-011	B1.5 Ia	21250	2.75	13	7.45	7.73 ± 0.07	8.41 ± 0.23	7.15 ± 0.26		7.19 ± 0.34	7.22 ± 0.66	7.14 ± 0.23
NGC2004-012	B1.5 Iab	21270	2.87	12	7.44	7.75 ± 0.09	8.43 ± 0.24	7.08 ± 0.23		7.19 ± 0.35	7.21 ± 0.64	7.12 ± 0.19
NGC2004-014	B3 Ib	17800	2.85	10	7.58	7.52 ± 0.26	8.24 ± 0.37	7.06 ± 0.22	7.22 ± 0.22	7.20 ± 0.40		7.17 ± 0.18
NGC2004-021	B1.5 Ib	21450	3.00	14	7.55	7.20 ± 0.10	8.47 ± 0.26	7.07 ± 0.22		7.18 ± 0.33	7.23 ± 0.57	7.19 ± 0.17
NGC2004-022	B1.5 Ib	21780	3.15	11	7.32	7.68 ± 0.11	8.55 ± 0.27	6.94 ± 0.19		7.23 ± 0.34	7.22 ± 0.58	7.00 ± 0.22
NGC2004-026	B2 II	22900	3.65	0	7.53	7.01 ± 0.12	8.18 ± 0.27	7.08 ± 0.17	7.24 ± 0.22	7.25 ± 0.36		7.35 ± 0.17
NGC2004-029	B1.5 e	23100	3.50	1	7.43	6.81 ± 0.05	8.29 ± 0.26	7.03 ± 0.19		7.21 ± 0.35	7.20 ± 0.56	7.35 ± 0.17
NGC2004-036	B1.5 III	22870	3.35	7	7.51	7.38 ± 0.07	8.48 ± 0.26	6.93 ± 0.18		7.21 ± 0.32	7.18 ± 0.56	7.29 ± 0.21
NGC2004-042	B2.5 III	20980	3.45	2	7.64	6.90 ± 0.19	8.16 ± 0.32	7.14 ± 0.22	7.18 ± 0.24	7.19 ± 0.36		7.20 ± 0.21
NGC2004-046	B1.5 III	26090	3.85	2	7.52	7.60 ± 0.11	8.44 ± 0.13	7.02 ± 0.19		7.22 ± 0.26	7.22 ± 0.50	

Table 6. Contd.

Star	Sp.Typ	$T_{\rm eff}$	log g	$\xi_{\rm 5Ave}$	C II	N II	O II	Mg II	Si II	Si III	Si IV	Fe III
NGC2004-053	B0.2 Ve	31500	4.15	6	7.83	7.64 ± 0.15	8.39 ± 0.17	7.24 ± 0.22		7.18 ± 0.26	7.18 ± 0.53	
NGC2004-061	B2 III	20990	3.35	1	7.75	6.99 ± 0.24	8.30 ± 0.45	7.13 ± 0.28	7.16 ± 0.29	7.17 ± 0.47		
NGC2004-064	B0.7-B1 III	25900	3.70	6	7.49	7.53 ± 0.09	8.37 ± 0.12	7.08 ± 0.25		7.18 ± 0.25	7.18 ± 0.53	
NGC2004-070	B0.7-B1 III	27400	3.90	4	7.58	7.43 ± 0.11	8.50 ± 0.20	7.15 ± 0.22		7.19 ± 0.36	7.20 ± 0.56	
NGC2004-084	B1.5 III	27395	4.00	3	7.64	7.28 ± 0.15	8.42 ± 0.13	7.17 ± 0.20		7.25 ± 0.24	7.25 ± 0.47	
NGC2004-090	O9.5 III	32500	4.10	< 0	7.63	7.65 ± 0.21	8.44 ± 0.24	6.97 ± 0.20		7.15 ± 0.27	7.16 ± 0.41	
NGC2004-091	B1.5 III	26520	4.05	0	7.80	7.29 ± 0.09	8.38 ± 0.14	7.29 ± 0.25		7.26 ± 0.27	7.26 ± 0.52	
NGC2004-108	B2.5 III	22600	4.00	< 0	7.29	6.89 ± 0.14	8.23 ± 0.30	6.99 ± 0.20	6.98 ± 0.23	6.98 ± 0.31		
NGC2004-119	B2 III	23210	3.75	< 0	7.48	6.95 ± 0.09	8.35 ± 0.27	7.17 ± 0.25	7.14 ± 0.24	7.14 ± 0.34		
NGC330-002	B3 Ib	14590	2.15	16	7.09	7.59 ± 0.33	7.98 ± 0.49	6.60 ± 0.23	6.81 ± 0.23	6.82 ± 0.46		6.70 ± 0.24
NGC330-003	B2 Ib	17210	2.25	20	7.25	7.69 ± 0.19	8.07 ± 0.34	6.79 ± 0.27	6.82 ± 0.25	6.81 ± 0.39		6.87 ± 0.22
NGC330-004	B2.5 Ib	17000	2.30	16	6.84	7.83 ± 0.14	7.86 ± 0.32	6.73 ± 0.21	6.76 ± 0.21	6.82 ± 0.39		6.83 ± 0.14
NGC330-005	B5 Ib	13700	2.25	8	6.77	7.49 ± 0.37	7.82 ± 0.45	6.58 ± 0.19	6.76 ± 0.23	6.81 ± 0.43		
NGC330-009	B5 Ib	13940	2.45	6	7.05	7.20 ± 0.41	8.30 ± 0.53	6.66 ± 0.31	6.80 ± 0.33	6.81 ± 0.49		
NGC330-010	B5 Ib	14820	2.60	4	7.17	7.14 ± 0.35	7.71 ± 0.43	6.63 ± 0.21	6.81 ± 0.30	6.84 ± 0.43		
NGC330-014	B1.5 Ib	20130	2.75	18	6.94	7.53 ± 0.13	8.11 ± 0.24	6.72 ± 0.21		6.83 ± 0.29	6.83 ± 0.52	
NGC330-016	B5: II	14220	2.60	5	7.36	7.18 ± 0.37	8.07 ± 0.51	6.69 ± 0.21	6.80 ± 0.31	6.81 ± 0.47		
NGC330-017	B2 II	22000	3.35	<0	7.07	7.12 ± 0.12	7.64 ± 0.25	6.47 ± 0.17		6.74 ± 0.33		6.90 ± 0.21
NGC330-018	B3 II	18000	2.95	5	7.17	7.24 ± 0.26	8.05 ± 0.37	6.61 ± 0.18	6.74 ± 0.18	6.80 ± 0.36		7.14 ± 0.21
NGC330-020	B3 II	16720	2.85	5	7.05	7.01 ± 0.44	7.80 ± 0.59	6.64 ± 0.28	6.82 ± 0.31	6.83 ± 0.57		
NGC330-022	B3 II	18860	3.00	1	7.14	7.29 ± 0.25	7.76 ± 0.39	6.85 ± 0.17	6.82 ± 0.20	6.83 ± 0.39		
NGC330-026	B2.5 II	22500	3.40	<0	7.30	7.23 ± 0.19	7.74 ± 0.30	7.02 ± 0.23		6.64 ± 0.39		
NGC330-027	B1 V	22040	3.20	7	7.13	7.40 ± 0.21	8.27 ± 0.43	6.44 ± 0.21		6.81 ± 0.36	6.82 ± 0.78	
NGC330-032	B0.5 V	29700	4.15	<0	7.16	7.37 ± 0.10	7.90 ± 0.07	6.80 ± 0.20		6.77 ± 0.19	6.77 ± 0.45	
NGC330-042	B2 II	25450	3.75	1	7.04	7.20 ± 0.05	7.73 ± 0.15	6.88 ± 0.18		6.82 ± 0.34	6.83 ± 0.52	
NGC330-047	B1 V	26700	4.05	0	7.20	6.76 ± 0.11	8.07 ± 0.13	6.57 ± 0.15		6.83 ± 0.23	6.84 ± 0.46	
NGC330-074	B0 V	32020	4.20	4	7.29	7.45 ± 0.19	7.87 ± 0.17	6.81 ± 0.18		6.83 ± 0.25	6.83 ± 0.47	
NGC330-114	B2 III	23800	3.90	4	7.23	7.32 ± 0.18	8.00 ± 0.27	6.97 ± 0.22		6.83 ± 0.32		
NGC330-124	B0.2 V	30980	4.25	2	7.55	7.36 ± 0.25	7.75 ± 0.17	6.75 ± 0.18		6.84 ± 0.23	6.84 ± 0.47	

Indeed from theoretical calculations involving 10,000 configurations the ratio of these two lines is found to be 0.69-0.70 (private comm.: A. Hibbert, Queen's University Belfast). However, from the observations of these stars we would require a ratio of 0.89 for these gf-values, to obtain consistent abundances from this multiplet. It is beyond the scope of this paper but this discrepancy clearly merits further investigation of the oscillator strengths in the future. In estimating the effective temperatures of these stars we have simply taken the mean of the two lines to represent the Si abundance as determined from the Si II spectrum.

Iron lines from Fe III at 4419 and 4430 Å have been detected in many of our targets, particularly in the more metal rich environs of the LMC and Milky Way Clusters. Unfortunately, whilst the Fe model atom is included in TLUSTY, apart from the ground level the higher energy states are bundled into superlevels to simplify and speed up the calculations. As a result it is difficult to isolate the levels associated with these transitions, and hence their departure coefficients. It was therefore necessary to calculate the abundances in LTE, as Thompson et al. (2007) have shown that non-LTE effects appear to be small.

In the Galactic clusters the Fe abundances from the higher gravity objects (log g > 3.3 dex), are higher in comparison to the lower gravity targets. For example, in NGC3293 the mean of the Fe abundance is 7.27 dex from the 3 stars with log g < 3.3 dex, whereas the mean is 7.62 dex from the 3 stars with log g > 3.3 dex. The weighted mean of this cluster is 7.49 dex and is reasonable for the Galaxy, yet clearly there is a large spread amongst the objects, which could be due to the microturbulences adopted. In addition to the objects analysed for this paper we have estimated the Fe abundances for a number of the objects from Paper IV (see Table B.1 & 9).

6. Discussion

6.1. Cluster Metallicities

In the following discussion we will compare the abundances derived for the older clusters analysed here with the younger clusters presented in Paper IV. In addition we will discuss all these results in relation to those available in the literature. The mean abundances for each cluster are presented in Table 9, and are based on the results presented in Table 6 weighted by their degree of uncertainty. Carbon has been omitted from Table 9 due to the uncertainties in the absolute abundances as discussed in Sect. 5.3. Objects for which the median silicon abundance of the cluster could not be reproduced, were omitted from the calculation of the mean cluster abundance (*i.e.* those objects with $\xi_{ave} < 0$). The abundances of the young clusters (NGC6611, N11 & NGC346) were taken from Paper IV except for the Fe abundances which were calculated in LTE using the methods described in Sect. 5.3.

6.1.1. Galactic Clusters: NGC3293, NGC4755, NGC6611

The α-processed elements, Mg & Si, and the heavier Fe nuclei provide good estimates of the metallicity of a cluster as they should be unaffected by any nuclear processes in the cores of these relatively young stars. As discussed above the Si results are sensitive to the atmospheric parameters, but nevertheless the mean Si abundances of the three clusters are in very good agreement as are those for Mg. In comparison to the solar composition from Asplund et al. (2005) these B-type star estimates are approximately 0.3 and 0.1 dex lower for Mg and Si.

Table 7. Comparison of NGC2004 analyses in this Paper with that from Korn et al. (2000, K00). In K00, NGC2004-022 is labeled with the Robertson (1974) identification - B30. K00 use LTE model atmospheres with NLTE line formations. Abundances are presented as [X]=12 + log([X/H]) in units of dex.

	NGC2004-022	
	This Paper	K00
$T_{\rm eff}$(K)	21780	23450
log g(cms^{-2})	3.15	3.45
ξ(kms^{-1})	11	14
C	7.32	7.60:
N	7.68 ± 0.11	7.50 ± 0.20
O	8.55 ± 0.27	8.35 ± 0.20
Mg	6.94 ± 0.19	7.00 ± 0.30
Si	7.23 ± 0.58	6.90 ± 0.20
Fe	7.00 ± 0.22	7.08 ± 0.30

Indeed solar abundances suggest that the Mg to Si ratio is almost 1:1 (Asplund et al. 2005, and references therein), but the B-type star results suggest something closer to 0.69:1. As discussed in Sect. 5.3, there is a large spread in Fe abundances within a cluster and between the Galactic clusters, although the mean Fe abundances from each cluster agree within the uncertainties, and with the solar estimate.

In Paper IV, we found that the oxygen abundances of NGC6611 were in very good agreement with those determined from H II regions. Yet both the stellar and H II regions whilst agreeing within the errors, were approximately 0.1 dex lower than the solar abundances from Asplund et al.. The oxygen abundances from the two older clusters are 8.73 dex, approximately 0.2 dex higher than those in NGC6611. As these two clusters are situated in the Carina arm of the Milky Way, it would be conceivable that the NGC6611 cluster has a different composition to these clusters. However the good agreement of the Si & Mg abundances would not support this. There are 3 objects with particularly high oxygen abundance in NGC4755 (#006, #040, & #048). The latter two objects have a very weak oxygen spectrum, whilst the oxygen abundance in #006 is very sensitive to the adopted microturbulence. Omitting these three objects would lower the mean abundance of NGC4755 to 8.66 dex, in better agreement with the solar abundance. It is therefore more likely that the difference is due to an artifact of the small number of objects per cluster, and the scatter from object to object, rather than a real metallicity difference between these clusters and their environments.

An LTE analysis of B-type stars in these three clusters by Rolleston et al. (2000), shows very good agreement in the oxygen abundances between these clusters. Besides the work by Rolleston et al., a number of the objects in NGC3293 and NGC4755 have been analysed by Mathys et al. (2002). However there are significant differences in the techniques used to determine the parameters in this work as they use Strömgren photometry to determine the atmospheric parameters. Whilst the microturbulences agree well in all the objects, for the hotter objects the $T_{\rm eff}$ and log g values differ significantly. This maybe a result of the insensitivity of the Strömgren colour index at high temperatures. Due to the large differences between these analyses we have not attempted any further comparisons.

Table 8. Comparison of NGC330 analyses in this Paper with those from Lennon et al. (2003, L03), and Korn et al. (2000, K00). In L03 and K00, NGC330-002,-004 and -018 are labeled with Robertson (1974) identifications, which are A02, B37 and B30. Fe has been omitted from this comparison as the other analyses did not consider this element. Abundances are presented as [X]=12 + log([X/H]) in units of dex.

	NGC330-002		NGC330-004		NGC330-018	
	This Paper	L03	This Paper	L03	This Paper	K00
$T_{\rm eff}$(K)	14590	16000	17000	18000	18000	16950
log g(cms^{-2})	2.15	2.30	2.30	2.40	2.95	2.77
ξ(kms^{-1})	16	8	16	10	5	6
C	7.09	6.91	6.84	6.71	7.17	7.30:
N	7.59 ± 0.33	7.71	7.83 ± 0.14	7.89	7.24 ± 0.26	
O	7.98 ± 0.49	8.14	7.86 ± 0.32	7.98	8.05 ± 0.37	8.25 ± 0.30
Mg	6.60 ± 0.23	6.69	6.73 ± 0.21	6.79	6.61 ± 0.18	6.85 ± 0.40
Si	6.82 ± 0.46	6.82	6.82 ± 0.39	7.12	6.80 ± 0.36	6.82 ± 0.30

Table 9. Weighted average abundances of the FLAMES clusters. Results for the clusters NGC6611, N11 & NGC346 are taken from Paper III, except for the Fe abundances which were derived from LTE calculations following the method described in Sect. 5.3. Solar abundances are taken from Asplund et al. (2005). Abundances are presented as [X]=12 + log([X/H]) in units of dex.

		Milky Way			LMC		SMC	
	Solar	NGC6611	NGC3293	NGC4755	N11	NGC2004	NGC346	NGC330
N	7.78 ± 0.06	7.59 ± 0.10	7.52 ± 0.07	7.85 ± 0.26	7.54 ± 0.40	7.33 ± 0.36	7.17 ± 0.29	7.27 ± 0.24
O	8.66 ± 0.05	8.55 ± 0.04	8.76 ± 0.05	8.73 ± 0.18	8.33 ± 0.08	8.40 ± 0.18	8.06 ± 0.10	7.90 ± 0.19
Mg	7.53 ± 0.09	7.32 ± 0.06	7.24 ± 0.10	7.23 ± 0.12	7.06 ± 0.09	7.08 ± 0.10	6.74 ± 0.07	6.72 ± 0.12
Si	7.51 ± 0.04	7.41 ± 0.05	7.47 ± 0.06	7.41 ± 0.04	7.19 ± 0.07	7.21 ± 0.03	6.79 ± 0.05	6.81 ± 0.02
Fe	7.45 ± 0.15	7.62 ± 0.15	7.49 ± 0.21	7.56 ± 0.19	7.23 ± 0.10	7.24 ± 0.12	6.98 ± 0.13	6.88 ± 0.16

6.1.2. LMC clusters: NGC2004, N11

From a literature search we found only one object in NGC2004 which had been analysed previously, (#022), by Korn et al. (2000) using LTE model atmospheres and non-LTE line formations. The comparison of their results with ours is shown in Table 7. Whilst there are significant differences in the derived atmospheric parameters, the abundances agree well within the errors, particularly the Fe & Mg abundances. A comparison of the silicon equivalent widths (A. Korn, private communication) show very good agreement for the Si III lines, although the Si IV 4116 Å line is weaker in the UVES data of Korn et al., than in our spectrum. This however would not explain the effective temperature difference of $\sim$ 1700K between the two analyses and would in fact require that the estimated temperatures of Korn et al. should be lower. We conclude that there is a significant difference in the fitting to the Balmer lines to determine the surface gravity, being 0.2 dex higher in the analysis by Korn et al. and this would lead to the higher $T_{\rm eff}$. Such a high gravity does not seem appropriate from the FLAMES data. There is also a difference in the adopted microturbulence which may explain some of the discrepancies in the abundances. Using the Si III equivalent widths provided by Korn et al. however we reproduce the value of 11 kms^{-1} as obtained from the FLAMES data.

Apart from the nitrogen abundances, the mean abundances in the two LMC clusters are in excellent agreement.

6.1.3. SMC Clusters: NGC330, NGC346

The mean elemental abundances of NGC330 presented here are in very good agreement, within the errors, with those derived for NGC346 in Paper IV. The O & Fe abundances in NGC346 are 0.10 & 0.16 dex higher than those in NGC330, but this is within the uncertainties and the excellent agreement between the magnesium and silicon abundances suggest it is insignificant.

Three of our targets have been analysed previously, NGC330-002, NGC330-004 and NGC330-018. The former two were analysed by Lennon et al. (2003) using LTE model atmospheres and making some non-LTE corrections to the abundances. Their estimated effective temperatures are hotter in both cases, whilst the microturbulences are lower (see Table 8), these differences are mainly due to the different analysis techniques. In particular, they use oxygen lines to determine the microturbulence and flux distributions to determine the effective temperature. Nevertheless, the abundances are in good agreement. NGC330-018 was analysed by Korn et al. and again, whilst quite different techniques and model atmospheres were applied, there is good agreement in the abundances.

6.2. Evolution of Nitrogen Abundances.

Photospheric nitrogen abundances of B-type stars are known to be good tracers of their evolution due to the wide range of abundances that have been estimated from their spectra, as evident from Table 6. Whilst it is clear that nitrogen can be produced in the core of these stars via the CNO cycle, the mechanism for transferring this nitrogen enriched material to the surface is still

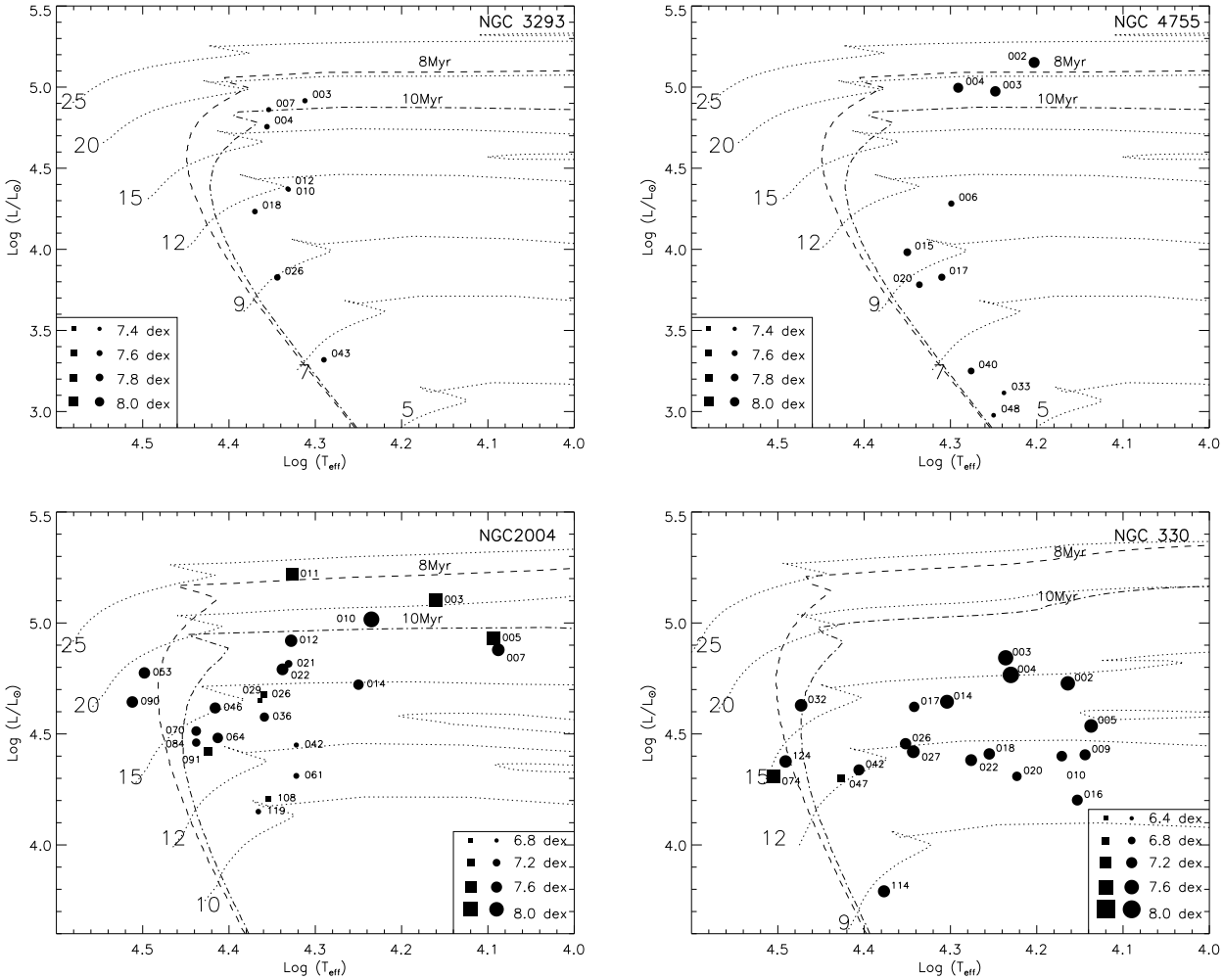

Fig. 2. Hertzsprung-Russell Diagrams of NGC3293, NGC4755, NGC2004 & NGC330 objects. Binaries are represented by squares, and single stars by solid circles. The nitrogen abundances in the stars are represented by the size of the symbols, as per the key in each diagram (*i.e.* the larger the symbol the more nitrogen at the surface of the star). The evolutionary tracks are shown as dotted lines and represent the non-rotating tracks from Meynet et al. (1994) and Schaller et al. (1992) for the Milky Way clusters, and Schaerer et al. (1993) and Charbonnel et al. (1993) for NGC2004 and NGC330, respectively. Isochrones are presented as dashed lines, but in the case of the Magellanic cloud HRDs they should be considered to be illustrative only (see Sect. 6.2).

under debate. In this section we will discuss the nitrogen abundances of these stars in terms of their evolution in an attempt to decipher the correlation of nitrogen with surface gravity and mass.

The targets from each field are shown on separate Hertzsprung-Russell diagrams (HRD) in Fig. 2, with the relative sizes of the symbols representing the degree of nitrogen in their atmospheres. The evolutionary tracks included are non-rotating tracks from Meynet et al. (1994) and Schaller et al. (1992) for the Milky Way clusters, and Schaerer et al. (1993) and Charbonnel et al. (1993) for NGC2004 and NGC330, respectively. Isochrones are also presented, but in the case of the Magellanic cloud HRD's they should be used for information only. The majority of the stars in these two sets of Magellanic Cloud FLAMES observations are expected to be field stars (the compactness of the clusters caused difficulties in putting fibres on objects close to their centre, see discussion in Paper II). On the contrary, amongst the Galactic objects only one star is thought to be a non-cluster member, this is NGC4755-033 (see Paper III).

It is important to note that these are intermediate age clusters or in the case of the Magellanic clouds, fields around such clusters and hence these objects are relatively low mass and can only be compared to the similarly low mass stars analysed in Paper IV. This can be seen in Fig. 2 where all but two objects, NGC4755-002 and NGC2004-011, lie below or on the 20 solar mass track. Meynet & Maeder (2000) and Maeder & Meynet (2001) have shown that mass-loss becomes an important factor in the evolution of stars with initial solar masses greater than 20 to 25 $M_{\odot}$, particularly for the evolution of the surface rotational velocities and angular momentum. We therefore exclude NGC4755-002 and NGC2004-011 from most of the following discussions and assume that mass-loss does not play an important role in the evolution of the surface nitrogen abundances of these stars.

From Fig. 2, it is immediately clear that the more massive and evolved objects have the larger absolute nitrogen abun-

dances. This has been discussed by Meynet & Maeder (2000), who showed that the surface nitrogen enrichments are more pronounced as the stellar mass is increased in their models. The HRDs of the Galactic clusters show that there is little variation in the nitrogen abundances of these objects, except for the three most massive and evolved objects in NGC4755 (#002, #003, & #004).

In Fig. 3 the absolute nitrogen abundances are shown as a function of the stellar surface gravity for each cluster, hence the main-sequence objects are to the right of the plot at high surface gravities and tend towards the more evolved objects at low values of log g. The baseline nitrogen abundances of the Galaxy, LMC and SMC are marked on these plots as adopted from H II region analyses (see Paper IV and references therein). The Galactic nitrogen abundance as estimated from H II regions is higher than the mean nitrogen abundances in these clusters. As can be seen from Fig. 3, the majority of Galactic objects have absolute nitrogen abundances below this baseline value. Omitting the three low gravity objects with log [N/H] > 8.0 dex (NGC4755-002,-003,-004) the mean nitrogen abundance from the three clusters is 7.58 dex, whereas that from H II regions is approx 7.64 dex, which is consistent within the errors of the analysis.

The NGC2004 & NGC330 objects span a very large range of nitrogen abundances, even if we exclude the supergiant objects. In NGC2004 the luminosity class V-II objects span a range of nitrogen abundances from the baseline LMC abundance to approximately 7.65 dex, whilst similar objects in NGC330 span a range from 6.75 dex (0.15 dex above baseline SMC abundances) to approx. 7.45 dex. We do not find many "normal" N abundance objects in NGC330 and indeed there is only one object (#47) with a nitrogen abundance in the range of 6.5 to 7 dex. However there are very few unevolved objects in our NGC330 sample, as can be seen from Fig. 2.

In the right panel of Fig. 3 we compare our results with those from Paper IV for the objects with masses less than 20 $M_{\odot}$. The LMC and Galactic objects from the young clusters analysed in Paper IV and the relatively older clusters studied here have the same range of abundances. In the SMC, the young cluster NGC346 has more objects than NGC330 with abundances close to the SMC baseline N abundance due to the larger sample of unevolved objects. The range of abundances for the relatively unevolved objects in the Magellanic clouds could be explained by the stellar sample having a range of initial rotational velocities. Hence if rotation is the dominant factor in producing the surface nitrogen enrichment one would expect a range in the nitrogen abundances. However, as stated in Paper IV and reconfirmed here, at least for the Magellanic Clouds, large nitrogen enrichment occurs for the stars close to the zero-age main-sequence. Additionally the nitrogen excesses for the luminosity class V-II objects in the Magellanic Clouds would results in an increase of a factor of two or less for the baseline Galactic nitrogen abundance, which is consistent with our results but indistinguishable from our uncertainties.

The majority of our supergiant or luminosity class I objects have higher surface nitrogen enrichments than seen in the dwarf or giant objects. In Fig. 4 we present histograms of the nitrogen abundances, separating the targets from each galaxy into a group of dwarfs and another of giants and supergiants. In the left panels of Fig. 4 are histograms which only include the objects analysed in this paper, it is clear from these that the more evolved objects have higher nitrogen abundances. As the histograms for these intermediate aged stars agree well with those presented in Paper IV for the younger objects in the survey, we present histograms of the complete sample of low $v \sin i$ objects in the right hand-side panel of Fig. 4. Whilst the giant/supergiant samples have objects with a similar range of surface nitrogen abundances as the dwarf objects, they also have a number of objects with higher nitrogen abundances. These latter objects are normally the more luminous supergiants, however not all the supergiants have highly nitrogen enriched atmospheres as a number of the Ib supergiants have abundances similar to the giant and dwarf objects (see Fig. 3). These low nitrogen abundances can again be accounted for by the objects evolving from a population of stars with a range of initial rotational velocities.

Our observations indicate that there are quite significant nitrogen enhancements during the supergiant phase in all three galaxies. The SMC evolutionary models from the Geneva group (Meynet & Maeder 2000; Maeder & Meynet 2001) show that between the end of the main sequence and the red supergiant phase at $\log(T_{\rm eff}) = 3.9$, there is a low level of nitrogen enrichment for 15-25 $M_{\odot}$ stars of approx 0.1 dex in the SMC. Lower mass objects that go through even a partial blue-loop show more significant nitrogen enrichments (see Fig.16 of Maeder & Meynet, 2001). However these N excesses are not produced in the Galactic models for stars crossing the HR diagram. Hence it is unclear if the unevolved Galactic objects exhibit surface nitrogen enrichments or the scatter in their abundances is simply a result of the uncertainties in the analysis.

In paper IV two distinct populations of radial velocity variable objects were found, (1) a group of unevolved objects with normal nitrogen abundances and (2) a group of evolved objects with large surface nitrogen enrichments. In this work we have discovered a number of objects which also fall into these two categories, as can be seen in Fig. 3. The first group are conceivably binary objects with low initial rotational velocities and hence have small or negligible surface nitrogen enrichments. The small rotational velocities may arise from tidal locking with the orbital velocity of the system within the main-sequence lifetime of the primary, thus slowing down these objects (Zahn 1992; Huang & Gies 2006). There are two unevolved objects that don't fall into these categories, these are N11-075 and NGC330-074 both of which have reasonably high nitrogen abundances. The second group of objects are all luminous objects, most of which have very small radial velocity variations of < 5 kms^{-1}. However further observations are required to determine if these objects are true binary systems. If these objects are in binary systems, the nitrogen excesses we are observing could suggest that they have gone through a mass-transfer process. That said, the nitrogen abundances are similar to other luminous objects for which we have not detected any radial velocity variations and may not necessarily be connected to binarity.

6.3. Effective Temperatures Scales.

Effective temperature scales of OB-type stars as a function of spectral type are important for determining their properties, such as luminosities and the number of ionising photons. In turn, these stellar properties are crucial for many topics in astrophysics; for comparisons with stellar evolution models, determining cluster properties such as age and distance and for understanding the properties of ionising stars. Due to most of their flux being emitted in the far-UV, the effective temperatures of OB-type stars can only be determined using indirect techniques involving the complex modelling of their atmospheres. These sophisticated model atmospheres need to take into account non-LTE effects, line blanketing and in some cases stellar wind effects. In recent years several revisions have been made to O and B-type star temperature scales in particular due to the inclusion of

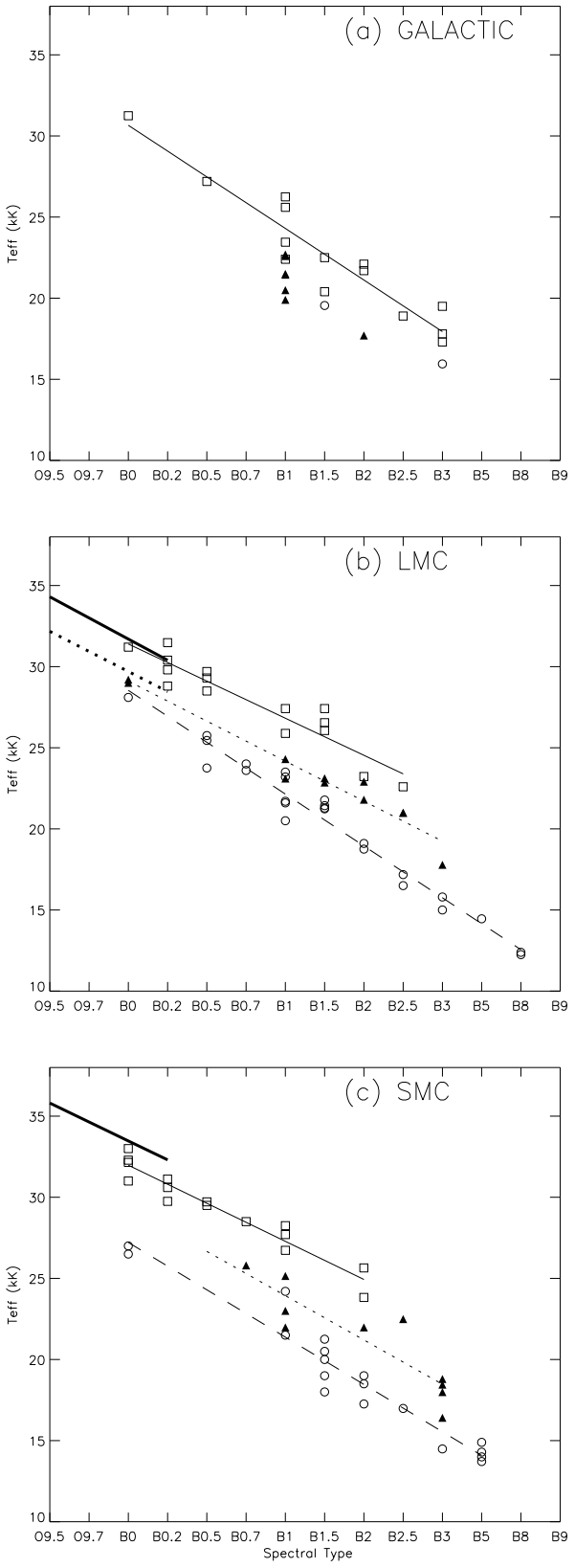

Fig. 5. Temperature Scales based on 107 B-type stars from the Flames Survey of 7 clusters; NGC6611, NGC3293, NGC4755, N11, NGC2004, NGC346 and NGC330. Also included are 9 SMC stars from Dufton et al. (2005). Comparison of the temperature scales as a function of **luminosity class** in the three galaxies (a) Milky Way, (b) LMC, (c) SMC. The thin lines are fits to the mean at each spectral type for the B-type stars and the thick lines are fits to the O star data presented in Mokiem et al. (2006, 2007). The different classes are identified by: V - open squares & solid line; III - filled triangles & dotted line; I - open

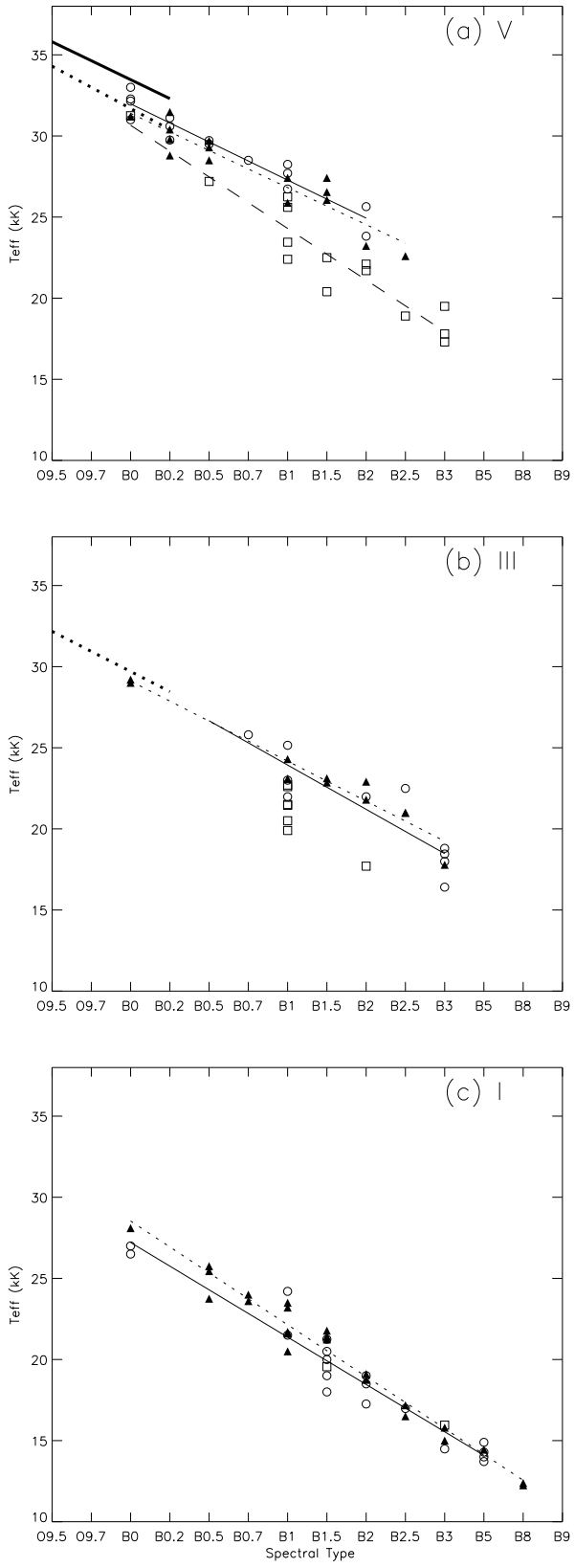

Fig. 6. Temperature Scales based on 107 B-type stars from the Flames Survey of 7 clusters; NGC6611, NGC3293, NGC4755, N11, NGC2004, NGC346 and NGC330. Also included are 9 SMC stars from Dufton et al. (2005). Comparison of the temperature scales as a function of **metallicity** for the three luminosity classes (a) V , (b) III and (c) I objects. The thin lines are fits to the mean at each spectral type for the B-type stars and the thick line are fits to the O star data presented in Mokiem et al. (2006, 2007). The open circles & solid lines, filled triangles & dotted lines and open squares & dashed lines represent the SMC, LMC

line blanketing and non-LTE effects in the model atmospheres (Martins et al. 2002; Crowther et al. 2002, 2006; Massey et al. 2004, 2005). These have revealed clear differences in the temperature scales depending on luminosity class and metallicity. In Paper III, the temperatures of 49 B-type stars in the spectral range of O9.5 to B2 were presented. The best sampled luminosity group in that work was the main sequence objects for which a clear difference in the temperature scales with metallicity was shown for the SMC and Galaxy, where the latter was cooler. Here we present the effective temperature scales based on the consistent analysis of 107 B-type stars studied in the Galaxy, LMC and SMC from the FLAMES dataset (60 from this paper and 47 from Paper IV, thus excluding O9 stars). In addition we have included nine supergiants from the work of Dufton et al. (2005), bringing the total to 116. Dufton et al. applied the same analysis techniques and so their results should be consistent with those presented here.

Firstly, the objects need to be separated into different luminosity classes. This is, in theory, easily done by adopting the luminosity classes assigned to the objects in Paper I & II based on the widths of the high order hydrogen Balmer lines. A small number of objects have atmospheric parameters that are inconsistent with their assigned classifications. This reflects the uncertainties of precise classification (e.g. with respect to rotation) and also the continuous nature of the physical gravities when compared to the discrete luminosity classes. For the purposes of investigating physical trends we have therefore reassigned some of the objects. Any luminosity class III objects with high gravities (> 3.7) were grouped with the class V objects, whilst any luminosity class V stars with low surface gravities (< 3.7) were grouped with the luminosity class III objects. The luminosity class II objects, as assigned in Paper I & II, were assigned to the luminosity class III or I scales depending on their surface gravity. Apart from the luminosity class II objects, this affected only 4 objects in the SMC: NGC346-039, NGC330-027, -042, -114, the former two having very high gravities for giants, and the latter two having too low gravities for dwarfs. In the LMC, 5 objects were affected; NGC2004-014, -046, -064, -119 having higher gravities than those expected for a giant, whereas N11-037 has a lower gravity and was included with the supergiants.

In Fig. 5 the effective temperatures of our sample are plotted as a function of spectral type for the Galaxy, LMC and SMC, where the luminosity classes are identified with different symbols. For the LMC and SMC, there is a clear separation of temperature scales depending on the luminosity class of the objects; the more luminous the object the cooler it is. From B0 to B2.5 the effective temperatures of the dwarfs are higher than those of the giants by $\sim$ 2300-3000 K in the LMC and $\sim$ 3100-3700 K in the SMC, whereas the supergiants are cooler than the giants by $\sim$ 550-3000 K in the LMC and $\sim$ 1600-2650 K in the SMC. For the Galactic sample there is insufficient sampling of luminosity classes III or I to characterize this separation, although the luminosity class V objects are clearly the hottest objects. The fact that the more evolved giants and supergiants are progressively cooler than the dwarfs is as expected since the former two classes are more evolved objects with lower gravities and hence require lower temperatures to fit the silicon ionisation equilibrium.

In the SMC and LMC plots we also show fits to the O-type star data, presented in Mokiem et al. (2006, 2007), for the different luminosity classes and which are based on all the data in the O3-B0.2 range. The sample size only allows a good fit to the dwarf and giant objects in the LMC and the dwarf objects in the SMC. There appears to be good agreement (within 500-700 K) in the crossover region from O to B-type stars (i.e O9-B0.2) for the dwarf and giant $T_{\rm eff}$ scales in the LMC. However, in the SMC, the O star dwarf scale is approximately 1500 K hotter than for the B-type star dwarf scale at B0 where the two scales cross. Mokiem et al. (2006) have analysed two B0 stars with FASTWIND, the $T_{\rm eff}$ of one agreeing well with the mean of the four B0 objects analysed with TLUSTY, the other however has a $T_{\rm eff}$ of 34400, 2300 K higher than derived with TLUSTY. However, the error on the $T_{\rm eff}$ estimation of this object is 2200 K. In addition the slope of the fit to the mean of the O-type stars is affected by the low $T_{\rm eff}$ of two O4 stars, omitting these objects would make the agreement at the crossover much better, and well within the uncertainties in the $T_{\rm eff}$ estimations. Martins et al. (2005) have produced observational effective temperature scales for Galactic O-type stars and their O9.5 dwarf point on the observational scale appears to be in good agreement, as it is 1200 K hotter than the B0 point on our scale.

In Fig. 6 the $T_{\rm eff}$ scale from each luminosity class is considered as a function of metallicity. In the case of the dwarf objects the SMC stars are substantially hotter than the Galactic stars ($\sim$ 1300 at B0 to 4000 K at B2), as expected due to the increased line blanketing in the more metal rich Galactic objects. Surprisingly, there is no apparent metallicity dependence on the $T_{\rm eff}$ between the SMC and LMC objects, with all luminosity classes showing a close agreement between the LMC and SMC objects. The largest difference is in the dwarf objects where the SMC stars are hotter by $\sim$ 800 K at B0 to 100 K at B2.

The analysis in this paper and Paper IV has provided an unprecedented, large and consistent set of atmospheric parameters based on non-LTE and line-blanketed model atmospheres. As such it is important to provide an up-to-date calibration of effective temperatures with spectral type. Using the linear fits to the mean at each spectral type we present the results in Table 10. This table is based on 116 objects analysed between B0-B8 in this paper, Paper IV and Dufton et al. (2005). Whilst we have chosen to present the LMC and SMC scales separately the reader should note the close agreement between these, particularly in the case of the luminosity class III and I objects.

7. Conclusions

In this paper we have completed a spectral analysis of 61 B-type stars, located in four fields; two centered on the Galactic clusters, NGC3293 & NGC4755, in the Carina arm, one centered on NGC2004 in the Large Magellanic cloud and the fourth centered on NGC330 in the Small Magellanic cloud. We have presented both their atmospheric parameters and abundances (C, N, O, Mg, Si) estimated using non-LTE line-blanketed TLUSTY model atmospheres. In addition we have calculated the LTE iron abundances for these objects plus 17 objects from Paper IV located in three fields toward the younger clusters observed within the FLAMES project for massive stars; NGC6611, N11, NGC346. In paper IV we presented the present day chemical composition of the LMC and SMC, these results are verified here and can now be extended to include the Fe abundances for these galaxies. In the LMC we derive an Fe abundance of 7.23 dex, and in the SMC 6.93 dex, this can be compared with that derived from the Galactic B-type stars, 7.53 dex, suggesting that the LMC is a factor of 2 less abundant than the Galaxy and the SMC is a factor of factor of 4 less abundant.

We have studied the nitrogen abundances of the 107 low $v \sin i$ B-type stars within the FLAMES survey of massive stars, and discussed them in terms of their evolution. We have observed a large range of nitrogen abundances in the LMC and SMC main-sequence objects which is likely to reflect the range

Table 10. Effective temperature scales of B-type stars in the Milky Way, LMC and SMC for different luminosity classes. These scales are based on parameters presented in this Paper and Paper IV, as well as a number of SMC stars from Dufton et al. (2005). The values in parenthesis are those for which we have no objects in the spectral type bin but for which we could interpolate. The $T_{\rm eff}$ values are presented in units of K.

	Milky Way		LMC		SMC		
Sp. Typ.	V	I	III	V	I	III	V
B0	30650	28550	29100	31400	27200		32000
B0.2	[29050]	[26950]	[27850]	30250	[25750]		30800
B0.5	27500	25350	[26650]	29100	[24300]		29650
B0.7	[25900]	23750	[25400]	[27950]	[22850]	25300	28450
B1	24300	22150	24150	26800	22350	23950	27300
B1.5	22700	20550	22950	25700	20650	[22550]	[26100]
B2	22100	18950	21700	24550	18950	21200	24950
B2.5	19550	17350	20450	23400	17200	19850	
B3	17950	15750	19250		15500	18450	
B5		14150			13800		
B8		12550					

of rotational velocities, and hence rotational-mixing, initially present in these stars. Whilst mass-loss may play some role in the evolution of these stars, the stars considered in this work have masses less than 20 $M_{\odot}$ masses and it is unlikely that it has a dominant role in altering their surface abundances. This is not the case for higher mass objects considered in Paper IV. The large spread of nitrogen abundances seen in the LMC and SMC main-sequence objects does not seem to be present in the Galactic objects but if we assume that these Galactic stars should undergo the same degree of enrichment as the LMC and SMC, a simple calculation shows that this would amount to only a factor of two or 0.30 dex enhancement of nitrogen in the Galaxy. This is similar to our degree of uncertainty so it is unclear if we are observing the scatter due to our uncertainties or the range of rotational velocities of this population of stars. The supergiants in the sample are significantly more enriched than their main-sequence counterparts, and hence there must be some method of enhancing the photospheric nitrogen abundance as the star evolves off the main-sequence and across the HRD. Models of single stars in the SMC (Meynet & Maeder 2000; Maeder & Meynet 2001), do not predict such large degrees of nitrogen enrichments and would require more efficient mixing mechanisms to match these observations.

Two populations of binary objects were identified in Paper IV and in this paper we have detected additional objects belonging to these groups; (1) unevolved, 'normal' nitrogen stars (2) evolved, nitrogen-rich stars. The former group have significant radial velocity variations, whilst the evolved objects have very small shifts which require verification by observations over multiple epochs. Binary evolution can be invoked to explain these two groups of objects using tidal locking to the orbital velocity to suppress nitrogen excesses in the first group, and mass-transfer to enhance the nitrogen in the more evolved objects, although the abundances observed in these objects are similar to those in the supposedly single stars. Clearly further observations of these objects are required to disentangle the binary objects from the single stars and to study the evolution of nitrogen abundances in these populations separately.

The results presented here and in Paper IV provide a consistent analysis of a large sample of Galactic objects, as well as the largest sample of Magellanic Cloud B-type stars studied to date. As a result, we have constructed effective temperature scales as a function of spectral type for B-type stars from B0 down to B8, for each of the galaxies and have shown that they are consistent with effective temperatures from O-type stars. In each of the three metallicity environments we have detected a dependency on luminosity, where the most luminous objects are the coolest. Due to the lower metallicity of the Magellanic Clouds and hence the expected reduction in line-blanketing, one would expect to detect higher temperatures with decreasing metallicity. Whilst we do see that the Galactic dwarf objects are cooler than the Magellanic cloud objects, we do not detect a significant difference in the temperature scales of the SMC and LMC supergiants and giants and the less luminous dwarf objects in the two clouds differ at the most by 600 K. We therefore present the effective temperature calibration of dwarf B-type stars in the Galaxy, LMC and SMC and giant and supergiant calibrations for LMC and SMC objects with the caveat that the latter are very similar.

This work has focused on the low $v \sin i$ population of B-type stars in 7 fields in 3 distinct metallicity environments. However we require knowledge of their high $v \sin i$ counterparts to get a complete picture of the evolution of their surface abundances in terms of their rotational velocities. We also require additional knowledge on whether or not these objects are binary or single stars, to unravel the evolution of these two distinct groups of stars. Future work will focus on these points, to place better constraints on the evolution of massive stars.

Acknowledgments

CT would like to thank A. Hibbert, N. Pryzbilla, M.F. Nieva and J. Eldridge for their insightful discussions on this work. We also acknowledge financial support from the UK Particle Physics and Astronomy Research Council (PPARC). This work, conducted as part of the award "Understanding the lives of massive stars from birth to supernovae" (S.J. Smartt) made under the European Heads of Research Councils and European Science Foundation EURYI (European Young Investigator) Awards scheme, was supported by funds from the Participating Organisations of EURYI and the EC Sixth Framework Programme. SJS also thanks the Leverhulme Trust for funding. We are also grateful to the referee, Dr. P. Bonifacio, for his constructive comments on this work.

Appendix A: Notes on Individual Objects:

NGC4755-005: Revisiting this spectrum we noticed weak absorption features from Si IV 4116/4089 Å and He II 4686 Å, that are inconsistent with the B2 II classification from Paper I. These lines are blue-shifted from their rest wavelengths by 5 $\rm kms^{-1}$, whereas the majority of the absorption lines in the spectrum are red-shifted by 40 $\rm kms^{-1}$. In addition, the metal lines are quite asymmetric and broad. Contrary to the statement in Paper I, this star appears to be a double-lined spectroscopic binary.

NGC4755-011: This object is also a possible double-lined spectroscopic binary. There are clear signs of double features in the Si III multiplet at 4560 Å and the Mg II line at 4481 Å is highly asymmetric.

References

Asplund, M., Grevesse, N., & Sauval, A. J. 2005, in ASP Conf. Ser. 336, Cosmic Abundances as Records of Stellar Evolution and Nucleosynthesis, ed. T.G. Barnes III & F.N. Bash (San Francisco:ASP), 25
Balona, L. A. 1994, MNRAS, 268, 119
Blecha, A., North, P., Royer, F., & Simond, G. 2003, BLDR Software-Reference Manual, 1st edn
Bouchet, P., Lequeux, J., Maurice, E., Prevot, L. & Prevot-Burnichon, M. L. 1985, A&A, 149, 330
Charbonnel, C., Meynet, G., Maeder, A., Schaller, G., & Schaerer, D. 1993, A&AS, 101, 415
Crowther, P. A., Hillier, D. J., Evans, C. J., et al. 2002, ApJ, 579, 774
Crowther, P. A., Lennon, D. J. & Walborn, N. R. 2006, A&A, 446, 279
Dufton, P. L. 1972, A&A, 16,301
Dufton, P. L., Ryans, R. S. I., Trundle, C., et al. 2005, A&A, 434, 1125
Dufton, P. L., Ryans, R. S. I., Simón-Díaz, S., Trundle, C. & Lennon, D.J. 2006, A&A, 451, 603
Dufton, P. L., Smartt, S. J., Lee, J.-K., et al. 2006, A&A, 457, 265, (Paper III)
Evans, C. J., Smartt, S. J., Lee, J.-K., et al. 2005, A&A, 437, 467, (Paper I)
Evans, C. J., Lennon, D. J., Smartt, S. J. & Trundle, C. 2006, A&A, 456, 623, (Paper II)
Gieren, W., Strom, J., Barnes, T. G., et al. 2005, ApJ, 627, 224
Heger, A. & Langer, N. 2000, ApJ, 528, 368
Herrero, A., Kudritzki, R.-P., Vilchez, J. M., Kunze, D., Butler, K., & Haser, S. 1992, A&A, 261, 209
Hilditch, R. W., Howarth, I. D., Harries, T. J. 2005, MNRAS, 357, 304
Howarth, I. D., Murray, J. & Mills, D. 1994, Starlink User Note, No. 50.15
Huang, W. & Gies, D. J. 2006, ApJ, 648, 591
Hubeny, I., Hummer D. G., & Lanz, T. 1994, A&A, 282, 151
Hunter, I., Dufton P. L., Smartt, S. J., et al. 2007, A&A, 466, 277, (Paper IV)
Hunter, I., Dufton P. L., Smartt, S. J., et al. 2007, A&A, in prep, (Paper V)
Jaschek, M., & Jaschek, C. 1967, ApJ, 150, 355
Korn, S. 2004, PASA, 21, 310
Korn, A. J., Becker, S. R., Gummersbach, C. A., et al. 2000, A&A, 353, 655
Korn, A. J., Keller, S. C., Kaufer, A., et al. 2002, A&A, 385, 143
Lennon, D. J. 1997, A&A, 317, 871
Lennon, D. J., Dufton, P. L. & Crowley, C. 2003, A&A, 398, 455
Lennon, D. J., Trundle, C. & Evans, C. J. 2006, ASPC, 353, 41
Maeder, A. & Meynet, G. 2001, A&A, 373, 555
Martayan, C., Frémat, Y., Hubert, A.-M, et al. 2006, A&A, 452, 273
Martins, F., Schaerer, D. & Hillier, D. J. 2002, 382, 999
Martins, F., Schaerer, D. & Hillier, D. J. 2005, 436, 1065
Massey, P., Bresolin, F., Kudritzki, R.-P., Puls, J. & Pauldrach, A. W. A. 2004, ApJ, 608, 1001
Massey, P., Puls, Pauldrach, A. W. A.J., Bresolin, F., Kudritzki, R.-P. & Simon, T. 2005, ApJ, 627, 477
Mathys, G., Andrievsky, S.M., Barbuy, B., Cunha, K. & Korotin, S.A. 2002, A&A, 387, 902
McErlean, N.D., Lennon, D.J., & Charbonnel, P.L. 1998, A&A, 329, 613
Meynet, G., Maeder, A., Schaller, G., Schaerer, D. & Charbonnel, C. 1994, A&AS, 103, 97
Meynet, G. & Maeder, A. 1997, A&A, 361, 159
Meynet, G. & Maeder, A. 2000, A&A, 321, 465
Mokiem, M. R., de Koter, A., Evans, C. J., et al. 2006, A&A, 456, 113
Mokiem, M. R., de Koter, A., Evans, C. J., et al. 2007, A&A, 465, 1003
Nieva, M. F., & Przybilla, N. 2006, ApJ, 639, L39
Nieva, M. F., & Przybilla, N. 2007, in prep
Robertson, J. W. 1974, A&AS, 15, 261
Rolleston, W. R. J., Smartt, S. J., Dufton, P. L. & Ryans, R. S. I. 2000, A&A, 363, 537
Ryans, R. S. I., Dufton, P. L., Rolleston, W. R. J., et al. 2002, MNRAS, 336, 577
Ryans, R. S. I., Dufton, P. L., Mooney, C. J., et al. 2003, A&A, 401, 1119
Sagar, R. & Richtler, T. 1991, A&AS, 90, 387
Schaerer, D., Meynet, G., Maeder, A. & Schaller, G. 1993, A&AS, 98, 523
Schaller, G., Schaerer, D., Meynet, G. & Maeder, A. 1992, A&AS, 96, 269
Simón-Díaz, S. & Herrero, A. 2007, A&A, in press (astroph/0702363)
Simón-Díaz, S., Herrero, A., Esteban, C. & Najarro, F. 2006, A&A, 448,351
Strom, S. E., Wolff, S. C., & Dror, D. H. A. 2005, AJ, 129, 809
Trundle, C., Lennon, D. J., Dufton,P. L., Smartt, S. J. & Urbaneja, M. A. 2002, A&A, 395, 519
Trundle, C., Lennon, D. J., Puls, J. & Dufton, P. L. 2004, A&A, 417, 217
Trundle, C. & Lennon, D. J. 2005, A&A, 434, 677
Thompson, H., Keenan, F. P., & Dufton, D. J., et al. 2007, A&A, in prep
Vacca, W. D., Garmany, C. D. & Shull, M. J. 1996, ApJ, 460, 914
Venn, K. A. 1999, ApJ 518, 405
Vidal, C. R., Cooper, J. & Smith, E.W. 1973, ApJS, 25, 37
Vrancken, M., Lennon, D. J., Dufton,P. L. & Lambert, D. L. 2000, A&A, 358, 639
Walborn, N. R. 1972, ApJ, 77, 312
Wolff, S. C., Strom, S. E., & Dror, D. H. A. 2007, AJ, in press (astroph/0702133)
Zahn, J.-P 1992, A&A, 265, 115

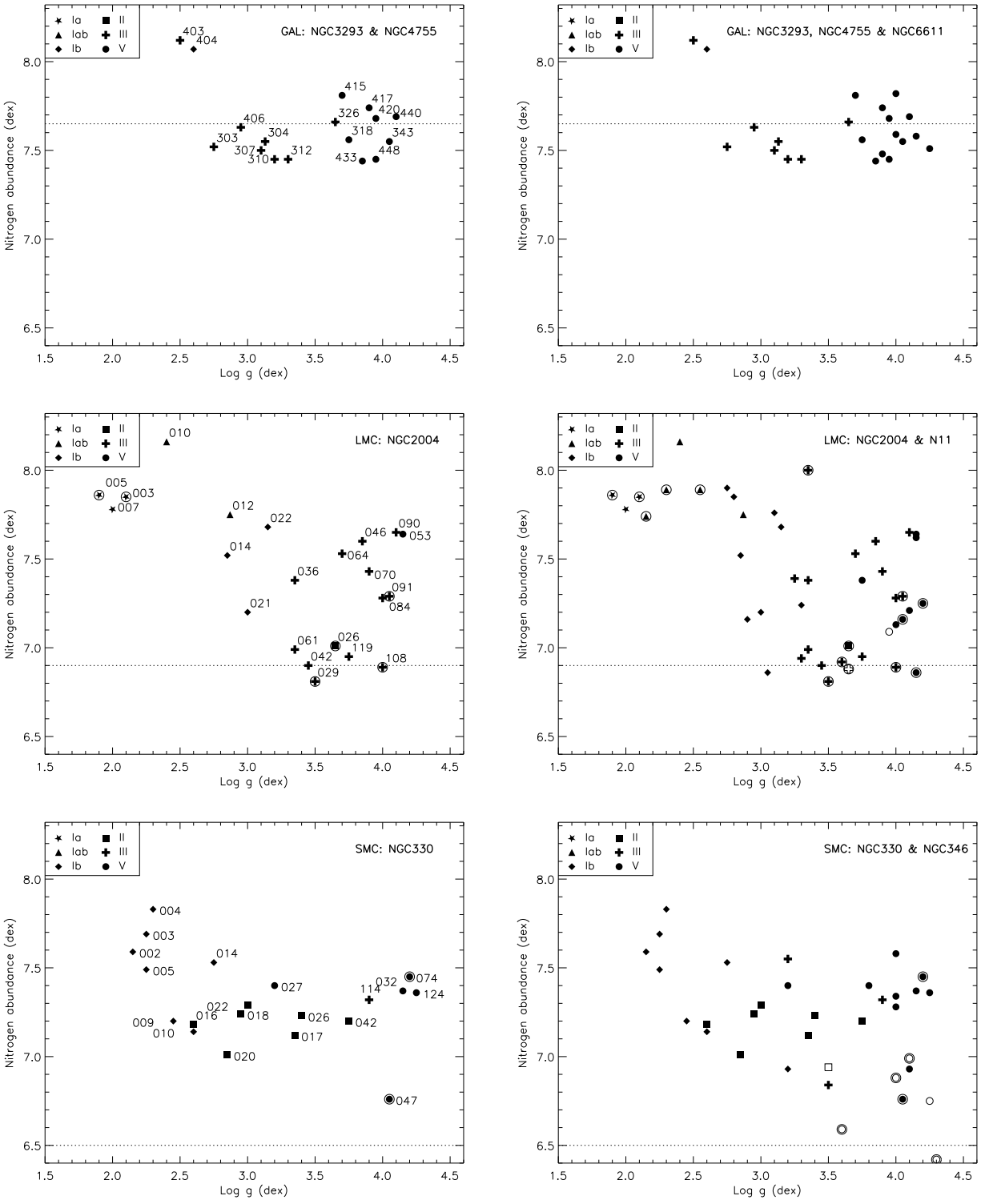

Fig. 3. Nitrogen abundances as a function of surface gravity (log g) for each galaxy. Only those objects with masses less than 20 solar masses are included. The left panel shows a plot for each of the galaxies with only those objects analysed in this paper included, whereas the right panel also contains objects from Paper IV with similar masses. Open circles represent upper limits to the nitrogen abundances, circled symbols are possible composite objects. Dotted lines in each plot represent the baseline abundance of the appropriate galaxy as estimated from H II regions.

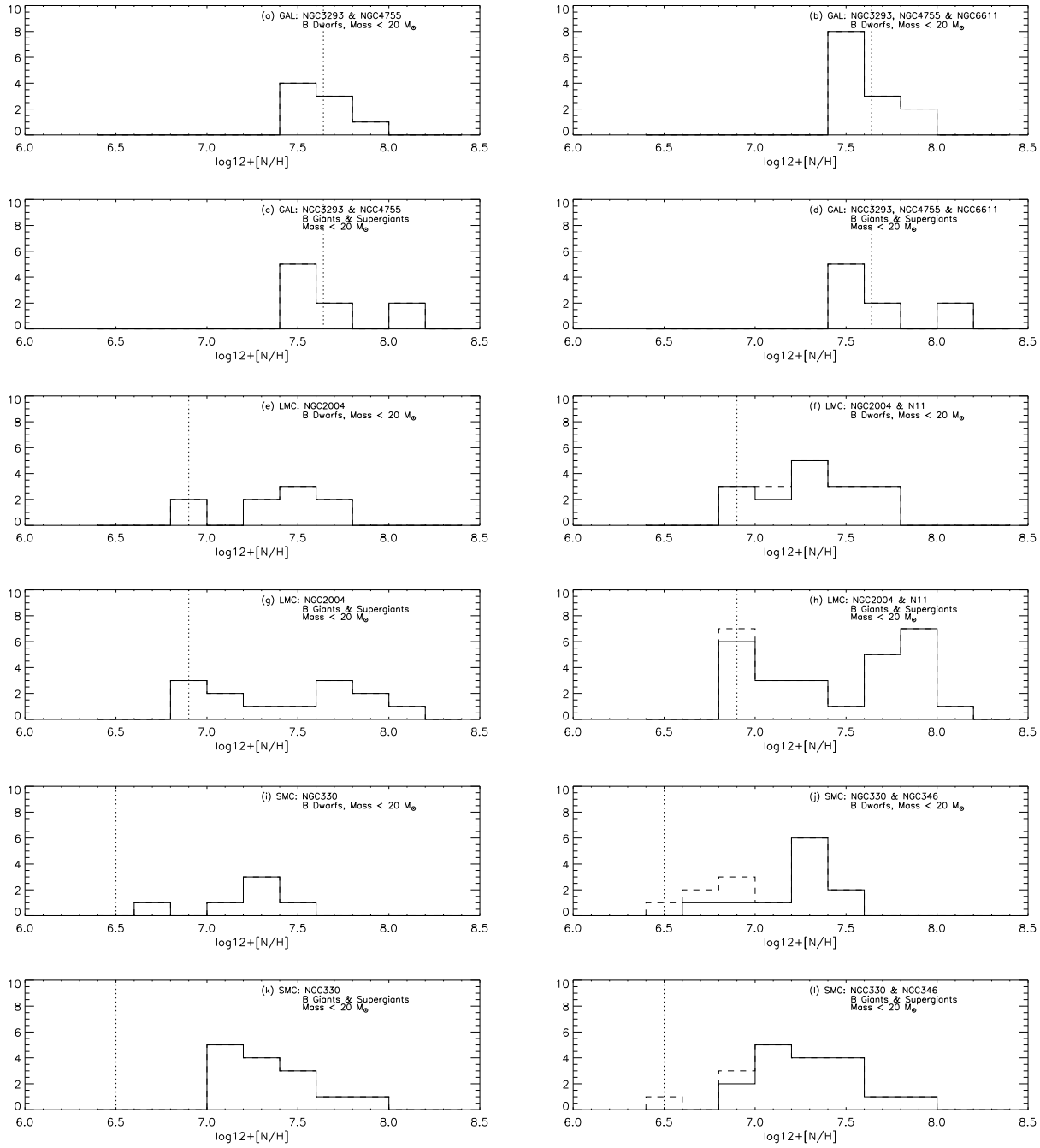

Fig. 4. Histograms of the 12+log[N/H] distributions in the Milky Way objects **(a-d)**, the LMC objects **(e-h)** and the SMC objects **(i-l)**. The left panels show plots for each of the galaxies including the objects analysed in this paper, whereas the right panel also contains objects with similar masses from Paper IV. The dotted line represents the baseline nitrogen abundance of the appropriate galaxy, and the dashed lines represent upper limits.

Online Material

Table A.1. Absolute Abundances of NGC3293, NGC4755, NGC2004 & NGC330 stars. The abundances presented below are the mean absolute abundances of each species studied, using the initial atmospheric parameters from Tables 3 & 4. Numbers in the parentheses represent the number of lines of each species observed in the star, only 1 line was considered for C II, Mg II & Si IV, 2 lines for Si II and 3 for Si III.Uncertainties on the abundances account for both random and systematic errors as discussed in Sect. 5.1. Abundances are presented as [X]=12 + log([X/H]) in units of dex.

Star	Sp.Typ	C II	N II		O II		Mg II	Si II	Si III	Si IV	Fe III	
NGC3293-003	B1 III	7.83	7.51 ± 0.05	(5)	8.66 ± 0.24	(27)	7.30 ± 0.26		7.31 ± 0.34	7.30 ± 0.65	7.27 ± 0.27	(1)
NGC3293-004	B1 III	7.89	7.55 ± 0.09	(5)	8.74 ± 0.23	(21)	7.44 ± 0.29		7.45 ± 0.31	7.45 ± 0.62		
NGC3293-007	B1 III	7.86	7.50 ± 0.08	(4)	8.67 ± 0.20	(28)	7.25 ± 0.21	7.35 ± 0.41	7.36 ± 0.30	7.34 ± 0.60	7.26 ± 0.22	(2)
NGC3293-010	B1 III	7.66	7.46 ± 0.12	(6)	8.88 ± 0.33	(28)	7.17 ± 0.25	6.86 ± 0.26	7.60 ± 0.43	7.63 ± 0.62	7.31 ± 0.26	(1)
NGC3293-012	B1 III	7.67	7.50 ± 0.17	(4)	8.96 ± 0.36	(25)	7.28 ± 0.23		7.66 ± 0.42	7.69 ± 0.61		
NGC3293-018	B1 V	7.67	7.61 ± 0.13	(5)	8.84 ± 0.30	(27)	7.20 ± 0.20	6.87 ± 0.22	7.71 ± 0.37	7.70 ± 0.55	7.68 ± 0.19	(2)
NGC3293-026	B2 III	7.81	7.78 ± 0.21	(4)	8.96 ± 0.33	(30)	7.29 ± 0.31	6.95 ± 0.25	7.76 ± 0.38	7.80 ± 0.56	7.66 ± 0.19	(2)
NGC3293-043	B3 V	7.91	7.55 ± 0.26	(7)	8.50 ± 0.34	(19)	7.14 ± 0.26	7.31 ± 0.37	7.31 ± 0.34		7.51 ± 0.25	(1)
NGC4755-002	B3 Ia	7.84	8.16 ± 0.30	(7)	8.57 ± 0.43	(26)	7.28 ± 0.32	7.38 ± 0.28	7.37 ± 0.45		7.53 ± 0.22	(2)
NGC4755-003	B2 III	7.74	8.09 ± 0.26	(7)	8.50 ± 0.37	(27)	7.27 ± 0.26	7.34 ± 0.25	7.34 ± 0.41		7.46 ± 0.18	(2)
NGC4755-004	B1.5 Ib	7.73	8.06 ± 0.14	(7)	8.65 ± 0.28	(31)	7.25 ± 0.28	7.34 ± 0.34	7.37 ± 0.37	7.35 ± 0.69	7.37 ± 0.24	(1)
NGC4755-006	B1 III	7.64	7.76 ± 0.23	(4)	9.16 ± 0.38	(24)	7.18 ± 0.23		7.76 ± 0.43	7.78 ± 0.54		
NGC4755-015	B1 V	7.66	7.98 ± 0.25	(5)	9.07 ± 0.33	(30)	7.16 ± 0.26		7.83 ± 0.35	7.84 ± 0.52	7.72 ± 0.23	(1)
NGC4755-017	B1.5 V	7.83	7.63 ± 0.35	(4)	8.57 ± 0.45	(14)	7.19 ± 0.31	7.22 ± 0.29	7.20 ± 0.42			
NGC4755-020	B2 V	7.95	7.61 ± 0.20	(6)	8.42 ± 0.30	(29)	7.34 ± 0.27	7.24 ± 0.25	7.20 ± 0.32		7.83 ± 0.29	(1)
NGC4755-033	B3 V	7.92	7.28 ± 0.27	(2)	8.41 ± 0.36	(3)	7.02 ± 0.25	7.06 ± 0.22	7.05 ± 0.31			
NGC4755-040	B2.5 V	8.45	7.87 ± 0.39	(2)	9.19 ± 0.32	(3)	7.28 ± 0.42	7.71 ± 0.58	7.70 ± 0.35			
NGC4755-048	B3 V	8.15	7.32 ± 0.31	(2)	8.81 ± 0.38	(4)	7.03 ± 0.27	7.19 ± 0.30	7.18 ± 0.33			
NGC2004-003	B5 Ia	7.68	7.86 ± 0.40	(7)	8.46 ± 0.55	(20)	7.04 ± 0.26	7.24 ± 0.26	7.25 ± 0.50		7.30 ± 0.23	(2)
NGC2004-005	B8 Ia	7.50	7.67 ± 0.37	(5)	8.56 ± 0.57	(4)	6.78 ± 0.46	6.95 ± 0.36	6.94 ± 0.44		7.13 ± 0.23	(2)
NGC2004-007	B8 Ia	7.36	7.47 ± 0.28	(2)	8.46 ± 0.53	(3)	6.67 ± 0.43	6.82 ± 0.39	6.82 ± 0.44		7.02 ± 0.26	(2)
NGC2004-010	B2.5 Iab	7.50	8.13 ± 0.28	(7)	8.29 ± 0.36	(27)	7.06 ± 0.26	7.15 ± 0.24	7.16 ± 0.41		7.25 ± 0.12	(2)
NGC2004-011	B1.5 Ia	7.45	7.72 ± 0.07	(7)	8.39 ± 0.21	(30)	7.15 ± 0.26		7.13 ± 0.32	7.16 ± 0.64	7.14 ± 0.22	(2)
NGC2004-012	B1.5 Iab	7.44	7.75 ± 0.09	(7)	8.43 ± 0.24	(31)	7.08 ± 0.23		7.19 ± 0.35	7.21 ± 0.64	7.12 ± 0.19	(2)
NGC2004-014	B3 Ib	7.52	7.51 ± 0.25	(7)	8.22 ± 0.37	(23)	6.96 ± 0.20	7.09 ± 0.19	7.08 ± 0.38		7.16 ± 0.17	(2)
NGC2004-021	B1.5 Ib	7.56	7.20 ± 0.10	(6)	8.53 ± 0.28	(29)	7.09 ± 0.23		7.31 ± 0.37	7.32 ± 0.60	7.19 ± 0.20	(2)
NGC2004-022	B1.5 Ib	7.31	7.70 ± 0.13	(7)	8.59 ± 0.28	(32)	6.94 ± 0.19		7.31 ± 0.37	7.31 ± 0.59	7.00 ± 0.25	(1)
NGC2004-026	B2 II	7.51	7.02 ± 0.11	(4)	8.19 ± 0.28	(30)	7.03 ± 0.18	7.16 ± 0.21	7.17 ± 0.34		7.31 ± 0.15	(2)
NGC2004-029	B1.5 e	7.43	6.81 ± 0.05	(4)	8.29 ± 0.26	(30)	7.03 ± 0.19		7.21 ± 0.35	7.20 ± 0.56	7.35 ± 0.17	(2)
NGC2004-036	B1.5 III	7.46	7.43 ± 0.11	(6)	8.72 ± 0.32	(28)	6.88 ± 0.20		7.57 ± 0.41	7.59 ± 0.58	7.32 ± 0.28	(1)
NGC2004-042	B2.5 III	7.62	6.89 ± 0.18	(2)	8.14 ± 0.31	(16)	7.09 ± 0.21	7.11 ± 0.22	7.11 ± 0.36		7.17 ± 0.20	(1)
NGC2004-046	B1.5 III	7.54	7.62 ± 0.11	(6)	8.53 ± 0.17	(30)	7.05 ± 0.22		7.43 ± 0.33	7.43 ± 0.53		

Table A.1. Abundances of NGC3293, NGC4755, NGC2004 & NGC330 stars. Contd.

Star	Sp.Typ	C II	N II		O II		Mg II	Si II	Si III	Si IV	Fe III	
NGC2004-053	B0.2 Ve	7.93	7.73 ± 0.16	(3)	8.51 ± 0.19	(28)	7.31 ± 0.24		7.41 ± 0.30	7.41 ± 0.60		
NGC2004-061	B2 III	7.78	7.00 ± 0.24	(3)	8.32 ± 0.46	(16)	7.20 ± 0.30	7.26 ± 0.31	7.27 ± 0.48		7.53 ± 0.34	(1)
NGC2004-064	B2 III	7.50	7.56 ± 0.09	(5)	8.50 ± 0.16	(29)	7.12 ± 0.29	0.00 ± 0.00	7.47 ± 0.31	7.49 ± 0.55		
NGC2004-070	B0.7-B1 III	7.59	7.48 ± 0.12	(4)	8.73 ± 0.19	(21)	7.23 ± 0.29	0.00 ± 0.00	7.60 ± 0.33	7.61 ± 0.51		
NGC2004-084	B0.7-B1 III	7.64	7.28 ± 0.14	(4)	8.57 ± 0.16	(26)	7.22 ± 0.23	0.00 ± 0.00	7.56 ± 0.32	7.57 ± 0.48		
NGC2004-090	O9.5 III	7.53	7.54 ± 0.19	(3)	8.32 ± 0.23	(24)	6.91 ± 0.19	0.00 ± 0.00	6.94 ± 0.29	6.93 ± 0.39		
NGC2004-091	B1.5 III	7.80	7.28 ± 0.08	(5)	8.34 ± 0.13	(27)	7.26 ± 0.24	0.00 ± 0.00	7.16 ± 0.24	7.16 ± 0.51		
NGC2004-108	B2.5 III	7.29	6.89 ± 0.14	(3)	8.23 ± 0.30	(28)	6.99 ± 0.20	6.98 ± 0.23	6.98 ± 0.31	0.00 ± 0.00	7.35 ± 0.21	(1)
NGC2004-119	B2 III	7.48	6.95 ± 0.09	(3)	8.35 ± 0.27	(29)	7.17 ± 0.25	7.14 ± 0.24	7.14 ± 0.34	0.00 ± 0.00	7.34 ± 0.25	(1)
NGC330-002	B3 Ib	7.08	7.58 ± 0.33	(8)	7.99 ± 0.52	(14)	6.55 ± 0.22	6.74 ± 0.22	6.78 ± 0.46		6.70 ± 0.25	(1)
NGC330-003	B2 Ib	7.28	7.74 ± 0.19	(8)	8.11 ± 0.36	(24)	6.82 ± 0.27	6.89 ± 0.27	6.95 ± 0.43		6.90 ± 0.25	(1)
NGC330-004	B2.5 Ib	6.84	7.83 ± 0.14	(8)	7.86 ± 0.32	(15)	6.73 ± 0.21	6.76 ± 0.21	6.82 ± 0.39		6.83 ± 0.14	(1)
NGC330-005	B5 Ib	6.77	7.49 ± 0.37	(4)	7.82 ± 0.45	(2)	6.58 ± 0.19	6.76 ± 0.23	6.81 ± 0.43			
NGC330-009	B5 Ib	6.99	7.14 ± 0.37	(2)	8.19 ± 0.52	(3)	6.57 ± 0.26	6.61 ± 0.22	6.65 ± 0.45			
NGC330-010	B5 Ib	7.07	7.05 ± 0.31	(2)	7.62 ± 0.40	(3)	6.52 ± 0.17	6.57 ± 0.18	6.65 ± 0.38			
NGC330-014	B1.5 Ib	6.93	7.56 ± 0.16	(7)	8.18 ± 0.27	(20)	6.72 ± 0.21		6.96 ± 0.33	6.96 ± 0.54		
NGC330-016	B5: II	7.24	7.08 ± 0.35	(1)	7.97 ± 0.50	(2)	6.57 ± 0.17	6.55 ± 0.16	6.61 ± 0.44			
NGC330-017	B2 II	7.07	7.12 ± 0.12	(8)	7.64 ± 0.25	(24)	6.47 ± 0.17		6.74 ± 0.33		6.90 ± 0.21	(1)
NGC330-018	B3 II	7.17	7.24 ± 0.26	(3)	8.05 ± 0.37	(7)	6.61 ± 0.18	6.74 ± 0.18	6.80 ± 0.36		7.14 ± 0.21	(1)
NGC330-020	B3 II	7.14	7.15 ± 0.49	(2)	7.99 ± 0.64	(4)	6.73 ± 0.34	7.05 ± 0.45	7.11 ± 0.60			
NGC330-022	B3 II	7.10	7.27 ± 0.24	(8)	7.76 ± 0.35	(8)	6.64 ± 0.14	6.53 ± 0.14	6.58 ± 0.34			
NGC330-026	B2.5 II	7.30	7.23 ± 0.19	(3)	7.74 ± 0.30	(6)	7.02 ± 0.23		6.64 ± 0.39			
NGC330-027	B1 V	7.13	7.45 ± 0.23	(2)	8.33 ± 0.45	(8)	6.44 ± 0.22		6.90 ± 0.39	6.88 ± 0.79		
NGC330-032	B0.5 V	7.16	7.37 ± 0.10	(3)	7.90 ± 0.07	(22)	6.80 ± 0.20		6.77 ± 0.19	6.77 ± 0.45		
NGC330-042	B2 II	7.06	7.20 ± 0.06	(7)	7.69 ± 0.12	(19)	6.86 ± 0.17		6.67 ± 0.28	6.66 ± 0.49		
NGC330-047	B1 V	7.20	6.76 ± 0.11	(2)	8.07 ± 0.13	(24)	6.57 ± 0.15		6.83 ± 0.23	6.84 ± 0.46		
NGC330-074	B0 V	7.29	7.52 ± 0.21	(2)	7.93 ± 0.17	(7)	6.83 ± 0.18		6.94 ± 0.24	6.95 ± 0.50		
NGC330-114	B2 III	7.24	7.34 ± 0.18	(3)	8.02 ± 0.28	(18)	6.99 ± 0.22		6.90 ± 0.34			
NGC330-124	B0.2 V	7.57	7.41 ± 0.26	(1)	7.81 ± 0.18	(3)	6.78 ± 0.18		6.98 ± 0.26	6.98 ± 0.48		

Table A.2. Absolute Abundances of the NGC3293, NGC4755, NGC2004 & NGC330 stars. The abundances presented below are the mean absolute abundances of each species studied, using the initial atmospheric parameters from Tables 3 & 4 but with the microturbulence corrected to obtain the mean Cluster silicon abundance in each star Uncertainties on the abundances account for both random and systematic errors as discussed in Sect. 5.1. Abundances are presented as [X]=12 + log([X/H]) in units of dex, and ξ in kms^{-1}.

Star	Sp.Typ	$\xi_{\rm Ave}$	$\xi_{\rm Si}$	C II	N II	O II	Mg II	Si II	Si III	Si IV	Fe III
NGC3293-003	B1 III	13	15	7.87	7.53 ± 0.05	8.72 ± 0.26	7.33 ± 0.28		7.45 ± 0.38	7.39 ± 0.67	7.29 ± 0.31
NGC3293-004	B1 III	13	13	7.89	7.55 ± 0.09	8.74 ± 0.23	7.44 ± 0.29		7.45 ± 0.31	7.45 ± 0.62	
NGC3293-007	B1 III	11	12	7.88	7.51 ± 0.08	8.70 ± 0.21	7.27 ± 0.22	7.36 ± 0.40	7.43 ± 0.33	7.40 ± 0.61	7.26 ± 0.24
NGC3293-010	B1 III	11	10	7.65	7.45 ± 0.12	8.84 ± 0.32	7.15 ± 0.24	6.86 ± 0.26	7.51 ± 0.40	7.58 ± 0.61	7.30 ± 0.24
NGC3293-012	B1 III	11	10	7.65	7.49 ± 0.17	8.92 ± 0.35	7.25 ± 0.22		7.58 ± 0.41	7.64 ± 0.61	
NGC3293-018	B1 V	5	3	7.64	7.56 ± 0.12	8.74 ± 0.30	7.14 ± 0.19	6.83 ± 0.21	7.51 ± 0.37	7.58 ± 0.56	7.68 ± 0.27
NGC3293-026	B2 III	2	< 0	7.75	7.70 ± 0.20	8.85 ± 0.32	7.18 ± 0.28	6.88 ± 0.24	7.54 ± 0.36	7.67 ± 0.59	7.66 ± 0.19
NGC3293-043	B3 V	<0	< 0	7.91	7.55 ± 0.26	8.50 ± 0.34	7.14 ± 0.26	7.31 ± 0.37	7.31 ± 0.34		7.51 ± 0.25
NGC4755-002	B3 Ia	18	19	7.87	8.18 ± 0.31	8.59 ± 0.43	7.30 ± 0.32	7.40 ± 0.30	7.40 ± 0.46		7.54 ± 0.22
NGC4755-003	B2 III	15	17	7.79	8.14 ± 0.28	8.54 ± 0.38	7.31 ± 0.26	7.39 ± 0.25	7.43 ± 0.43		7.48 ± 0.18
NGC4755-004	B1.5 Ib	17	18	7.75	8.08 ± 0.15	8.67 ± 0.29	7.26 ± 0.28	7.35 ± 0.33	7.42 ± 0.39	7.38 ± 0.70	7.38 ± 0.26
NGC4755-006	B1 III	21	14	7.54	7.67 ± 0.19	8.95 ± 0.36	7.07 ± 0.20		7.41 ± 0.37	7.55 ± 0.56	
NGC4755-015	B1 V	6	2	7.58	7.80 ± 0.22	8.85 ± 0.33	7.02 ± 0.23		7.43 ± 0.36	7.60 ± 0.59	7.56 ± 0.31
NGC4755-017	B1.5 V	3	6	7.92	7.72 ± 0.37	8.68 ± 0.46	7.33 ± 0.33	7.45 ± 0.36	7.41 ± 0.44		
NGC4755-020	B2 V	1	3	8.02	7.67 ± 0.21	8.49 ± 0.31	7.45 ± 0.29	7.39 ± 0.29	7.37 ± 0.34		7.83 ± 0.25
NGC4755-033	B3 V	2	10	8.19	7.39 ± 0.33	8.63 ± 0.40	7.44 ± 0.43	8.00 ± 0.80	7.39 ± 0.39		
NGC4755-040	B2.5 V	5	< 0	8.28	7.72 ± 0.36	9.02 ± 0.38	6.98 ± 0.35	7.03 ± 0.32	7.41 ± 0.33		
NGC4755-048	B3 V	2	6	8.29	7.39 ± 0.33	8.93 ± 0.37	7.25 ± 0.34	7.74 ± 0.51	7.38 ± 0.34		
NGC2004-003	B5 Ia	15	14	7.66	7.85 ± 0.40	8.45 ± 0.55	7.02 ± 0.26	7.22 ± 0.25	7.22 ± 0.50		7.29 ± 0.23
NGC2004-005	B8 Ia	9	24	7.79	7.82 ± 0.37	8.78 ± 0.57	7.17 ± 0.46	7.49 ± 0.36	7.20 ± 0.44		7.19 ± 0.23
NGC2004-007	B8 Ia	6	29	7.74	7.75 ± 0.28	8.74 ± 0.53	7.37 ± 0.43	8.02 ± 0.39	7.20 ± 0.44		7.10 ± 0.26
NGC2004-010	B2.5 Iab	14	16	7.53	8.18 ± 0.29	8.32 ± 0.37	7.10 ± 0.27	7.19 ± 0.25	7.24 ± 0.43		7.26 ± 0.12
NGC2004-011	B1.5 Ia	13	14	7.46	7.73 ± 0.07	8.41 ± 0.22	7.16 ± 0.26		7.18 ± 0.33	7.20 ± 0.64	7.14 ± 0.23
NGC2004-012	B1.5 Iab	12	12	7.44	7.75 ± 0.09	8.43 ± 0.24	7.08 ± 0.23		7.19 ± 0.35	7.21 ± 0.64	7.12 ± 0.19
NGC2004-014	B3 Ib	11	14	7.58	7.54 ± 0.26	8.26 ± 0.39	7.02 ± 0.22	7.16 ± 0.21	7.19 ± 0.40		7.18 ± 0.17
NGC2004-021	B1.5 Ib	13	12	7.55	7.20 ± 0.10	8.50 ± 0.27	7.08 ± 0.23		7.25 ± 0.35	7.28 ± 0.59	7.19 ± 0.18
NGC2004-022	B1.5 Ib	11	10	7.31	7.68 ± 0.12	8.56 ± 0.28	6.94 ± 0.19		7.24 ± 0.34	7.26 ± 0.58	7.00 ± 0.22
NGC2004-026	B2 II	0	1	7.52	7.02 ± 0.12	8.22 ± 0.28	7.07 ± 0.19	7.21 ± 0.22	7.29 ± 0.37		7.35 ± 0.17
NGC2004-029	B1.5 e	1	1	7.43	6.81 ± 0.05	8.29 ± 0.26	7.03 ± 0.19		7.21 ± 0.35	7.20 ± 0.56	7.35 ± 0.17
NGC2004-036	B1.5 III	8	5	7.42	7.38 ± 0.09	8.57 ± 0.27	6.84 ± 0.16		7.22 ± 0.31	7.38 ± 0.58	7.26 ± 0.20
NGC2004-042	B2.5 III	2	3	7.64	6.91 ± 0.19	8.17 ± 0.32	7.13 ± 0.22	7.17 ± 0.23	7.20 ± 0.36		7.21 ± 0.21
NGC2004-046	B1.5 III	2	< 0	7.50	7.57 ± 0.10	8.43 ± 0.14	7.01 ± 0.20		7.20 ± 0.26	7.26 ± 0.51	

Table A.2. Contd.

Star	Sp.Typ	$\xi_{\rm Ave}$	$\xi_{\rm Si}$	C II	N II	O II	Mg II	Si II	Si III	Si IV	Fe III
NGC2004-053	B0.2 Ve	7	3	7.89	7.70 ± 0.16	8.44 ± 0.18	7.25 ± 0.22		7.23 ± 0.26	6.98 ± 0.46	
NGC2004-061	B2 III	1	<0	7.75	6.98 ± 0.23	8.28 ± 0.45	7.14 ± 0.28	7.18 ± 0.29	7.15 ± 0.47		7.44 ± 0.31
NGC2004-064	B2 III	6	3	7.48	7.51 ± 0.08	8.37 ± 0.13	7.06 ± 0.25		7.17 ± 0.25	7.24 ± 0.54	
NGC2004-070	B0.7-B1 III	4	<0	7.56	7.42 ± 0.11	8.51 ± 0.20	7.14 ± 0.22		7.19 ± 0.36	7.26 ± 0.56	
NGC2004-084	B0.7-B1 III	3	<0	7.61	7.26 ± 0.14	8.43 ± 0.13	7.15 ± 0.19		7.24 ± 0.24	7.31 ± 0.47	
NGC2004-090	O9.5 III	<0	3	7.54	7.57 ± 0.19	8.36 ± 0.23	6.94 ± 0.19		7.05 ± 0.29	7.24 ± 0.42	
NGC2004-091	B1.5 III	0	1	7.81	7.29 ± 0.09	8.38 ± 0.14	7.29 ± 0.25		7.26 ± 0.27	7.24 ± 0.52	
NGC2004-108	B2.5 III	<0	<0	7.29	6.89 ± 0.14	8.23 ± 0.30	6.99 ± 0.20	6.98 ± 0.23	6.98 ± 0.31		7.35 ± 0.21
NGC2004-119	B2 III	<0	<0	7.48	6.95 ± 0.09	8.35 ± 0.27	7.17 ± 0.25	7.14 ± 0.24	7.14 ± 0.34		7.34 ± 0.25
NGC330-002	B3 Ib	18	20	7.09	7.60 ± 0.32	8.00 ± 0.52	6.57 ± 0.23	6.77 ± 0.23	6.81 ± 0.47		6.70 ± 0.24
NGC330-003	B2 Ib	19	15	7.25	7.69 ± 0.19	8.07 ± 0.34	6.80 ± 0.27	6.85 ± 0.26	6.82 ± 0.39		6.88 ± 0.22
NGC330-004	B2.5 Ib	16	16	6.84	7.83 ± 0.14	7.86 ± 0.32	6.73 ± 0.21	6.76 ± 0.21	6.82 ± 0.39		6.83 ± 0.14
NGC330-005	B5 Ib	8	8	6.77	7.49 ± 0.37	7.82 ± 0.45	6.58 ± 0.19	6.76 ± 0.23	6.81 ± 0.43		
NGC330-009	B5 Ib	6	10	7.04	7.18 ± 0.41	8.27 ± 0.53	6.67 ± 0.31	6.81 ± 0.32	6.78 ± 0.49		
NGC330-010	B5 Ib	4	9	7.15	7.11 ± 0.33	7.69 ± 0.41	6.64 ± 0.20	6.82 ± 0.31	6.82 ± 0.42		
NGC330-014	B1.5 Ib	19	15	6.93	7.53 ± 0.15	8.12 ± 0.24	6.70 ± 0.21		6.82 ± 0.29	6.89 ± 0.51	
NGC330-016	B5: II	4	10	7.36	7.17 ± 0.38	8.06 ± 0.52	6.77 ± 0.25	6.91 ± 0.38	6.82 ± 0.48		
NGC330-017	B2 II	<0	<0	7.07	7.12 ± 0.12	7.64 ± 0.25	6.47 ± 0.17		6.74 ± 0.33		6.90 ± 0.21
NGC330-018	B3 II	5	5	7.17	7.24 ± 0.26	8.05 ± 0.37	6.61 ± 0.18	6.74 ± 0.18	6.80 ± 0.36		7.14 ± 0.19
NGC330-020	B3 II	8	2	7.06	7.06 ± 0.44	7.87 ± 0.61	6.55 ± 0.26	6.66 ± 0.27	6.81 ± 0.55		
NGC330-022	B3 II	3	7	7.13	7.33 ± 0.26	7.84 ± 0.37	6.73 ± 0.16	6.66 ± 0.17	6.80 ± 0.37		
NGC330-026	B2.5 II	<0	<0	7.30	7.23 ± 0.19	7.74 ± 0.30	7.02 ± 0.23		6.64 ± 0.39		
NGC330-027	B1 V	7	6	7.13	7.40 ± 0.22	8.28 ± 0.44	6.44 ± 0.22		6.82 ± 0.36	6.84 ± 0.78	
NGC330-032	B0.5 V	<0	< 0	7.16	7.37 ± 0.10	7.90 ± 0.07	6.80 ± 0.20		6.77 ± 0.19	6.77 ± 0.50	
NGC330-042	B2 II	1	3	7.06	7.22 ± 0.06	7.73 ± 0.13	6.89 ± 0.18		6.83 ± 0.34	6.76 ± 0.52	
NGC330-047	B1 V	0	0	7.20	6.76 ± 0.11	8.07 ± 0.13	6.57 ± 0.15		6.83 ± 0.23	6.84 ± 0.46	
NGC330-074	B0 V	6	2	7.31	7.49 ± 0.21	7.88 ± 0.17	6.81 ± 0.19		6.81 ± 0.25	6.62 ± 0.39	
NGC330-114	B2 III	4	3	7.23	7.32 ± 0.18	8.00 ± 0.27	6.97 ± 0.22		6.83 ± 0.32		
NGC330-124	B0.2 V	3	<0	7.57	7.37 ± 0.25	7.76 ± 0.18	6.75 ± 0.18		6.82 ± 0.23	6.73 ± 0.45	

Table B.1. Iron equivalent widths and absolute abundances for the objects analysed in Paper IV. The last column contains the weighted mean abundance and uncertainties of the iron abundance in each star.

ID	Fe III 4419 Å		Fe III 4431 Å		
	EW(mÅ)	Abund.	EW(mÅ)	Abund	[Fe/H]
NGC6611-030	24	7.55	19	7.69	7.62 ± 0.15
N11-001	92	7.59	34	7.30	7.45 ± 0.17
N11-002	55	7.27	41	7.41	7.34 ± 0.15
N11-009	38	7.20	26	7.29	7.24 ± 0.13
N11-012	42	7.20	14	7.00	7.10 ± 0.27
N11-014	52	7.25	28	7.22	7.23 ± 0.17
N11-015	23	7.21			7.21 ± 0.26
N11-016	44	7.26			7.26 ± 0.28
N11-017	47	7.21	26	7.20	7.20 ± 0.15
N11-024	36	7.15	16	7.07	7.11 ± 0.16
N11-036	23	7.17			7.17 ± 0.23
N11-110	27	7.17	12	7.08	7.12 ± 0.16
NGC346-021	17	7.14			7.14 ± 0.18
NGC346-037	11	6.83			6.83 ± 0.21
NGC346-039	10	6.94			6.94 ± 0.17
NGC346-044	18	6.99			6.99 ± 0.18

Table C.1. Equivalent widths and line by line absolute abundances of the NGC3293 stars:#3, #4, #7. The first and second columns represent the ion and wavelength of the line. There are four columns per star the first represents the equivalent width of the line, the following three are abundance estimates from the lines and they show the results from the 3 steps in determining the abundances as described in Sect. 4. The energy levels and oscillator strenghts relating to the transitions for the metal lines are available online at http://star.pst.qub.ac.uk/ pld/line_identifications.html.

		NGC3293-003				NGC3293-004				NGC3293-007			
ION	λ	EW (mÅ)	(1)	(2)	(3)	EW (mÅ)	(1)	(2)	(3)	EW (mÅ)	(1)	(2)	(3)
C II	3920.68	146	8.03	8.07	8.03					110	8.03	8.04	8.03
C II(B)	4267.00	237	7.83	7.87	7.84	214	7.89	7.89	7.89	200	7.86	7.88	7.86
C II	6578.05												
C II	6582.88												
N II	3955.85									27	7.57	7.57	7.56
N II	3995.00	127	7.39	7.43	7.41	115	7.39	7.39	7.39	123	7.47	7.49	7.48
N II	4447.03	65	7.51	7.52	7.52	78	7.63	7.63	7.63	59	7.49	7.49	7.49
N II	4601.48	68	7.63	7.65	7.64	69	7.71	7.71	7.71				
N II	4613.86	37	7.55	7.55	7.55	35	7.58	7.58	7.58				
N II	4630.54	115	7.49	7.51	7.50	94	7.43	7.43	7.43	101	7.49	7.50	7.49
N II	4643.08												
O II(B)	3912.00	94	8.42	8.45	8.48					140	8.66	8.68	8.69
O II	3945.04	78	8.51	8.54	8.56	105	8.67	8.67	8.67	92	8.58	8.60	8.61
O II	3954.36	118	8.45	8.50	8.53	151	8.61	8.61	8.61	121	8.44	8.46	8.48
O II	3982.71	106	8.70	8.74	8.77					89	8.55	8.57	8.58
O II(B)	4069.00	242	8.62	8.69	8.73	361	9.12	9.12	9.12	271	8.72	8.76	8.78
O II	4072.15	209	8.65	8.77	8.81	208	8.61	8.61	8.61	220	8.74	8.82	8.83
O II	4075.86	261	8.74	8.88	8.93	313	9.03	9.03	9.03	243	8.68	8.76	8.78
O II	4078.84	58	8.45	8.49	8.51					55	8.36	8.38	8.38
O II	4132.80					89	8.54	8.54	8.54	87	8.54	8.55	8.56
O II	4156.53	41	8.89	8.92	8.93								
O II(B)	4317.00	182	8.91	9.00	9.04	188	8.91	8.91	8.91	176	8.88	8.93	8.94
O II	4319.63	178	8.88	8.97	9.01	189	8.92	8.92	8.92	184	8.93	8.98	9.00
O II	4325.76	39	8.55	8.57	8.59					64	8.81	8.83	8.84
O II	4349.43												
O II(B)	4351.00												
O II	4353.58												
O II(B)	4366.00	180	8.81	8.89	8.93	222	9.01	9.01	9.01	191	8.87	8.93	8.94
O II	4369.27	30	8.39	8.40	8.42					40	8.47	8.48	8.49
O II	4395.94	72	8.71	8.73	8.76	67	8.59	8.59	8.59	70	8.62	8.63	8.64
O II	4414.90	267	8.77	8.87	8.92	274	8.77	8.77	8.77	253	8.71	8.76	8.78
O II	4416.98	194	8.69	8.77	8.81	196	8.66	8.66	8.66	190	8.66	8.70	8.71
O II	4452.38	81	8.77	8.81	8.83	79	8.70	8.70	8.70	82	8.74	8.75	8.76
O II	4590.97	179	8.63	8.71	8.75	201	8.68	8.68	8.68	186	8.63	8.67	8.69
O II(B)	4596.18	148	8.57	8.63	8.67	173	8.64	8.64	8.64	161	8.59	8.62	8.64
O II	4638.86	195	8.83	8.90	8.94	206	8.83	8.83	8.83	193	8.79	8.84	8.85
O II	4641.81					395	9.21	9.21	9.21	296	8.82	8.89	8.90
O II(B)	4650.00												
O II	4661.63	206	8.80	8.87	8.91	233	8.88	8.88	8.88	206	8.78	8.82	8.83
O II	4673.73	57	8.77	8.79	8.81					65	8.80	8.81	8.82
O II	4676.23	195	8.88	8.95	8.99					138	8.54	8.57	8.58
O II	4699.00	105	8.32	8.35	8.38	97	8.19	8.19	8.19	135	8.41	8.43	8.44
O II	4705.35	120	8.41	8.46	8.50	134	8.41	8.41	8.41	148	8.51	8.54	8.55
O II	4710.00	49	8.73	8.76	8.79	40	8.55	8.55	8.55	61	8.80	8.82	8.83
Mg II(B)	4481.00	191	7.30	7.33	7.29	198	7.44	7.44	7.44	152	7.25	7.27	7.26
Si II	4128.05									24	7.42	7.43	7.39
Si II	4130.89									27	7.28	7.29	7.25
Si III	4552.62	393	7.31	7.49	7.53	390	7.44	7.44	7.44	350	7.33	7.43	7.44
Si III	4567.84	321	7.30	7.44	7.48	330	7.46	7.46	7.46	300	7.38	7.47	7.48
Si III	4574.75	199	7.33	7.41	7.44	206	7.44	7.44	7.44	184	7.36	7.40	7.41
Si IV	4116.10	91	7.30	7.39	7.49	121	7.45	7.45	7.45	110	7.34	7.40	7.44
Fe III	4419.60	52	7.27	7.29	7.27					33	7.23	7.23	7.22
Fe III	4431.02									20	7.28	7.28	7.27

Table C.1. Contd. STARS:#10, #12, #18

		NGC3293-010				NGC3293-012				NGC3293-018			
ION	λ	EW (mÅ)	(1)	(2)	(3)	EW (mÅ)	(1)	(2)	(3)	EW (mÅ)	(1)	(2)	(3)
C II	3920.68	97	7.71	7.70	7.71					72	7.80	7.74	7.77
C II(B)	4267.00	194	7.66	7.65	7.66	201	7.67	7.65	7.67	155	7.67	7.64	7.66
C II	6578.05												
C II	6582.88												
N II	3955.85	27	7.52	7.51	7.51					22	7.58	7.56	7.57
N II	3995.00	116	7.40	7.38	7.37	94	7.27	7.26	7.23	94	7.55	7.47	7.47
N II	4447.03	49	7.36	7.35	7.34					50	7.54	7.50	7.50
N II	4601.48	39	7.38	7.38	7.37	40	7.43	7.43	7.40				
N II	4613.86	46	7.69	7.68	7.67	47	7.75	7.74	7.71				
N II	4630.54	95	7.44	7.43	7.42	101	7.54	7.52	7.48	83	7.66	7.58	7.58
N II	4643.08									51	7.73	7.69	7.69
O II(B)	3912.00	124	8.83	8.80	8.78	103	8.76	8.73	8.66	94	8.82	8.75	8.72
O II	3945.04	77	8.69	8.67	8.65	88	8.89	8.86	8.80	55	8.67	8.61	8.58
O II	3954.36	90	8.48	8.45	8.43	99	8.66	8.63	8.56	82	8.72	8.63	8.60
O II	3982.71					92	8.95	8.92	8.85	56	8.73	8.66	8.63
O II(B)	4069.00	245	8.98	8.93	8.90	254	9.16	9.10	9.01	185	8.97	8.85	8.81
O II	4072.15	196	9.04	8.95	8.92	187	9.09	9.01	8.91	105	8.71	8.57	8.54
O II	4075.86	203	8.89	8.81	8.78	230	9.22	9.12	9.02	131	8.86	8.70	8.67
O II	4078.84	59	8.65	8.63	8.60	53	8.65	8.63	8.57	43	8.62	8.56	8.53
O II	4132.80	92	8.83	8.79	8.77					54	8.60	8.53	8.50
O II	4156.53	35	8.89	8.88	8.86								
O II(B)	4317.00	164	9.17	9.11	9.08	142	9.10	9.05	8.97	96	8.97	8.85	8.83
O II	4319.63	165	9.17	9.11	9.09	137	9.06	9.01	8.93	102	9.06	8.93	8.91
O II	4325.76	51	8.87	8.85	8.83								
O II	4349.43												
O II(B)	4351.00												
O II	4353.58												
O II(B)	4366.00	164	9.07	9.01	8.98	147	9.04	9.00	8.91	100	8.94	8.80	8.78
O II	4369.27	45	8.74	8.73	8.71					29	8.59	8.55	8.53
O II	4395.94	78	8.95	8.93	8.90	72	8.98	8.96	8.89	60	8.99	8.91	8.88
O II	4414.90	215	8.95	8.88	8.85	168	8.76	8.71	8.62	140	8.85	8.73	8.70
O II	4416.98	167	8.91	8.85	8.82	135	8.78	8.74	8.66	116	8.92	8.80	8.77
O II	4452.38	83	9.01	8.98	8.96	71	8.97	8.95	8.88	58	8.95	8.88	8.85
O II	4590.97	154	8.87	8.82	8.79	149	8.97	8.92	8.82	100	8.80	8.68	8.65
O II(B)	4596.18	146	8.89	8.85	8.82	146	9.03	8.98	8.89	104	8.85	8.77	8.73
O II	4638.86	172	9.07	9.01	8.98	152	9.05	9.00	8.91	112	9.02	8.89	8.86
O II	4641.81	212	8.84	8.78	8.75	268	9.31	9.23	9.13	142	8.88	8.72	8.69
O II(B)	4650.00												
O II	4661.63	88	8.32	8.30	8.28	159	9.01	8.96	8.87	111	8.92	8.80	8.76
O II	4673.73	63	9.02	9.00	8.98	56	9.03	9.01	8.94	40	8.88	8.83	8.80
O II	4676.23	137	8.86	8.82	8.80	145	9.05	9.00	8.92	92	8.83	8.73	8.69
O II	4699.00	130	8.73	8.70	8.67	106	8.67	8.64	8.56	108	8.71	8.66	8.62
O II	4705.35	126	8.74	8.71	8.68	112	8.76	8.72	8.64	86	8.65	8.58	8.54
O II	4710.00	71	9.24	9.21	9.18	48	9.05	9.02	8.95	49	9.19	9.11	9.07
Mg II(B)	4481.00	168	7.17	7.15	7.17	199	7.28	7.25	7.29	126	7.20	7.14	7.15
Si II	4128.05	24	6.95	6.94	6.97					19	7.12	7.07	7.12
Si II	4130.89	25	6.78	6.77	6.80					12	6.62	6.59	6.63
Si III	4552.62	313	7.59	7.49	7.46	306	7.66	7.57	7.48	192	7.69	7.48	7.46
Si III	4567.84	269	7.62	7.53	7.50	256	7.66	7.57	7.49	164	7.71	7.50	7.49
Si III	4574.75	174	7.58	7.52	7.50	172	7.67	7.61	7.54	113	7.72	7.54	7.53
Si IV	4116.10	64	7.63	7.58	7.53	54	7.69	7.64	7.51	44	7.70	7.58	7.49
Fe III	4419.60	46	7.31	7.30	7.30					33	7.71	7.71	7.72
Fe III	4431.02									22	7.66	7.66	7.68

Table C.1. Contd. STARS:#26, #43

		NGC3293-026				NGC3293-043			
ION	λ	EW (mÅ)	(1)	(2)	(3)	EW (mÅ)	(1)	(2)	(3)
C II	3920.68	90	8.06	7.94	7.97	74	8.02	8.02	8.02
C II(B)	4267.00	181	7.81	7.75	7.79	169	7.91	7.91	7.91
C II	6578.05	131	8.01	7.90	7.93	104	8.14	8.14	8.14
C II	6582.88	112	8.08	7.97	8.00	65	7.89	7.89	7.89
N II	3955.85	26	7.79	7.74	7.72	10	7.74	7.74	7.74
N II	3995.00	89	7.74	7.62	7.58	34	7.35	7.35	7.35
N II	4447.03	55	7.81	7.74	7.69	18	7.56	7.56	7.56
N II	4601.48	42	7.78	7.71	7.67	11	7.42	7.42	7.42
N II	4613.86					11	7.64	7.64	7.64
N II	4630.54					25	7.49	7.49	7.49
N II	4643.08					17	7.67	7.67	7.67
O II(B)	3912.00	71	8.90	8.82	8.73				
O II	3945.04	45	8.83	8.75	8.66	13	8.64	8.64	8.64
O II	3954.36	66	8.92	8.80	8.70	20	8.71	8.71	8.71
O II	3982.71	45	8.90	8.81	8.72				
O II(B)	4069.00	131	8.95	8.83	8.73	31	8.36	8.36	8.36
O II	4072.15	83	8.92	8.76	8.65	25	8.47	8.47	8.47
O II	4075.86	113	9.20	9.01	8.91	40	8.76	8.76	8.76
O II	4078.84	39	8.91	8.81	8.73				
O II	4132.80								
O II	4156.53	46	9.54	9.47	9.42				
O II(B)	4317.00	76	9.13	8.99	8.90	18	8.55	8.55	8.55
O II	4319.63	71	9.03	8.90	8.81	13	8.32	8.32	8.32
O II	4325.76	32	9.04	8.97	8.89				
O II	4349.43								
O II(B)	4351.00								
O II	4353.58								
O II(B)	4366.00	75	9.05	8.90	8.81	15	8.38	8.38	8.38
O II	4369.27	22	8.69	8.64	8.56				
O II	4395.94	50	9.23	9.13	9.03	14	9.03	9.03	9.03
O II	4414.90	104	8.94	8.81	8.71	29	8.43	8.43	8.43
O II	4416.98	89	9.08	8.94	8.84	23	8.55	8.55	8.55
O II	4452.38	42	9.01	8.93	8.84				
O II	4590.97	73	8.93	8.80	8.69	15	8.41	8.41	8.41
O II(B)	4596.18	76	8.95	8.86	8.75	13	8.41	8.41	8.41
O II	4638.86	78	9.06	8.93	8.82	19	8.59	8.59	8.59
O II	4641.81	100	8.95	8.78	8.67	24	8.36	8.36	8.36
O II(B)	4650.00	117	8.31	8.21	8.11				
O II	4661.63	77	8.97	8.83	8.73	17	8.44	8.44	8.44
O II	4673.73	30	8.98	8.92	8.83				
O II	4676.23	67	8.93	8.81	8.71	15	8.47	8.47	8.47
O II	4699.00	79	8.81	8.75	8.64	11	8.22	8.22	8.22
O II	4705.35	66	8.83	8.74	8.63	14	8.41	8.41	8.41
O II	4710.00	38	9.38	9.28	9.18				
Mg II(B)	4481.00	135	7.29	7.18	7.22	151	7.14	7.14	7.14
Si II	4128.05	22	7.09	7.00	7.07	35	7.36	7.36	7.36
Si II	4130.89	21	6.82	6.75	6.82	41	7.25	7.25	7.25
Si III	4552.62	141	7.73	7.50	7.43	60	7.34	7.34	7.34
Si III	4567.84	116	7.72	7.49	7.42	43	7.24	7.24	7.24
Si III	4574.75	85	7.84	7.63	7.56	28	7.34	7.34	7.34
Si IV	4116.10	24	7.80	7.67	7.46				
Fe III	4419.60	33	7.69	7.69	7.68	17	7.51	7.51	7.51
Fe III	4431.02	22	7.64	7.64	7.64				

Table C.2. Equivalent widths and line by line absolute abundances of NGC4755 for stars:#2, #3, #4. Columns are as for Table C.1.

		NGC4755-002				NGC4755-003				NGC4755-004			
ION	λ	EW (mÅ)	(1)	(2)	(3)	EW (mÅ)	(1)	(2)	(3)	EW (mÅ)	(1)	(2)	(3)
C II	3920.68	164	7.86	7.88	7.88	172	7.88	7.93	7.93	115	7.71	7.72	7.74
C II(B)	4267.00	289	7.84	7.87	7.87	274	7.74	7.79	7.78	240	7.73	7.75	7.76
C II	6578.05												
C II	6582.88												
N II	3955.85	66	8.23	8.25	8.25	62	8.04	8.07	8.05	78	8.06	8.07	8.06
N II	3995.00	192	8.02	8.06	8.06	219	7.98	8.06	8.04	269	7.97	8.00	7.99
N II	4447.03	85	8.02	8.04	8.04	106	7.99	8.03	8.01	140	8.00	8.02	8.00
N II	4601.48	103	8.22	8.24	8.24	118	8.16	8.20	8.18	161	8.19	8.22	8.20
N II	4613.86	65	8.14	8.15	8.15	78	8.10	8.13	8.11	99	8.09	8.10	8.09
N II	4630.54	189	8.24	8.27	8.27	211	8.16	8.24	8.21	264	8.09	8.13	8.11
N II	4643.08	103	8.23	8.25	8.25	122	8.18	8.23	8.21	128	8.02	8.03	8.02
O II(B)	3912.00	46	8.65	8.67	8.67	52	8.45	8.48	8.45	105	8.60	8.62	8.59
O II	3945.04					38	8.45	8.47	8.45	71	8.53	8.55	8.52
O II	3954.36	38	8.36	8.38	8.38	48	8.27	8.29	8.27	102	8.43	8.45	8.42
O II	3982.71												
O II(B)	4069.00	72	8.37	8.38	8.38	102	8.35	8.39	8.36	192	8.49	8.51	8.47
O II	4072.15	84	8.58	8.61	8.61	113	8.57	8.64	8.61	204	8.69	8.74	8.70
O II	4075.86	95	8.52	8.55	8.55	118	8.43	8.51	8.48	219	8.59	8.63	8.59
O II	4078.84									37	8.25	8.26	8.24
O II	4132.80					48	8.61	8.64	8.62	76	8.61	8.63	8.60
O II	4156.53									24	8.70	8.70	8.68
O II(B)	4317.00	59	8.72	8.74	8.74	75	8.64	8.68	8.65	154	8.83	8.86	8.83
O II	4319.63	62	8.76	8.78	8.78	78	8.66	8.71	8.68	168	8.91	8.94	8.91
O II	4325.76	15	8.59	8.60	8.60	20	8.52	8.54	8.52	41	8.65	8.66	8.64
O II	4349.43	87	8.67	8.69	8.69					246	8.92	8.96	8.92
O II(B)	4351.00									93	8.36	8.37	8.35
O II	4353.58												
O II(B)	4366.00	55	8.59	8.60	8.60	78	8.59	8.63	8.61	161	8.79	8.82	8.78
O II	4369.27	26	9.00	9.01	9.01								
O II	4395.94	49	9.24	9.26	9.26	51	8.96	8.99	8.97	65	8.75	8.77	8.74
O II	4414.90	85	8.50	8.53	8.53	111	8.46	8.52	8.49	233	8.70	8.73	8.70
O II	4416.98	61	8.49	8.52	8.52	86	8.50	8.55	8.53	169	8.65	8.68	8.64
O II	4452.38	19	8.52	8.53	8.53	29	8.53	8.56	8.54	66	8.73	8.74	8.72
O II	4590.97	42	8.40	8.42	8.42	64	8.41	8.45	8.42	146	8.57	8.59	8.56
O II(B)	4596.18	44	8.55	8.57	8.57	59	8.47	8.50	8.47	123	8.55	8.57	8.53
O II	4638.86	56	8.59	8.61	8.61	74	8.54	8.59	8.56	166	8.78	8.80	8.77
O II	4641.81	101	8.61	8.63	8.63	121	8.50	8.56	8.53	295	8.89	8.93	8.89
O II(B)	4650.00	105	8.19	8.20	8.20	136	8.11	8.15	8.12	421	8.63	8.66	8.62
O II	4661.63	44	8.36	8.37	8.37	84	8.56	8.61	8.58	184	8.79	8.81	8.78
O II	4673.73	24	8.91	8.92	8.92	27	8.73	8.75	8.73	64	8.93	8.95	8.92
O II	4676.23	54	8.63	8.64	8.64	73	8.59	8.63	8.61	161	8.80	8.83	8.79
O II	4699.00	26	8.27	8.28	8.28	48	8.35	8.38	8.35	84	8.31	8.32	8.29
O II	4705.35	36	8.44	8.46	8.46	48	8.33	8.37	8.34	108	8.46	8.48	8.44
O II	4710.00					20	8.72	8.74	8.72	42	8.76	8.77	8.74
Mg II(B)	4481.00	350	7.28	7.30	7.30	294	7.27	7.31	7.33	215	7.25	7.26	7.29
Si II	4128.05	141	7.45	7.48	7.48	107	7.40	7.45	7.47	61	7.38	7.39	7.44
Si II	4130.89	149	7.30	7.33	7.33	118	7.28	7.32	7.34	73	7.29	7.31	7.35
Si III	4552.62	241	7.37	7.41	7.41	281	7.34	7.46	7.42	415	7.36	7.42	7.38
Si III	4567.84	192	7.37	7.41	7.41	224	7.33	7.43	7.40	343	7.36	7.42	7.38
Si III	4574.75	108	7.36	7.39	7.39	132	7.34	7.41	7.38	208	7.38	7.41	7.38
Si IV	4116.10									77	7.35	7.38	7.32
Fe III	4419.60	78	7.47	7.48	7.48	77	7.44	7.47	7.46	70	7.37	7.38	7.38
Fe III	4431.02	57	7.59	7.60	7.60	48	7.48	7.50	7.49				

Table C.2. Contd. STARS:#6, #15, #17

		NGC4755-006				NGC4755-015				NGC4755-017			
ION	λ	EW (mÅ)	(1)	(2)	(3)	EW (mÅ)	(1)	(2)	(3)	EW (mÅ)	(1)	(2)	(3)
C II	3920.68	286	8.59	8.27	8.41	63	7.59	7.50	7.57	95	7.86	8.01	8.02
C II(B)	4267.00	223	7.64	7.54	7.60	165	7.66	7.58	7.64	203	7.83	7.92	7.93
C II	6578.05												
C II	6582.88												
N II	3955.85					40	8.06	7.95	7.96				
N II	3995.00	131	7.53	7.41	7.39	117	7.96	7.71	7.74	61	7.41	7.51	7.53
N II	4447.03					45	7.56	7.48	7.46	52	7.91	8.00	8.02
N II	4601.48	88	7.94	7.85	7.81								
N II	4613.86	54	7.86	7.80	7.75								
N II	4630.54	127	7.72	7.61	7.58	117	8.26	7.96	8.00	49	7.53	7.63	7.65
N II	4643.08					64	8.06	7.91	7.91	30	7.67	7.73	7.75
O II(B)	3912.00	120	8.99	8.82	8.77	96	9.13	8.95	8.90				
O II	3945.04	96	9.03	8.88	8.83	50	8.83	8.68	8.63				
O II	3954.36	129	8.96	8.77	8.73	80	9.00	8.78	8.74				
O II	3982.71	104	9.12	8.94	8.90								
O II(B)	4069.00	246	9.18	8.93	8.88	153	9.02	8.79	8.73	65	8.43	8.52	8.55
O II	4072.15	205	9.19	8.86	8.85	118	9.25	8.90	8.90	56	8.58	8.73	8.76
O II	4075.86	251	9.29	8.91	8.91	116	9.03	8.69	8.68	78	8.76	8.94	8.97
O II	4078.84					50	9.05	8.86	8.82				
O II	4132.80	118	9.24	9.04	8.99								
O II	4156.53	36	9.10	9.01	8.94	24	8.91	8.83	8.77				
O II(B)	4317.00	164	9.31	9.07	9.03	107	9.43	9.14	9.12	46	8.76	8.88	8.91
O II	4319.63	172	9.36	9.12	9.08	87	9.14	8.89	8.86	31	8.45	8.53	8.56
O II	4325.76												
O II	4349.43					104	9.10	8.81	8.77				
O II(B)	4351.00					86	8.97	8.81	8.73				
O II	4353.58												
O II(B)	4366.00	197	9.44	9.18	9.14	93	9.15	8.88	8.85	40	8.57	8.68	8.71
O II	4369.27					33	8.93	8.81	8.75				
O II	4395.94					60	9.28	9.09	9.04	33	9.11	9.21	9.24
O II	4414.90	204	9.03	8.76	8.73	123	9.00	8.75	8.71	40	8.15	8.24	8.27
O II	4416.98	150	8.95	8.73	8.68	117	9.26	8.98	8.96	43	8.49	8.61	8.64
O II	4452.38	85	9.21	9.06	9.00	46	8.99	8.85	8.80				
O II	4590.97	171	9.18	8.94	8.88	91	9.04	8.79	8.74	46	8.72	8.84	8.87
O II(B)	4596.18	156	9.18	8.97	8.90	103	9.17	8.97	8.91	40	8.69	8.77	8.80
O II	4638.86	178	9.27	9.03	8.99	100	9.22	8.95	8.91	40	8.62	8.72	8.75
O II	4641.81					124	9.05	8.73	8.70	41	8.21	8.31	8.34
O II(B)	4650.00					190	8.74	8.50	8.45				
O II	4661.63	198	9.31	9.05	9.01	99	9.12	8.85	8.81	34	8.42	8.51	8.55
O II	4673.73	44	8.96	8.86	8.80	39	9.12	8.99	8.93				
O II	4676.23	204	9.48	9.22	9.18	93	9.18	8.93	8.89				
O II	4699.00	113	8.87	8.73	8.65	96	8.92	8.79	8.70				
O II	4705.35	136	9.06	8.85	8.79	84	8.97	8.78	8.71				
O II	4710.00	42	9.07	8.97	8.89	57	9.58	9.42	9.38				
Mg II(B)	4481.00	230	7.18	7.07	7.21	131	7.16	7.02	7.09	184	7.19	7.33	7.32
Si II	4128.05									50	7.33	7.59	7.58
Si II	4130.89									51	7.10	7.32	7.31
Si III	4552.62	357	7.75	7.34	7.38	179	7.84	7.40	7.46	111	7.24	7.49	7.51
Si III	4567.84	304	7.77	7.40	7.43	144	7.78	7.37	7.41	79	7.12	7.33	7.36
Si III	4574.75	196	7.77	7.50	7.49	104	7.87	7.51	7.53	52	7.25	7.41	7.44
Si IV	4116.10	54	7.78	7.55	7.47	30	7.84	7.60	7.46				
Fe III	4419.60					34	7.72	7.56	7.73				
Fe III	4431.02												

Table C.2. Contd. STARS:#20, #33, #40

		NGC4755-020				NGC4755-033				NGC4755-040			
ION	λ	EW (mÅ)	(1)	(2)	(3)	EW (mÅ)	(1)	(2)	(3)	EW (mÅ)	(1)	(2)	(3)
C II	3920.68	96	7.99	8.11	8.11	76	7.75	8.10	8.01	99	8.58	8.26	8.38
C II(B)	4267.00	213	7.95	8.02	8.01	190	7.92	8.19	8.17	219	8.45	8.28	8.31
C II	6578.05	155	8.14	8.28	8.28	111	8.02	8.29	8.26	144	8.80	8.45	8.57
C II	6582.88	137	8.24	8.39	8.39	98	8.10	8.40	8.35	138	9.03	8.64	8.79
N II	3955.85	15	7.53	7.56	7.57								
N II	3995.00	67	7.42	7.49	7.51	21	7.12	7.18	7.23	39	7.75	7.59	7.58
N II	4447.03												
N II	4601.48	40	7.78	7.84	7.85								
N II	4613.86	24	7.66	7.70	7.71								
N II	4630.54	58	7.57	7.65	7.67	21	7.45	7.59	7.63	33	7.99	7.84	7.81
N II	4643.08	37	7.70	7.75	7.76								
O II(B)	3912.00	39	8.45	8.50	8.52								
O II	3945.04	27	8.48	8.53	8.56								
O II	3954.36	37	8.43	8.50	8.53								
O II	3982.71	20	8.38	8.42	8.45								
O II(B)	4069.00	75	8.35	8.42	8.45	22	8.31	8.44	8.53	36	8.84	8.72	8.64
O II	4072.15	57	8.43	8.54	8.56	18	8.30	8.51	8.57	36	9.18	8.98	8.94
O II	4075.86	86	8.74	8.87	8.89	35	8.63	8.93	8.95	63	9.54	9.35	9.35
O II	4078.84	16	8.26	8.29	8.32								
O II	4132.80	22	8.28	8.32	8.35								
O II	4156.53	12	8.50	8.53	8.55								
O II(B)	4317.00	47	8.61	8.69	8.71								
O II	4319.63	38	8.42	8.49	8.51								
O II	4325.76												
O II	4349.43												
O II(B)	4351.00												
O II	4353.58												
O II(B)	4366.00	41	8.42	8.50	8.52								
O II	4369.27												
O II	4395.94	34	8.93	9.00	9.03								
O II	4414.90	62	8.36	8.44	8.47								
O II	4416.98	51	8.47	8.56	8.59								
O II	4452.38	23	8.60	8.64	8.66								
O II	4590.97	36	8.29	8.35	8.38								
O II(B)	4596.18	36	8.37	8.42	8.45								
O II	4638.86	46	8.54	8.61	8.64								
O II	4641.81	61	8.37	8.47	8.50								
O II(B)	4650.00	57	7.76	7.81	7.83								
O II	4661.63	40	8.35	8.42	8.44								
O II	4673.73	15	8.60	8.63	8.65								
O II	4676.23	36	8.39	8.45	8.47								
O II	4699.00	37	8.29	8.32	8.35								
O II	4705.35	35	8.33	8.38	8.41								
O II	4710.00	18	8.87	8.92	8.95								
Mg II(B)	4481.00	167	7.34	7.45	7.44	233	7.02	7.44	7.09	185	7.28	6.98	7.19
Si II	4128.05	34	7.31	7.46	7.45	75	7.15	8.15	7.36	51	7.84	7.13	7.56
Si II	4130.89	38	7.17	7.31	7.30	77	6.96	7.85	7.12	54	7.58	6.94	7.30
Si III	4552.62	111	7.23	7.42	7.44	62	7.09	7.54	7.44	62	7.68	7.35	7.40
Si III	4567.84	83	7.13	7.30	7.32	35	6.91	7.23	7.19	49	7.67	7.37	7.41
Si III	4574.75	56	7.24	7.38	7.40	24	7.14	7.41	7.39	32	7.76	7.50	7.52
Si IV	4116.10												
Fe III	4419.60	33	7.83	7.83	7.84								
Fe III	4431.02												

Table C.2. Contd. STARS:#48

ION	λ	NGC4755-048 EW (mÅ)	(1)	(2)	(3)
C II	3920.68	90	8.07	8.29	8.25
C II(B)	4267.00	207	8.15	8.29	8.30
C II	6578.05	109	8.12	8.27	8.27
C II	6582.88	107	8.29	8.49	8.47
N II	3955.85				
N II	3995.00	24	7.19	7.25	7.30
N II	4447.03				
N II	4601.48				
N II	4613.86				
N II	4630.54	20	7.46	7.53	7.59
N II	4643.08				
O II(B)	3912.00				
O II	3945.04				
O II	3954.36				
O II	3982.71				
O II(B)	4069.00	29	8.52	8.60	8.69
O II	4072.15	30	8.75	8.90	8.96
O II	4075.86	50	9.06	9.24	9.28
O II	4078.84				
O II	4132.80	15	8.89	8.99	9.08
O II	4156.53				
O II(B)	4317.00				
O II	4319.63				
O II	4325.76				
O II	4349.43				
O II(B)	4351.00				
O II	4353.58				
O II(B)	4366.00				
O II	4369.27				
O II	4395.94				
O II	4414.90				
O II	4416.98				
O II	4452.38				
O II	4590.97				
O II(B)	4596.18				
O II	4638.86				
O II	4641.81				
O II(B)	4650.00				
O II	4661.63				
O II	4673.73				
O II	4676.23				
O II	4699.00				
O II	4705.35				
O II	4710.00				
Mg II(B)	4481.00	202	7.03	7.25	7.08
Si II	4128.05	60	7.22	7.75	7.38
Si II	4130.89	72	7.17	7.74	7.35
Si III	4552.62	59	7.22	7.46	7.45
Si III	4567.84	35	7.01	7.20	7.22
Si III	4574.75	27	7.31	7.48	7.50
Si IV	4116.10				
Fe III	4419.60				
Fe III	4431.02				

Table C.3. Equivalent widths and line by line absolute abundances of NGC2004 for stars #3, #5, & #7. Columns are as for Table C.1.

		NGC2004-003				NGC2004-005				NGC2004-007			
ION	λ	EW (mÅ)	Abundance			EW (mÅ)	Abundance			EW (mÅ)	Abundance		
C II	3920.68	90	7.68	7.66	7.66	49	7.48	7.70	7.68	42	7.40	7.74	7.69
C II(B)	4267.00	173	7.68	7.66	7.66	105	7.50	7.79	7.77	86	7.36	7.74	7.73
C II	6578.05												
C II	6582.88												
N II	3955.85	21	7.90	7.89	7.89								
N II	3995.00	83	7.81	7.79	7.79	34	7.52	7.76	7.77	28	7.43	7.78	7.78
N II	4447.03	31	7.82	7.81	7.81	11	7.69	7.79	7.85				
N II	4601.48	31	7.88	7.86	7.86	11	7.72	7.82	7.87				
N II	4613.86	19	7.81	7.80	7.80								
N II	4630.54	60	7.86	7.84	7.84	27	7.75	7.94	7.98	15	7.51	7.72	7.77
N II	4643.08	34	7.94	7.93	7.93	10	7.69	7.77	7.83				
O II(B)	3912.00	12	8.39	8.38	8.38								
O II	3945.04	8	8.31	8.30	8.30								
O II	3954.36	15	8.35	8.33	8.33								
O II	3982.71	8	8.31	8.30	8.30								
O II(B)	4069.00	29	8.36	8.35	8.35								
O II	4072.15	28	8.45	8.43	8.43								
O II	4075.86	37	8.50	8.47	8.47								
O II	4078.84												
O II	4132.80												
O II	4156.53												
O II(B)	4317.00	19	8.49	8.48	8.48								
O II	4319.63	23	8.63	8.62	8.62								
O II	4325.76												
O II	4349.43												
O II(B)	4351.00												
O II	4353.58												
O II(B)	4366.00	18	8.38	8.37	8.37								
O II	4369.27												
O II	4395.94												
O II	4414.90	32	8.43	8.41	8.41	26	8.82	9.13	9.15				
O II	4416.98	30	8.63	8.61	8.61	17	8.79	9.07	9.10	12	8.64	9.00	9.06
O II	4452.38	10	8.69	8.68	8.68								
O II	4590.97	17	8.50	8.48	8.48								
O II(B)	4596.18	16	8.57	8.55	8.55								
O II	4638.86	20	8.51	8.49	8.49	8	8.53	8.69	8.78	8	8.61	8.89	9.02
O II	4641.81	37	8.50	8.48	8.48	8	8.12	8.24	8.32	7	8.13	8.34	8.45
O II(B)	4650.00												
O II	4661.63												
O II	4673.73												
O II	4676.23	21	8.61	8.59	8.59								
O II	4699.00	8	8.22	8.21	8.21								
O II	4705.35	11	8.38	8.37	8.37								
O II	4710.00												
Mg II(B)	4481.00	302	7.04	7.02	7.02	370	6.78	7.17	6.98	363	6.67	7.37	6.95
Si II	4128.05	133	7.31	7.28	7.28	167	7.02	7.56	7.28	164	6.90	8.13	7.28
Si II	4130.89	144	7.18	7.15	7.15	177	6.88	7.43	7.15	171	6.74	7.92	7.14
Si III	4552.62	107	7.27	7.23	7.23	44	6.97	7.30	7.30	34	6.85	7.34	7.31
Si III	4567.84	77	7.21	7.18	7.18	27	6.87	7.14	7.16	20	6.76	7.13	7.14
Si III	4574.75	44	7.27	7.24	7.24	14	6.98	7.16	7.20	10	6.86	7.12	7.18
Si IV	4116.10												
Fe III	4419.60	37	7.26	7.25	7.25	18	7.08	7.15	7.16	14	7.02	7.12	7.13
Fe III	4431.02	25	7.34	7.33	7.33	12	7.18	7.23	7.25	7	7.01	7.07	7.10

Table C.3. Contd. STARS:#10, #11, #12

		NGC2004-010				NGC2004-011				NGC2004-012			
ION	λ	EW (mÅ)	(1)	(2)	(3)	EW (mÅ)	(1)	(2)	(3)	EW (mÅ)	(1)	(2)	(3)
C II	3920.68	91	7.46	7.48	7.48	51	7.46	7.46	7.45				
C II(B)	4267.00	194	7.50	7.53	7.53	130	7.45	7.46	7.45	134	7.44	7.44	7.44
C II	6578.05									75	7.46	7.46	7.46
C II	6582.88									56	7.48	7.48	7.48
N II	3955.85	64	8.17	8.21	8.19	52	7.84	7.85	7.85	48	7.80	7.80	7.80
N II	3995.00	202	8.05	8.13	8.11	196	7.74	7.76	7.76	177	7.69	7.69	7.69
N II	4447.03	93	8.03	8.07	8.04	76	7.59	7.60	7.60	69	7.54	7.54	7.54
N II	4601.48	97	8.15	8.20	8.17	95	7.84	7.85	7.85	105	7.94	7.94	7.94
N II	4613.86	65	8.10	8.14	8.11	60	7.80	7.81	7.81	56	7.77	7.77	7.77
N II	4630.54	180	8.17	8.24	8.21	153	7.66	7.68	7.68	152	7.71	7.71	7.71
N II	4643.08	108	8.24	8.29	8.26	58	7.55	7.55	7.55	83	7.77	7.77	7.77
O II(B)	3912.00	29	8.25	8.27	8.24	84	8.30	8.32	8.32	86	8.39	8.39	8.39
O II	3945.04	19	8.19	8.21	8.18	57	8.28	8.29	8.30	56	8.34	8.34	8.34
O II	3954.36	30	8.13	8.15	8.12	86	8.20	8.21	8.22	84	8.27	8.27	8.27
O II	3982.71	20	8.22	8.24	8.21	75	8.44	8.45	8.46	55	8.32	8.32	8.32
O II(B)	4069.00	62	8.15	8.17	8.14	188	8.30	8.32	8.33	189	8.43	8.43	8.43
O II	4072.15	74	8.40	8.46	8.42	181	8.45	8.50	8.51	170	8.55	8.55	8.55
O II	4075.86	69	8.17	8.22	8.19	190	8.31	8.36	8.37	173	8.38	8.38	8.38
O II	4078.84					31	8.03	8.04	8.04	37	8.19	8.19	8.19
O II	4132.80					60	8.31	8.32	8.33	71	8.48	8.48	8.48
O II	4156.53					15	8.32	8.32	8.32	21	8.51	8.51	8.51
O II(B)	4317.00	43	8.38	8.41	8.38	133	8.57	8.59	8.60	117	8.57	8.57	8.57
O II	4319.63	43	8.38	8.41	8.38	142	8.62	8.65	8.66	127	8.64	8.64	8.64
O II	4325.76	14	8.46	8.47	8.44	34	8.43	8.44	8.44	33	8.47	8.47	8.47
O II	4349.43	74	8.43	8.47	8.43	227	8.67	8.72	8.73	193	8.67	8.67	8.67
O II(B)	4351.00	24	8.04	8.06	8.02	87	8.10	8.11	8.12	88	8.20	8.20	8.20
O II	4353.58												
O II(B)	4366.00	36	8.18	8.20	8.18	127	8.44	8.46	8.47	122	8.52	8.52	8.52
O II	4369.27									13	8.03	8.03	8.03
O II	4395.94	29	8.78	8.81	8.77	45	8.41	8.42	8.42	45	8.46	8.46	8.46
O II	4414.90	65	8.21	8.26	8.22	223	8.54	8.58	8.59	188	8.52	8.52	8.52
O II	4416.98	46	8.21	8.25	8.22	154	8.45	8.48	8.48	143	8.51	8.51	8.51
O II	4452.38	19	8.44	8.46	8.43	54	8.48	8.49	8.50	54	8.55	8.55	8.55
O II	4590.97	36	8.20	8.23	8.19	137	8.33	8.35	8.36	124	8.39	8.39	8.39
O II(B)	4596.18	30	8.20	8.22	8.19	109	8.27	8.28	8.29	103	8.34	8.34	8.34
O II	4638.86	42	8.30	8.32	8.29	155	8.55	8.57	8.58	139	8.58	8.58	8.58
O II	4641.81	75	8.27	8.31	8.28	272	8.64	8.69	8.70	229	8.62	8.62	8.62
O II(B)	4650.00												
O II	4661.63	51	8.35	8.39	8.35	170	8.55	8.57	8.58	152	8.58	8.58	8.58
O II	4673.73	11	8.38	8.40	8.37	41	8.52	8.53	8.53	33	8.46	8.46	8.46
O II	4676.23	41	8.34	8.37	8.33	154	8.59	8.62	8.63	131	8.58	8.58	8.58
O II	4699.00	20	8.03	8.04	8.01	64	8.02	8.02	8.02	69	8.11	8.11	8.11
O II	4705.35	26	8.14	8.16	8.13	82	8.13	8.15	8.15	87	8.26	8.26	8.26
O II	4710.00	15	8.73	8.75	8.71	23	8.30	8.30	8.31	32	8.53	8.53	8.53
Mg II(B)	4481.00	228	7.06	7.10	7.11	136	7.15	7.16	7.15	132	7.08	7.08	7.08
Si II	4128.05	84	7.22	7.26	7.28								
Si II	4130.89	91	7.08	7.12	7.14								
Si III	4552.62	205	7.16	7.26	7.22	350	7.12	7.20	7.21	308	7.18	7.18	7.18
Si III	4567.84	161	7.16	7.24	7.21	286	7.13	7.19	7.20	256	7.20	7.20	7.20
Si III	4574.75	89	7.16	7.21	7.18	166	7.13	7.16	7.17	151	7.18	7.18	7.18
Si IV	4116.10					87	7.16	7.20	7.22	69	7.21	7.21	7.21
Fe III	4419.60	45	7.19	7.20	7.19	40	7.17	7.17	7.17	32	7.08	7.08	7.08
Fe III	4431.02	33	7.31	7.33	7.32	19	7.11	7.11	7.11	21	7.16	7.16	7.16

Table C.3. Contd. STARS:#14, #21, #22

		NGC2004-014				NGC2004-021				NGC2004-022			
ION	λ	EW (mÅ)	(1)	(2)	(3)	EW (mÅ)	(1)	(2)	(3)	EW (mÅ)	(1)	(2)	(3)
C II	3920.68	98	7.55	7.60	7.61	83	7.63	7.62	7.62	46	7.29	7.29	7.30
C II(B)	4267.00	191	7.52	7.58	7.58	167	7.56	7.55	7.55	119	7.31	7.31	7.32
C II	6578.05	273	8.06	8.16	8.17					61	7.31	7.31	7.31
C II	6582.88	207	8.05	8.13	8.14					47	7.34	7.34	7.35
N II	3955.85	19	7.56	7.58	7.56	18	7.27	7.27	7.26	38	7.71	7.70	7.70
N II	3995.00	82	7.41	7.47	7.47	82	7.10	7.09	7.07	149	7.61	7.58	7.58
N II	4447.03	33	7.48	7.51	7.49	22	6.93	6.93	6.93	68	7.55	7.54	7.54
N II	4601.48	30	7.54	7.57	7.55	42	7.38	7.38	7.37	88	7.88	7.86	7.86
N II	4613.86	17	7.47	7.48	7.46	30	7.42	7.42	7.42	55	7.80	7.79	7.79
N II	4630.54	59	7.49	7.53	7.51	59	7.13	7.13	7.13	118	7.58	7.56	7.56
N II	4643.08	34	7.62	7.65	7.63					73	7.74	7.73	7.73
O II(B)	3912.00	23	8.23	8.26	8.23	94	8.48	8.46	8.43	94	8.55	8.52	8.51
O II	3945.04	18	8.30	8.33	8.31	67	8.48	8.47	8.45	59	8.46	8.45	8.44
O II	3954.36	25	8.17	8.21	8.19	88	8.34	8.32	8.30	86	8.41	8.38	8.37
O II	3982.71	10	8.03	8.04	8.02					59	8.47	8.45	8.44
O II(B)	4069.00	48	8.14	8.18	8.15	197	8.52	8.48	8.44	192	8.60	8.56	8.54
O II	4072.15	39	8.10	8.17	8.15	159	8.52	8.47	8.41	153	8.63	8.56	8.55
O II	4075.86	55	8.19	8.28	8.27	182	8.49	8.43	8.37	157	8.47	8.41	8.39
O II	4078.84					42	8.29	8.28	8.26	41	8.34	8.32	8.31
O II	4132.80					54	8.30	8.28	8.26	58	8.41	8.39	8.38
O II	4156.53					20	8.49	8.49	8.48	28	8.72	8.71	8.70
O II(B)	4317.00	29	8.29	8.32	8.30	128	8.70	8.67	8.63	120	8.75	8.71	8.70
O II	4319.63	32	8.35	8.40	8.38	135	8.75	8.71	8.67	119	8.74	8.70	8.69
O II	4325.76					38	8.57	8.56	8.54	35	8.58	8.57	8.56
O II	4349.43	48	8.36	8.41	8.38	198	8.77	8.73	8.67	183	8.84	8.79	8.77
O II(B)	4351.00	17	8.06	8.08	8.06	86	8.23	8.22	8.19	100	8.44	8.41	8.40
O II	4353.58									24	8.55	8.54	8.52
O II(B)	4366.00	25	8.12	8.15	8.12	136	8.67	8.63	8.59	124	8.69	8.65	8.63
O II	4369.27					14	8.06	8.06	8.06	24	8.36	8.35	8.34
O II	4395.94					53	8.58	8.57	8.55	48	8.57	8.56	8.55
O II	4414.90	44	8.11	8.17	8.16	201	8.65	8.61	8.56	179	8.67	8.61	8.60
O II	4416.98	38	8.27	8.33	8.31	153	8.63	8.59	8.55	136	8.63	8.59	8.58
O II	4452.38	17	8.53	8.57	8.55	61	8.66	8.65	8.62	56	8.67	8.65	8.64
O II	4590.97	20	8.06	8.09	8.07	140	8.56	8.53	8.49	126	8.59	8.55	8.53
O II(B)	4596.18	19	8.14	8.17	8.15	116	8.50	8.48	8.45	109	8.55	8.52	8.51
O II	4638.86	36	8.41	8.46	8.44	163	8.79	8.75	8.70	145	8.80	8.75	8.74
O II	4641.81	57	8.30	8.36	8.35					212	8.75	8.70	8.68
O II(B)	4650.00												
O II	4661.63	35	8.32	8.37	8.34	171	8.75	8.71	8.67	148	8.73	8.69	8.67
O II	4673.73					41	8.61	8.60	8.58	44	8.72	8.70	8.69
O II	4676.23	30	8.35	8.39	8.37	149	8.75	8.72	8.67	130	8.74	8.70	8.69
O II	4699.00	16	8.08	8.10	8.07	80	8.24	8.23	8.21	84	8.34	8.32	8.31
O II	4705.35	19	8.15	8.18	8.16	95	8.37	8.35	8.32	92	8.43	8.41	8.39
O II	4710.00					28	8.51	8.50	8.48	43	8.83	8.81	8.80
Mg II(B)	4481.00	214	6.96	7.02	7.06	144	7.09	7.08	7.07	116	6.94	6.94	6.94
Si II	4128.05	80	7.15	7.23	7.28								
Si II	4130.89	89	7.02	7.10	7.16								
Si III	4552.62	146	7.08	7.22	7.24	318	7.30	7.22	7.14	270	7.28	7.20	7.19
Si III	4567.84	112	7.08	7.20	7.21	266	7.32	7.25	7.18	231	7.34	7.26	7.25
Si III	4574.75	60	7.08	7.16	7.15	163	7.31	7.27	7.22	142	7.31	7.26	7.25
Si IV	4116.10					63	7.32	7.28	7.23	52	7.31	7.26	7.22
Fe III	4419.60	30	7.14	7.16	7.15	39	7.17	7.17	7.16	23	7.00	7.00	7.00
Fe III	4431.02	18	7.19	7.20	7.19	24	7.22	7.22	7.22				

Table C.3. Contd. STARS:#26, #29, #36

		NGC2004-026				NGC2004-029				NGC2004-036			
ION	λ	EW (mÅ)	(1)	(2)	(3)	EW (mÅ)	(1)	(2)	(3)	EW (mÅ)	(1)	(2)	(3)
C II	3920.68	64	7.70	7.74	7.75	56	7.64	7.64	7.64	56	7.49	7.45	7.54
C II(B)	4267.00	131	7.51	7.52	7.53	112	7.43	7.43	7.43	131	7.46	7.42	7.51
C II	6578.05	124	7.91	7.97	7.98	85	7.59	7.59	7.59	95	7.54	7.49	7.56
C II	6582.88	98	7.91	7.96	7.97	77	7.71	7.71	7.71	68	7.51	7.48	7.55
N II	3955.85									22	7.49	7.45	7.46
N II	3995.00					41	6.87	6.87	6.87	88	7.37	7.27	7.28
N II	4447.03					12	6.75	6.75	6.75	41	7.35	7.31	7.30
N II	4601.48	21	7.21	7.22	7.20								
N II	4613.86	10	7.04	7.05	7.03					30	7.55	7.51	7.51
N II	4630.54	27	6.91	6.91	6.90	23	6.80	6.80	6.80	65	7.34	7.28	7.27
N II	4643.08	12	6.92	6.91	6.90	10	6.82	6.82	6.82	42	7.51	7.47	7.46
O II(B)	3912.00	42	8.24	8.27	8.23	48	8.20	8.20	8.20	88	8.69	8.57	8.49
O II	3945.04	26	8.20	8.22	8.19	37	8.33	8.33	8.33	54	8.58	8.48	8.41
O II	3954.36	35	8.10	8.13	8.09	52	8.27	8.27	8.27	80	8.59	8.45	8.37
O II	3982.71	23	8.17	8.19	8.15	32	8.24	8.24	8.24	53	8.58	8.48	8.41
O II(B)	4069.00	87	8.22	8.26	8.22	107	8.27	8.27	8.27	174	8.79	8.60	8.51
O II	4072.15	51	8.05	8.10	8.06	74	8.30	8.30	8.30	130	8.93	8.60	8.54
O II	4075.86	63	8.10	8.16	8.12	80	8.21	8.21	8.21	133	8.76	8.44	8.37
O II	4078.84	20	8.15	8.17	8.14	27	8.23	8.23	8.23	45	8.61	8.49	8.42
O II	4132.80	27	8.17	8.20	8.16	29	8.09	8.09	8.09	49	8.46	8.36	8.28
O II	4156.53	9	8.14	8.15	8.13					25	8.74	8.69	8.62
O II(B)	4317.00	44	8.27	8.31	8.27	64	8.50	8.50	8.50				
O II	4319.63	47	8.33	8.38	8.33	67	8.55	8.55	8.55	106	8.99	8.76	8.69
O II	4325.76	13	8.22	8.23	8.20	19	8.32	8.32	8.32	33	8.69	8.61	8.54
O II	4349.43	56	8.23	8.28	8.23	75	8.33	8.33	8.33				
O II(B)	4351.00	35	8.03	8.05	8.01	44	8.00	8.00	8.00	103	8.70	8.57	8.45
O II	4353.58												
O II(B)	4366.00	46	8.26	8.31	8.26	63	8.42	8.42	8.42	101	8.82	8.61	8.54
O II	4369.27	11	8.10	8.11	8.08	16	8.18	8.18	8.18	24	8.44	8.40	8.32
O II	4395.94	30	8.57	8.60	8.56	36	8.56	8.56	8.56				
O II	4414.90	62	8.11	8.16	8.12	82	8.24	8.24	8.24	157	8.91	8.66	8.59
O II	4416.98	46	8.14	8.18	8.14	68	8.36	8.36	8.36	127	8.94	8.70	8.63
O II	4452.38	21	8.29	8.31	8.28	28	8.36	8.36	8.36	53	8.82	8.71	8.63
O II	4590.97	47	8.20	8.24	8.19	60	8.23	8.23	8.23	109	8.80	8.58	8.48
O II(B)	4596.18	39	8.12	8.14	8.10	65	8.36	8.36	8.36	95	8.67	8.54	8.43
O II	4638.86	49	8.29	8.33	8.28	68	8.43	8.43	8.43	114	8.91	8.69	8.60
O II	4641.81	70	8.21	8.27	8.22	88	8.28	8.28	8.28	162	8.90	8.61	8.53
O II(B)	4650.00												
O II	4661.63	48	8.20	8.24	8.20	65	8.31	8.31	8.31	115	8.83	8.61	8.53
O II	4673.73	16	8.36	8.37	8.34	22	8.42	8.42	8.42	36	8.74	8.66	8.58
O II	4676.23	42	8.21	8.24	8.20	54	8.25	8.25	8.25	92	8.71	8.54	8.45
O II	4699.00	38	8.02	8.03	8.00	51	8.07	8.07	8.07	75	8.37	8.32	8.21
O II	4705.35	33	7.99	8.01	7.97	44	8.05	8.05	8.05	74	8.47	8.35	8.25
O II	4710.00					19	8.44	8.44	8.44	34	8.83	8.75	8.65
Mg II(B)	4481.00	100	7.03	7.07	7.08	93	7.03	7.03	7.03	96	6.88	6.84	6.93
Si II	4128.05	24	7.28	7.34	7.37								
Si II	4130.89	24	7.04	7.08	7.12								
Si III	4552.62	114	7.17	7.30	7.26	129	7.22	7.22	7.22	205	7.56	7.14	7.14
Si III	4567.84	95	7.18	7.31	7.27	106	7.19	7.19	7.19	180	7.62	7.24	7.23
Si III	4574.75	60	7.17	7.27	7.23	69	7.21	7.21	7.21	115	7.54	7.27	7.25
Si IV	4116.10					28	7.20	7.20	7.20	46	7.59	7.38	7.18
Fe III	4419.60	24	7.33	7.38	7.38	27	7.37	7.37	7.37	35	7.32	7.26	7.29
Fe III	4431.02	14	7.22	7.31	7.31	16	7.28	7.32	7.32				

Table C.3. Contd. STARS:#42, #46, #53

		NGC2004-042				NGC2004-046				NGC2004-053			
ION	λ	EW (mÅ)	(1)	(2)	(3)	EW (mÅ)	(1)	(2)	(3)	EW (mÅ)	(1)	(2)	(3)
C II	3920.68	82	7.77	7.81	7.81	29	7.45	7.44	7.47	17	7.93	7.93	7.84
C II(B)	4267.00	165	7.62	7.64	7.64	95	7.52	7.50	7.52	76	7.93	7.89	7.83
C II	6578.05	147	7.91	7.96	7.96	62	7.58	7.54	7.56	37	7.81	7.80	7.71
C II	6582.88	111	7.86	7.90	7.90	48	7.61	7.58	7.60	21	7.76	7.76	7.67
N II	3955.85					13	7.43	7.41	7.44				
N II	3995.00	37	6.87	6.89	6.88	81	7.59	7.52	7.54	50	7.74	7.70	7.63
N II	4447.03					42	7.51	7.47	7.49				
N II	4601.48												
N II	4613.86					33	7.88	7.83	7.86				
N II	4630.54	25	6.92	6.93	6.92	68	7.69	7.61	7.64	35	7.71	7.66	7.61
N II	4643.08					34	7.61	7.58	7.61	16	7.75	7.73	7.67
O II(B)	3912.00	34	8.27	8.29	8.28	68	8.39	8.34	8.35	50	8.38	8.34	8.29
O II	3945.04	17	8.09	8.10	8.09	48	8.48	8.42	8.43	31	8.47	8.43	8.39
O II	3954.36	26	8.05	8.07	8.06	60	8.33	8.26	8.27	49	8.42	8.36	8.32
O II	3982.71					44	8.43	8.38	8.39	29	8.44	8.41	8.36
O II(B)	4069.00	58	8.05	8.08	8.07	144	8.53	8.41	8.41	145	8.65	8.52	8.49
O II	4072.15	36	7.91	7.95	7.93	93	8.53	8.35	8.35	66	8.18	8.07	8.04
O II	4075.86	55	8.15	8.20	8.18	98	8.40	8.22	8.22	82	8.21	8.06	8.04
O II	4078.84	12	8.00	8.01	8.00	33	8.31	8.25	8.26	40	8.70	8.61	8.57
O II	4132.80					54	8.51	8.43	8.43				
O II	4156.53					16	8.35	8.33	8.34				
O II(B)	4317.00	34	8.23	8.25	8.24	75	8.66	8.53	8.54	55	8.70	8.63	8.57
O II	4319.63	28	8.07	8.09	8.08	74	8.63	8.51	8.52	60	8.77	8.69	8.62
O II	4325.76					27	8.54	8.50	8.52				
O II	4349.43					120	9.07	8.82	8.83				
O II(B)	4351.00					79	8.32	8.26	8.26	55	8.09	8.04	8.01
O II	4353.58									12	8.20	8.18	8.16
O II(B)	4366.00	33	8.13	8.17	8.15	74	8.57	8.43	8.44	58	8.67	8.60	8.53
O II	4369.27									12	8.22	8.22	8.17
O II	4395.94					54	8.81	8.72	8.73	30	8.51	8.48	8.45
O II	4414.90	47	8.04	8.07	8.06	111	8.49	8.38	8.39	79	8.49	8.41	8.35
O II	4416.98	38	8.15	8.19	8.18	100	8.70	8.57	8.58	69	8.62	8.54	8.48
O II	4452.38	23	8.53	8.56	8.55	48	8.70	8.64	8.65	25	8.65	8.63	8.56
O II	4590.97					91	8.59	8.45	8.46	69	8.45	8.35	8.31
O II(B)	4596.18					87	8.53	8.44	8.45	59	8.42	8.36	8.30
O II	4638.86	42	8.36	8.39	8.38	86	8.61	8.50	8.50	73	8.77	8.67	8.61
O II	4641.81	52	8.11	8.16	8.14	118	8.60	8.42	8.43	107	8.73	8.57	8.52
O II(B)	4650.00												
O II	4661.63	36	8.16	8.19	8.18	85	8.52	8.41	8.42	72	8.69	8.59	8.53
O II	4673.73					37	8.73	8.68	8.69	30	9.01	8.97	8.89
O II	4676.23					68	8.39	8.31	8.32	49	8.52	8.48	8.41
O II	4699.00					77	8.22	8.19	8.19	61	8.30	8.29	8.23
O II	4705.35					61	8.17	8.12	8.12	57	8.30	8.25	8.20
O II	4710.00					38	8.83	8.76	8.76	26	8.67	8.63	8.60
Mg II(B)	4481.00	134	7.09	7.13	7.14	76	7.05	7.01	7.02	80	7.31	7.25	7.24
Si II	4128.05	27	7.04	7.09	7.10								
Si II	4130.89	41	7.17	7.25	7.26								
Si III	4552.62	111	7.15	7.25	7.24	129	7.36	7.10	7.13	103	7.37	7.13	7.09
Si III	4567.84	83	7.04	7.13	7.12	113	7.43	7.19	7.21	89	7.46	7.26	7.21
Si III	4574.75	55	7.14	7.21	7.20	79	7.50	7.30	7.33	45	7.41	7.30	7.23
Si IV	4116.10					54	7.43	7.26	7.22	133	7.41	6.98	7.18
Fe III	4419.60	22	7.17	7.21	7.20								
Fe III	4431.02												

Table C.3. Contd. STARS:#61, #64, #70

		NGC2004-061				NGC2004-064				NGC2004-070			
ION	λ	EW (mÅ)	(1)	(2)	(3)	EW (mÅ)	(1)	(2)	(3)	EW (mÅ)	(1)	(2)	(3)
C II	3920.68	84	7.97	7.90	7.90								
C II(B)	4267.00	175	7.78	7.75	7.75	94	7.50	7.48	7.49	88	7.59	7.56	7.58
C II	6578.05	138	7.98	7.92	7.92	47	7.37	7.35	7.36	67	7.75	7.67	7.68
C II	6582.88	110	7.97	7.92	7.92	40	7.48	7.46	7.47	47	7.71	7.66	7.68
N II	3955.85					17	7.56	7.53	7.55				
N II	3995.00	41	6.95	6.93	6.94	96	7.65	7.54	7.56	82	7.70	7.58	7.59
N II	4447.03	18	6.99	6.98	6.99	46	7.52	7.47	7.48	34	7.45	7.40	7.42
N II	4601.48					31	7.52	7.48	7.50				
N II	4613.86												
N II	4630.54	33	7.05	7.04	7.05					45	7.44	7.38	7.40
N II	4643.08					34	7.56	7.52	7.54	17	7.32	7.31	7.33
O II(B)	3912.00	28	8.09	8.07	8.09	27	7.70	7.68	7.68				
O II	3945.04					52	8.44	8.37	8.37	53	8.55	8.45	8.45
O II	3954.36	36	8.27	8.24	8.26	68	8.31	8.22	8.22	62	8.34	8.23	8.22
O II	3982.71	18	8.12	8.10	8.12	54	8.48	8.41	8.41	51	8.54	8.44	8.44
O II(B)	4069.00	71	8.23	8.19	8.21	169	8.55	8.38	8.38	180	8.84	8.56	8.55
O II	4072.15	54	8.36	8.30	8.32	113	8.55	8.30	8.29	127	9.06	8.63	8.62
O II	4075.86	65	8.41	8.34	8.37	112	8.32	8.09	8.08	133	8.92	8.49	8.48
O II	4078.84	18	8.23	8.20	8.22	35	8.26	8.19	8.19	51	8.70	8.54	8.53
O II	4132.80									54	8.47	8.34	8.33
O II	4156.53												
O II(B)	4317.00	32	8.15	8.12	8.14	88	8.65	8.49	8.49	90	8.92	8.64	8.64
O II	4319.63	39	8.33	8.29	8.32	103	8.87	8.66	8.66	103	9.16	8.81	8.81
O II	4325.76					43	8.82	8.73	8.74	42	8.93	8.80	8.80
O II	4349.43					137	8.90	8.61	8.62	117	9.00	8.59	8.59
O II(B)	4351.00					91	8.32	8.22	8.22	86	8.33	8.21	8.20
O II	4353.58												
O II(B)	4366.00	30	8.05	8.02	8.04	87	8.54	8.38	8.39	88	8.80	8.52	8.51
O II	4369.27					14	8.02	8.01	8.01	25	8.36	8.32	8.31
O II	4395.94					35	8.35	8.30	8.30	50	8.69	8.57	8.56
O II	4414.90	63	8.35	8.30	8.32	128	8.47	8.33	8.33	131	8.69	8.46	8.46
O II	4416.98	53	8.49	8.44	8.46	125	8.76	8.58	8.58	119	8.90	8.65	8.64
O II	4452.38	37	8.91	8.87	8.90	49	8.61	8.55	8.55	48	8.69	8.59	8.59
O II	4590.97					112	8.62	8.44	8.43				
O II(B)	4596.18					91	8.42	8.32	8.31				
O II	4638.86	46	8.44	8.39	8.42	107	8.67	8.51	8.51	119	9.08	8.76	8.75
O II	4641.81	66	8.39	8.32	8.35	154	8.70	8.45	8.45	95	8.26	8.06	8.05
O II(B)	4650.00												
O II	4661.63	44	8.33	8.28	8.31	105	8.57	8.41	8.41				
O II	4673.73					40	8.69	8.63	8.63				
O II	4676.23					87	8.49	8.37	8.38				
O II	4699.00					75	8.14	8.11	8.11				
O II	4705.35					74	8.23	8.15	8.15				
O II	4710.00					51	8.95	8.85	8.85				
Mg II(B)	4481.00	125	7.20	7.14	7.13	90	7.12	7.06	7.08	86	7.23	7.14	7.15
Si II	4128.05	33	7.49	7.39	7.38								
Si II	4130.89	28	7.03	6.97	6.95								
Si III	4552.62	99	7.22	7.10	7.12	174	7.45	7.09	7.10	139	7.55	7.09	7.09
Si III	4567.84	82	7.23	7.11	7.13	152	7.51	7.18	7.19	124	7.65	7.20	7.21
Si III	4574.75	58	7.35	7.25	7.27	97	7.45	7.23	7.24	81	7.60	7.27	7.28
Si IV	4116.10					75	7.49	7.24	7.18	77	7.61	7.26	7.20
Fe III	4419.60	30	7.53	7.44	7.44								
Fe III	4431.02												

Table C.3. Contd. STARS:#84, #90, #91

		NGC2004-084				NGC2004-090				NGC2004-091			
ION	λ	EW (mÅ)	(1)	(2)	(3)	EW (mÅ)	(1)	(2)	(3)	EW (mÅ)	(1)	(2)	(3)
C II	3920.68	36	7.71	7.68	7.71					60	8.02	8.04	8.04
C II(B)	4267.00	96	7.64	7.61	7.64	41	7.53	7.54	7.63	125	7.80	7.81	7.80
C II	6578.05	76	7.85	7.77	7.80					100	8.04	8.09	8.08
C II	6582.88	59	7.88	7.82	7.84					82	8.10	8.14	8.13
N II	3955.85												
N II	3995.00	35	7.00	6.98	6.99	40	7.59	7.62	7.72	50	7.19	7.21	7.21
N II	4447.03					20	7.43	7.45	7.51	33	7.38	7.40	7.39
N II	4601.48												
N II	4613.86	18	7.58	7.55	7.57					15	7.42	7.43	7.43
N II	4630.54	36	7.29	7.26	7.28	30	7.60	7.64	7.73	34	7.19	7.21	7.20
N II	4643.08	15	7.24	7.23	7.26					16	7.22	7.22	7.22
O II(B)	3912.00	79	8.51	8.43	8.42	45	8.32	8.35	8.42	66	8.37	8.40	8.40
O II	3945.04	62	8.71	8.61	8.60	15	8.06	8.08	8.15	42	8.38	8.41	8.41
O II	3954.36	75	8.55	8.43	8.42	29	8.08	8.11	8.18	55	8.26	8.29	8.30
O II	3982.71	50	8.54	8.46	8.45	22	8.27	8.29	8.38	33	8.25	8.26	8.27
O II(B)	4069.00	168	8.73	8.53	8.51	126	8.51	8.61	8.68	121	8.26	8.31	8.31
O II	4072.15	93	8.48	8.25	8.23	65	8.18	8.29	8.36	70	8.07	8.12	8.13
O II	4075.86	109	8.54	8.26	8.25	66	8.01	8.12	8.19	92	8.22	8.31	8.31
O II	4078.84	33	8.29	8.22	8.21	18	8.17	8.21	8.29	37	8.40	8.43	8.43
O II	4132.80	54	8.47	8.37	8.36	24	8.13	8.15	8.22				
O II	4156.53	24	8.60	8.58	8.58								
O II(B)	4317.00	85	8.83	8.62	8.61	45	8.58	8.62	8.72	62	8.39	8.43	8.44
O II	4319.63	79	8.71	8.53	8.52	40	8.51	8.54	8.63	53	8.22	8.26	8.26
O II	4325.76	23	8.44	8.41	8.40					22	8.42	8.44	8.44
O II	4349.43									120	9.02	9.15	9.16
O II(B)	4351.00	80	8.30	8.20	8.18					76	8.30	8.33	8.34
O II	4353.58												
O II(B)	4366.00	94	8.91	8.66	8.65	43	8.49	8.54	8.63				
O II	4369.27												
O II	4395.94	52	8.73	8.63	8.62	24	8.41	8.43	8.48	35	8.42	8.45	8.45
O II	4414.90	120	8.58	8.42	8.40	67	8.38	8.43	8.53	100	8.35	8.40	8.40
O II	4416.98	99	8.66	8.50	8.49	51	8.43	8.48	8.57	78	8.38	8.43	8.44
O II	4452.38	46	8.65	8.58	8.57					40	8.55	8.57	8.58
O II	4590.97	98	8.67	8.46	8.45	51	8.22	8.28	8.36	67	8.20	8.24	8.25
O II(B)	4596.18	90	8.54	8.43	8.41	43	8.21	8.25	8.34	62	8.20	8.23	8.23
O II	4638.86	102	8.84	8.64	8.62	48	8.47	8.51	8.61	73	8.41	8.46	8.46
O II	4641.81	132	8.77	8.49	8.48					98	8.30	8.38	8.38
O II(B)	4650.00												
O II	4661.63					55	8.50	8.56	8.65	69	8.28	8.32	8.33
O II	4673.73					15	8.62	8.63	8.75	23	8.41	8.42	8.43
O II	4676.23	42	7.96	7.91	7.90	38	8.39	8.41	8.51	60	8.27	8.31	8.31
O II	4699.00	84	8.25	8.21	8.20	48	8.18	8.18	8.25	55	7.99	8.00	8.01
O II	4705.35	90	8.53	8.41	8.39	47	8.19	8.23	8.29	49	7.99	8.01	8.01
O II	4710.00					15	8.40	8.42	8.47	36	8.77	8.80	8.81
Mg II(B)	4481.00	87	7.22	7.15	7.17	44	6.91	6.94	6.97	98	7.26	7.29	7.29
Si II	4128.05												
Si II	4130.89												
Si III	4552.62	138	7.54	7.18	7.18	68	6.93	7.09	7.19	120	7.18	7.30	7.30
Si III	4567.84	118	7.57	7.23	7.23	51	6.94	7.05	7.15	94	7.10	7.21	7.21
Si III	4574.75	80	7.58	7.32	7.33	23	6.94	7.00	7.12	63	7.19	7.27	7.27
Si IV	4116.10	68	7.57	7.31	7.25	101	6.93	7.24	7.16	44	7.16	7.24	7.26
Fe III	4419.60												
Fe III	4431.02												

Table C.3. Contd. STARS:#108, #119

		NGC2004-108				NGC2004-119			
ION	λ	EW (mÅ)	(1)	(2)	(3)	EW (mÅ)	(1)	(2)	(3)
C II	3920.68	50	7.50	7.50	7.50	58	7.67	7.67	7.67
C II(B)	4267.00	103	7.29	7.29	7.29	123	7.48	7.48	7.48
C II	6578.05	86	7.63	7.63	7.63	95	7.71	7.71	7.71
C II	6582.88	70	7.66	7.66	7.66				
N II	3955.85					7	6.97	6.97	6.97
N II	3995.00	36	6.94	6.94	6.94	40	6.91	6.91	6.91
N II	4447.03	13	6.91	6.91	6.91				
N II	4601.48								
N II	4613.86								
N II	4630.54	18	6.83	6.83	6.83				
N II	4643.08					13	6.96	6.96	6.96
O II(B)	3912.00	32	8.30	8.30	8.30	50	8.39	8.39	8.39
O II	3945.04	20	8.27	8.27	8.27	36	8.46	8.46	8.46
O II	3954.36	35	8.41	8.41	8.41	46	8.35	8.35	8.35
O II	3982.71	15	8.19	8.19	8.19	25	8.23	8.23	8.23
O II(B)	4069.00	63	8.20	8.20	8.20	88	8.24	8.24	8.24
O II	4072.15	36	8.02	8.02	8.02	53	8.10	8.10	8.10
O II	4075.86	47	8.10	8.10	8.10	67	8.20	8.20	8.20
O II	4078.84	12	8.05	8.05	8.05	21	8.18	8.18	8.18
O II	4132.80	16	8.05	8.05	8.05	37	8.43	8.43	8.43
O II	4156.53								
O II(B)	4317.00	32	8.27	8.27	8.27	63	8.69	8.69	8.69
O II	4319.63	35	8.36	8.36	8.36	60	8.62	8.62	8.62
O II	4325.76					21	8.54	8.54	8.54
O II	4349.43	35	8.21	8.21	8.21	63	8.40	8.40	8.40
O II(B)	4351.00	24	8.13	8.13	8.13	38	8.08	8.08	8.08
O II	4353.58								
O II(B)	4366.00	27	8.09	8.09	8.09	49	8.34	8.34	8.34
O II	4369.27					15	8.27	8.27	8.27
O II	4395.94	21	8.57	8.57	8.57	43	8.89	8.89	8.89
O II	4414.90	52	8.22	8.22	8.22	65	8.17	8.17	8.17
O II	4416.98	46	8.42	8.42	8.42				
O II	4452.38	15	8.30	8.30	8.30	33	8.62	8.62	8.62
O II	4590.97	29	8.11	8.11	8.11	46	8.18	8.18	8.18
O II(B)	4596.18	32	8.27	8.27	8.27	59	8.47	8.47	8.47
O II	4638.86	35	8.30	8.30	8.30	52	8.36	8.36	8.36
O II	4641.81	47	8.15	8.15	8.15	66	8.17	8.17	8.17
O II(B)	4650.00								
O II	4661.63	35	8.24	8.24	8.24	53	8.31	8.31	8.31
O II	4673.73	11	8.38	8.38	8.38	18	8.43	8.43	8.43
O II	4676.23	26	8.12	8.12	8.12	46	8.29	8.29	8.29
O II	4699.00	24	7.97	7.97	7.97	40	8.03	8.03	8.03
O II	4705.35	30	8.18	8.18	8.18	38	8.08	8.08	8.08
O II	4710.00	13	8.63	8.63	8.63	21	8.68	8.68	8.68
Mg II(B)	4481.00	98	6.99	6.99	6.99	108	7.17	7.17	7.17
Si II	4128.05	20	7.15	7.15	7.15	19	7.20	7.20	7.20
Si II	4130.89	18	6.81	6.81	6.81	22	7.07	7.07	7.07
Si III	4552.62	76	6.95	6.95	6.95	100	7.09	7.09	7.09
Si III	4567.84	62	6.97	6.97	6.97	85	7.13	7.13	7.13
Si III	4574.75	39	7.02	7.02	7.02	58	7.21	7.21	7.21
Si IV	4116.10								
Fe III	4419.60	19	7.35	7.35	7.35	22	7.34	7.34	7.34
Fe III	4431.02								

Table C.4. Equivalent Widths and line by line absolute abundances of NGC330 for stars #2, #3, & #4. Columns are as for Table C.1.

		NGC330-002				NGC330-003				NGC330-004			
ION	λ	EW (mÅ)	(1)	(2)	(3)	EW (mÅ)	(1)	(2)	(3)	EW (mÅ)	(1)	(2)	(3)
C II	3920.68	33	7.01	7.02	7.02	75	7.36	7.33	7.32	31	6.87	6.87	6.87
C II(B)	4267.00	82	7.08	7.09	7.09	134	7.28	7.25	7.25	62	6.84	6.84	6.84
C II	6578.05												
C II	6582.88												
N II	3955.85												
N II	3995.00	56	7.45	7.48	7.49	150	7.73	7.64	7.62	146	7.75	7.75	7.75
N II	4447.03	23	7.69	7.71	7.70	68	7.79	7.75	7.74	64	7.80	7.80	7.80
N II	4601.48	18	7.60	7.62	7.61	52	7.70	7.67	7.67	64	7.87	7.87	7.87
N II	4613.86	11	7.60	7.61	7.59	34	7.69	7.67	7.67	41	7.85	7.85	7.85
N II	4630.54	36	7.54	7.56	7.56	118	7.75	7.68	7.67	126	7.86	7.86	7.86
N II	4643.08	18	7.64	7.65	7.64	66	7.84	7.80	7.80	70	7.91	7.91	7.91
O II(B)	3912.00					27	8.16	8.12	8.12				
O II	3945.04					19	8.15	8.13	8.13				
O II	3954.36	14	8.33	8.35	8.34	18	7.80	7.78	7.78	15	7.79	7.79	7.79
O II	3982.71												
O II(B)	4069.00	12	7.86	7.87	7.86	61	8.04	7.98	7.98	36	7.81	7.81	7.81
O II	4072.15	14	8.00	8.02	8.01	56	8.08	7.99	7.99	32	7.81	7.81	7.81
O II	4075.86	15	7.89	7.92	7.91	70	8.07	7.98	7.97	38	7.75	7.75	7.75
O II	4078.84	3	8.00	8.01	7.99	8	7.80	7.77	7.78				
O II	4132.80												
O II	4156.53												
O II(B)	4317.00	9	8.08	8.09	8.06	43	8.31	8.27	8.26	19	7.89	7.89	7.89
O II	4319.63	10	8.16	8.17	8.15	46	8.35	8.30	8.30	23	7.98	7.98	7.98
O II	4325.76					6	7.97	7.96	7.96				
O II	4349.43	11	7.88	7.88	7.86	71	8.29	8.23	8.22	35	7.88	7.88	7.88
O II(B)	4351.00					22	7.85	7.83	7.83				
O II	4353.58												
O II(B)	4366.00					46	8.28	8.23	8.23	19	7.82	7.82	7.82
O II	4369.27												
O II	4395.94												
O II	4414.90	13	7.85	7.86	7.86	70	8.19	8.10	8.10	41	7.89	7.89	7.89
O II	4416.98	12	8.05	8.07	8.06	49	8.18	8.11	8.11	31	7.95	7.95	7.95
O II	4452.38												
O II	4590.97					33	8.04	8.00	8.00				
O II(B)	4596.18					26	8.00	7.97	7.98				
O II	4638.86	5	7.82	7.83	7.81	43	8.20	8.15	8.15	19	7.83	7.83	7.83
O II	4641.81	13	7.88	7.89	7.88	82	8.22	8.15	8.14	40	7.84	7.84	7.84
O II(B)	4650.00					173	8.32	8.24	8.23	79	7.87	7.87	7.87
O II	4661.63	8	7.94	7.95	7.93	50	8.23	8.17	8.17	24	7.89	7.89	7.89
O II	4673.73												
O II	4676.23	8	8.07	8.08	8.06	43	8.26	8.21	8.21	17	7.83	7.83	7.83
O II	4699.00					17	7.87	7.86	7.87				
O II	4705.35					27	8.09	8.05	8.06				
O II	4710.00												
Mg II(B)	4481.00	175	6.55	6.57	6.60	131	6.82	6.80	6.79	128	6.73	6.73	6.73
Si II	4128.05	75	6.80	6.82	6.86	41	6.91	6.87	6.85	40	6.81	6.81	6.81
Si II	4130.89	85	6.68	6.71	6.75	52	6.87	6.82	6.80	48	6.71	6.71	6.71
Si III	4552.62	66	6.79	6.83	6.84	185	6.94	6.79	6.77	150	6.82	6.82	6.82
Si III	4567.84	47	6.77	6.81	6.82	146	6.96	6.82	6.81	114	6.82	6.82	6.82
Si III	4574.75	21	6.77	6.79	6.79	77	6.95	6.86	6.85	56	6.81	6.81	6.81
Si IV	4116.10												
Fe III	4419.60	12	6.70	6.71	6.70	29	6.90	6.88	6.87	24	6.83	6.83	6.83
Fe III	4431.02												

Table C.4. Contd. STARS:#5, #9, #10

		NGC330-005				NGC330-009				NGC330-010			
ION	λ	EW (mÅ)	(1)	(2)	(3)	EW (mÅ)	(1)	(2)	(3)	EW (mÅ)	(1)	(2)	(3)
C II	3920.68	17	6.88	6.88	6.88	27	7.14	7.22	7.24	29	7.09	7.20	7.21
C II(B)	4267.00	33	6.77	6.77	6.77	48	6.99	7.04	7.05	64	7.07	7.15	7.17
C II	6578.05												
C II	6582.88												
N II	3955.85												
N II	3995.00	25	7.41	7.41	7.41	16	7.11	7.17	7.19	16	6.96	7.04	7.06
N II	4447.03												
N II	4601.48	7	7.51	7.51	7.51								
N II	4613.86												
N II	4630.54	13	7.42	7.42	7.42	8	7.16	7.19	7.21	10	7.14	7.19	7.21
N II	4643.08												
O II(B)	3912.00												
O II	3945.04												
O II	3954.36												
O II	3982.71												
O II(B)	4069.00					6	7.98	8.02	8.05				
O II	4072.15					9	8.31	8.41	8.44	4	7.65	7.72	7.75
O II	4075.86	5	7.83	7.83	7.83	11	8.29	8.39	8.42	5	7.59	7.67	7.69
O II	4078.84												
O II	4132.80												
O II	4156.53												
O II(B)	4317.00												
O II	4319.63												
O II	4325.76												
O II	4349.43												
O II(B)	4351.00												
O II	4353.58												
O II(B)	4366.00												
O II	4369.27												
O II	4395.94												
O II	4414.90												
O II	4416.98												
O II	4452.38												
O II	4590.97												
O II(B)	4596.18												
O II	4638.86												
O II	4641.81												
O II(B)	4650.00	8	7.82	7.82	7.82					8	7.63	7.68	7.70
O II	4661.63												
O II	4673.73												
O II	4676.23												
O II	4699.00												
O II	4705.35												
O II	4710.00												
Mg II(B)	4481.00	193	6.58	6.58	6.58	202	6.57	6.67	6.66	161	6.52	6.64	6.63
Si II	4128.05	74	6.84	6.84	6.84	68	6.67	6.87	6.87	54	6.65	6.92	6.90
Si II	4130.89	78	6.68	6.68	6.68	74	6.54	6.75	6.74	56	6.49	6.73	6.72
Si III	4552.62	27	6.82	6.82	6.82	24	6.69	6.84	6.86	29	6.66	6.87	6.90
Si III	4567.84	18	6.79	6.79	6.79	15	6.62	6.73	6.76	20	6.64	6.81	6.84
Si III	4574.75	9	6.81	6.81	6.81					9	6.65	6.77	6.79
Si IV	4116.10												
Fe III	4419.60												
Fe III	4431.02												

Table C.4. Contd. STARS:#14, #16, #17

		NGC330-014				NGC330-016				NGC330-017			
ION	λ	EW (mÅ)	(1)	(2)	(3)	EW (mÅ)	(1)	(2)	(3)	EW (mÅ)	(1)	(2)	(3)
C II	3920.68					22	7.01	7.12	7.12	34	7.20	7.20	7.20
C II(B)	4267.00	67	6.93	6.93	6.94	69	7.24	7.36	7.36	75	7.07	7.07	7.07
C II	6578.05									59	7.24	7.24	7.24
C II	6582.88									46	7.27	7.27	7.27
N II	3955.85												
N II	3995.00	157	7.53	7.45	7.47	15	7.08	7.17	7.18	49	7.04	7.04	7.04
N II	4447.03	69	7.57	7.53	7.54					24	7.12	7.12	7.12
N II	4601.48	64	7.64	7.61	7.61					20	7.18	7.18	7.18
N II	4613.86	35	7.53	7.52	7.52					16	7.28	7.28	7.28
N II	4630.54	113	7.50	7.45	7.46					39	7.12	7.12	7.12
N II	4643.08									20	7.15	7.15	7.15
O II(B)	3912.00	40	8.04	8.01	8.00					28	7.99	7.99	7.99
O II	3945.04	38	8.24	8.22	8.21					11	7.70	7.70	7.70
O II	3954.36									21	7.75	7.75	7.75
O II	3982.71												
O II(B)	4069.00	129	8.24	8.17	8.16	5	7.83	7.87	7.89	54	7.84	7.84	7.84
O II	4072.15	101	8.17	8.07	8.06					26	7.50	7.50	7.50
O II	4075.86	115	8.10	7.99	7.98	8	8.10	8.24	8.25	36	7.58	7.58	7.58
O II	4078.84	24	8.07	8.03	8.02					11	7.79	7.79	7.79
O II	4132.80	31	8.07	8.03	8.02					15	7.82	7.82	7.82
O II	4156.53												
O II(B)	4317.00	70	8.32	8.26	8.25					17	7.56	7.56	7.56
O II	4319.63	78	8.39	8.33	8.32					23	7.75	7.75	7.75
O II	4325.76												
O II	4349.43									34	7.75	7.75	7.75
O II(B)	4351.00									19	7.59	7.59	7.59
O II	4353.58												
O II(B)	4366.00	70	8.24	8.18	8.17					17	7.51	7.51	7.51
O II	4369.27												
O II	4395.94												
O II	4414.90	99	8.10	8.02	8.02					25	7.41	7.41	7.41
O II	4416.98	63	8.02	7.97	7.96					22	7.60	7.60	7.60
O II	4452.38	34	8.41	8.37	8.36								
O II	4590.97	71	8.19	8.13	8.11					16	7.45	7.45	7.45
O II(B)	4596.18	62	8.22	8.17	8.14					18	7.63	7.63	7.63
O II	4638.86	82	8.31	8.25	8.24					21	7.63	7.63	7.63
O II	4641.81									35	7.59	7.59	7.59
O II(B)	4650.00									60	7.51	7.51	7.51
O II	4661.63	85	8.26	8.21	8.20					20	7.56	7.56	7.56
O II	4673.73												
O II	4676.23	69	8.25	8.20	8.19					21	7.69	7.69	7.69
O II	4699.00	31	7.87	7.86	7.84					13	7.45	7.45	7.45
O II	4705.35	43	8.02	7.99	7.97					17	7.60	7.60	7.60
O II	4710.00												
Mg II(B)	4481.00	92	6.72 1	6.70	6.72	200	6.57	6.77	6.69	47	6.47	6.47	6.47
Si II	4128.05					64	6.63	7.02	6.90				
Si II	4130.89					65	6.46	6.80	6.69				
Si III	4552.62	247	6.94	6.77	6.78	22	6.63	6.86	6.84	77	6.75	6.75	6.75
Si III	4567.84	200	6.97	6.82	6.83	15	6.60	6.78	6.78	61	6.72	6.72	6.72
Si III	4574.75	107	6.96	6.88	6.88					37	6.74	6.74	6.74
Si IV	4116.10	29	6.96	6.89	6.83								
Fe III	4419.60									14	6.90	6.90	6.90
Fe III	4431.02												

Table C.4. Contd. STARS:#18, #20, #22

		NGC330-018				NGC330-020				NGC330-022			
ION	λ	EW (mÅ)	(1)	(2)	(3)	EW (mÅ)	(1)	(2)	(3)	EW (mÅ)	(1)	(2)	(3)
C II	3920.68	57	7.37	7.37	7.37	27	7.04	6.95	6.95	37	7.03	7.09	7.12
C II(B)	4267.00	103	7.17	7.17	7.17	77	7.14	7.06	7.05	95	7.10	7.13	7.14
C II	6578.05												
C II	6582.88												
N II	3955.85												
N II	3995.00	50	7.31	7.31	7.31	23	7.08	6.96	6.93	51	7.19	7.31	7.30
N II	4447.03									16	7.13	7.17	7.12
N II	4601.48									17	7.30	7.35	7.30
N II	4613.86									14	7.39	7.44	7.39
N II	4630.54	27	7.18	7.18	7.18	16	7.23	7.15	7.10	32	7.19	7.27	7.23
N II	4643.08									19	7.35	7.40	7.35
O II(B)	3912.00												
O II	3945.04												
O II	3954.36												
O II	3982.71												
O II(B)	4069.00	35	8.13	8.13	8.13	17	8.15	8.05	7.96	26	7.77	7.83	7.74
O II	4072.15	22	7.99	7.99	7.99	11	8.04	7.90	7.85	20	7.75	7.86	7.78
O II	4075.86	30	8.09	8.09	8.09	14	8.04	7.88	7.84	28	7.81	7.95	7.88
O II	4078.84												
O II	4132.80												
O II	4156.53												
O II(B)	4317.00												
O II	4319.63												
O II	4325.76												
O II	4349.43	18	7.90	7.90	7.90					18	7.75	7.81	7.71
O II(B)	4351.00												
O II	4353.58												
O II(B)	4366.00									14	7.80	7.86	7.78
O II	4369.27												
O II	4395.94												
O II	4414.90	27	8.05	8.05	8.05								
O II	4416.98	24	8.26	8.26	8.26								
O II	4452.38												
O II	4590.97												
O II(B)	4596.18												
O II	4638.86												
O II	4641.81									21	7.69	7.78	7.69
O II(B)	4650.00	45	7.94	7.94	7.94	15	7.72	7.64	7.55	41	7.71	7.79	7.70
O II	4661.63									14	7.80	7.85	7.76
O II	4673.73												
O II	4676.23												
O II	4699.00												
O II	4705.35												
O II	4710.00												
Mg II(B)	4481.00	108	6.61	6.61	6.61	134	6.73	6.55	6.64	110	6.64	6.73	6.85
Si II	4128.05	31	6.75	6.75	6.75	47	7.18	6.76	6.92	24	6.57	6.69	6.84
Si II	4130.89	41	6.74	6.74	6.74	48	6.92	6.56	6.72	30	6.50	6.63	6.80
Si III	4552.62	64	6.81	6.81	6.81	44	7.07	6.72	6.77	66	6.60	6.89	6.95
Si III	4567.84	49	6.80	6.80	6.80	37	7.14	6.82	6.85	46	6.54	6.76	6.79
Si III	4574.75	26	6.80	6.80	6.80	20	7.11	6.88	6.88	25	6.60	6.75	6.74
Si IV	4116.10												
Fe III	4419.60	23	7.15	7.15	7.15								
Fe III	4431.02												

Table C.4. Contd. STARS:#26, #27, #32

		NGC330-026				NGC330-027				NGC330-032			
ION	λ	EW (mÅ)	(1)	(2)	(3)	EW (mÅ)	(1)	(2)	(3)	EW (mÅ)	(1)	(2)	(3)
C II	3920.68	39	7.33	7.33	7.33								
C II(B)	4267.00	97	7.3	7.30	7.30	82	7.13	7.13	7.13	34	7.16	7.16	7.16
C II	6578.05	80	7.47	7.47	7.47								
C II	6582.88	64	7.5	7.50	7.50					22	7.44	7.44	7.44
N II	3955.85												
N II	3995.00	78	7.45	7.45	7.45	10	7.43	7.38	7.38	43	7.33	7.33	7.33
N II	4447.03									24	7.38	7.38	7.38
N II	4601.48	22	7.22	7.22	7.22								
N II	4613.86												
N II	4630.54	34	7.01	7.01	7.01	81	7.47	7.43	7.43	31	7.40	7.40	7.40
N II	4643.08												
O II(B)	3912.00									26	7.78	7.78	7.78
O II	3945.04												
O II	3954.36									3	7.92	7.92	7.92
O II	3982.71												
O II(B)	4069.00	44	7.61	7.61	7.61	141	8.46	8.42	8.41	4	7.42	7.42	7.42
O II	4072.15	32	7.6	7.60	7.60	95	8.39	8.31	8.30	53	7.80	7.80	7.80
O II	4075.86	44	7.7	7.70	7.70	104	8.32	8.23	8.23	72	7.93	7.93	7.93
O II	4078.84									3	8.29	8.29	8.29
O II	4132.80									16	7.66	7.66	7.66
O II	4156.53												
O II(B)	4317.00									35	8.00	8.00	8.00
O II	4319.63									4	8.09	8.09	8.09
O II	4325.76												
O II	4349.43									65	8.24	8.24	8.24
O II(B)	4351.00									39	7.70	7.70	7.70
O II	4353.58												
O II(B)	4366.00									37	7.98	7.98	7.98
O II	4369.27												
O II	4395.94												
O II	4414.90									56	7.91	7.91	7.91
O II	4416.98									47	8.04	8.04	8.04
O II	4452.38												
O II	4590.97					54	8.06	8.03	8.02	36	7.74	7.74	7.74
O II(B)	4596.18					52	8.13	8.11	8.10	33	7.82	7.82	7.82
O II	4638.86	38	8.02	8.02	8.02					41	8.00	8.00	8.00
O II	4641.81									64	7.95	7.95	7.95
O II(B)	4650.00	87	7.74	7.74	7.74	218	8.36	8.29	8.28				
O II	4661.63	30	7.76	7.76	7.76	79	8.34	8.30	8.29	46	8.02	8.02	8.02
O II	4673.73												
O II	4676.23					88	8.59	8.53	8.52	39	8.00	8.00	8.00
O II	4699.00									37	7.82	7.82	7.82
O II	4705.35									35	7.79	7.79	7.79
O II	4710.00												
Mg II(B)	4481.00	92	7.02	7.02	7.02	47	6.44	6.44	6.44	41	6.80	6.80	6.80
Si II	4128.05												
Si II	4130.89												
Si III	4552.62	73	6.62	6.62	6.62	145	6.87	6.77	6.76	66	6.65	6.65	6.65
Si III	4567.84	58	6.61	6.61	6.61	123	6.94	6.85	6.84	59	6.82	6.82	6.82
Si III	4574.75	37	6.7	6.70	6.70	68	6.88	6.83	6.83	32	6.84	6.84	6.84
Si IV	4116.10					23	6.88	6.84	6.82	49	6.77	6.77	6.77
Fe III	4419.60												
Fe III	4431.02												

Table C.4. Contd. STARS:#42, #47, #74

		NGC330-042				NGC330-047				NGC330-074			
ION	λ	EW (mÅ)	(1)	(2)	(3)	EW (mÅ)	(1)	(2)	(3)	EW (mÅ)	(1)	(2)	(3)
C II	3920.68												
C II(B)	4267.00	48	7.06	7.06	7.04	54	7.20	7.20	7.20	23	7.29	7.31	7.26
C II	6578.05	31	7.09	7.09	7.08								
C II	6582.88	22	7.12	7.11	7.10								
N II	3955.85												
N II	3995.00	60	7.2	7.24	7.22	2	6.61	6.61	6.61	25	7.32	7.30	7.26
N II	4447.03	29	7.21	7.23	7.21								
N II	4601.48	16	7.15	7.15	7.14								
N II	4613.86	12	7.2	7.20	7.19								
N II	4630.54	38	7.15	7.17	7.16	2	6.91	6.91	6.91	31	7.71	7.67	7.65
N II	4643.08	18	7.17	7.18	7.16								
O II(B)	3912.00					5	8.19	8.19	8.19				
O II	3945.04												
O II	3954.36	25	7.66	7.68	7.68	45	8.14	8.14	8.14				
O II	3982.71					24	8.07	8.07	8.07				
O II(B)	4069.00	65	7.63	7.67	7.68	88	7.97	7.97	7.97	77	8.07	8.01	8.00
O II	4072.15	49	7.62	7.68	7.69	52	7.79	7.79	7.79	45	7.86	7.80	7.80
O II	4075.86	54	7.51	7.58	7.59	65	7.84	7.84	7.84	49	7.76	7.68	7.69
O II	4078.84					22	8.03	8.03	8.03				
O II	4132.80					34	8.14	8.14	8.14				
O II	4156.53												
O II(B)	4317.00	29	7.7	7.72	7.72	51	8.22	8.22	8.22				
O II	4319.63	32	7.75	7.78	7.77	54	8.28	8.28	8.28				
O II	4325.76					16	8.23	8.23	8.23				
O II	4349.43	47	7.72	7.76	7.77	62	8.14	8.14	8.14	46	8.25	8.22	8.19
O II(B)	4351.00	28	7.49	7.51	7.52	46	7.90	7.90	7.90	38	7.83	7.79	7.79
O II	4353.58												
O II(B)	4366.00	26	7.58	7.60	7.60	47	8.09	8.09	8.09				
O II	4369.27												
O II	4395.94												
O II	4414.90	40	7.49	7.52	7.52	78	8.13	8.13	8.13				
O II	4416.98	67	8.15	8.22	8.23	59	8.17	8.17	8.17				
O II	4452.38												
O II	4590.97	35	7.63	7.66	7.67	51	8.01	8.01	8.01	26	7.83	7.81	7.78
O II(B)	4596.18	36	7.76	7.78	7.79	47	8.03	8.03	8.03	24	7.89	7.88	7.85
O II	4638.86	39	7.8	7.83	7.83	49	8.07	8.07	8.07				
O II	4641.81	67	7.78	7.85	7.85	79	8.12	8.12	8.12				
O II(B)	4650.00												
O II	4661.63	45	7.82	7.86	7.87	53	8.07	8.07	8.07				
O II	4673.73												
O II	4676.23	32	7.72	7.75	7.75	53	8.20	8.20	8.20				
O II	4699.00	27	7.59	7.59	7.60	46	7.90	7.90	7.90				
O II	4705.35	35	7.73	7.75	7.76	45	7.95	7.95	7.95				
O II	4710.00												
Mg II(B)	4481.00	64	6.86	6.89	6.88	37	6.57	6.57	6.57	38	6.83	6.81	6.81
Si II	4128.05												
Si II	4130.89												
Si III	4552.62	98	6.62	6.81	6.81	76	6.66	6.66	6.66	75	7.01	6.81	6.87
Si III	4567.84	85	6.72	6.89	6.88	71	6.84	6.84	6.84	49	6.88	6.75	6.77
Si III	4574.75	44	6.68	6.78	6.77	49	7.00	7.00	7.00	24	6.94	6.86	6.85
Si IV	4116.10	29	6.66	6.76	6.83	28	6.84	6.84	6.84	91	6.95	6.62	6.83
Fe III	4419.60												
Fe III	4431.02												

Table C.4. Contd. STARS:#114, #124

		NGC330-114				NGC330-124			
ION	λ	EW (mÅ)	(1)	(2)	(3)	EW (mÅ)	(1)	(2)	(3)
C II	3920.68	39	7.37	7.36	7.36				
C II(B)	4267.00	83	7.24	7.23	7.23	54	7.57	7.57	7.55
C II	6578.05								
C II	6582.88								
N II	3955.85								
N II	3995.00	53	7.10	7.08	7.08	38	7.41	7.37	7.36
N II	4447.03								
N II	4601.48								
N II	4613.86								
N II	4630.54	51	7.33	7.31	7.31				
N II	4643.08	36	7.58	7.57	7.57				
O II(B)	3912.00								
O II	3945.04								
O II	3954.36								
O II	3982.71								
O II(B)	4069.00	68	7.95	7.92	7.92	50	7.66	7.63	7.62
O II	4072.15	59	8.12	8.08	8.08				
O II	4075.86	56	7.88	7.84	7.84	56	7.78	7.70	7.70
O II	4078.84								
O II	4132.80								
O II	4156.53								
O II(B)	4317.00	52	8.38	8.35	8.35				
O II	4319.63	29	7.91	7.89	7.89				
O II	4325.76								
O II	4349.43	63	8.32	8.27	8.27	39	7.99	7.95	7.94
O II(B)	4351.00	24	7.75	7.74	7.74				
O II	4353.58								
O II(B)	4366.00	25	7.76	7.74	7.74				
O II	4369.27								
O II	4395.94								
O II	4414.90	52	7.89	7.86	7.86				
O II	4416.98	53	8.20	8.16	8.16				
O II	4452.38								
O II	4590.97	48	8.17	8.14	8.14				
O II(B)	4596.18	45	8.21	8.19	8.19				
O II	4638.86	39	8.05	8.03	8.03				
O II	4641.81	60	7.97	7.94	7.94				
O II(B)	4650.00	111	7.95	7.92	7.92				
O II	4661.63	32	7.85	7.83	7.83				
O II	4673.73								
O II	4676.23	39	8.11	8.09	8.09				
O II	4699.00								
O II	4705.35	33	7.96	7.94	7.94				
O II	4710.00								
Mg II(B)	4481.00	95	6.99	6.97	6.97	37	6.78	6.75	6.75
Si II	4128.05								
Si II	4130.89								
Si III	4552.62	100	6.83	6.75	6.75	76	7.02	6.79	6.83
Si III	4567.84	91	6.98	6.90	6.90	52	6.87	6.71	6.73
Si III	4574.75	49	6.89	6.84	6.84	34	7.05	6.95	6.96
Si IV	4116.10					67	6.98	6.73	6.84
Fe III	4419.60								
Fe III	4431.02								